MEASUREMENT OF HYDROPHOBICITY OF SULPHIDE MINERALS BY USING ELECTROCHEMICAL METHODS

SÜLFÜRLÜ MİNERALLERDE HİDROFOBİKLİK DERECESİNİN ELEKTROKİMYASAL YÖNTEMLERLE BELİRLENMESİ

ESRA BAĞCI TEKEŞ

Submitted to the Institute of Sciences of

Hacettepe University as a partial fulfillment to the requirements

for the award degree of

DOCTOR OF PHILOSOPHY

in MINING ENGINEERING

2012

To the Directory of the Institute for Graduade Studies in Science and Engineering,

This study has been accepted as a thesis for the degree of **PHILOSOPHY OF DOCTORATE** in **MINING ENGINEERING** by our Examining Committee.

Head : ….....
Prof. Dr. Çetin HOŞTEN

Advisor : ….....
Prof. Dr. Zafir EKMEKÇİ

Member : ….....
Prof. Dr. Özcan Y. GÜLSOY

Member : ….....
Prof. Dr. Kadir PEKMEZ

Member :….....
Assis. Prof. Dr. N. Metin CAN

APPROVAL

Pursuant to the relevant articles of the “Hacettepe University Graduate Education and Examination Regulation”, this thesis was accepted by the abovementioned members of the Examining Committee on ...../...../..... and was approved by the Board of Directors of the Institute for Graduade Studies in Science and Engineering on ...../...../.....

Prof. Dr. Fatma SEVİN DÜZ
Director of Institute for Graduade Studies
in Science and Engineering

MEASUREMENT OF HYDROPHOBICITY OF SULPHIDE MINERALS BY USING ELECTROCHEMICAL METHODS

ESRA BAĞCI TEKEŞ

ABSTRACT

In froth flotation, the amount of valuable mineral recovered to the concentrate correlates with its degree of hydrophobicity. Some minerals, such as talc, graphite, molybdenite, etc., have natural floatability. However, since most of the minerals demonstrate hydrophilic behavior, collectors are required to acquire hydrophobic surface. Hydrophobicity can be defined as the minerals' tendency to remove the water from its surface and attach to the bubble. Measurement of hydrophobicity of mineral surfaces is very important in terms of observing and evaluating the flotation process. There is a correlation between the amount of adsorbed collectors and the degree of hydrophobicity.

Up to now, various experimental techniques have been used for measurement of degree of hydrophobicity. Contact angle, bubble induction time, microflotation and spectroscopic methods (UV visible spectroscopy, FTIR, HPLC, ToF-SIMS) are the most commonly used techniques. However, most of these techniques provide qualitative and at most semi-quantitative measurements. Besides, requirement of preparing a special sample and ex-situ operation method are disadvantages of these methods.

This study addresses measurement of the degree of hydrophobicity of sulphide minerals by using electrochemical techniques, utilizing their semi-conductive property. Since the mineral-collector interaction is electrochemical in nature, the degree of hydrophobicity of a sulphide mineral can be measured by electrochemical techniques.

In this study, open circuit potential measurements, voltammetric methods, chronoamperometry and electrochemical impedance spectroscopy (EIS) were used to quantify the degree of hydrophobicity. Chalcopyrite and pyrite were used in the experiments. Sodium iso propyl xanthate (SIPX) and sodium di-isobutyl dithiophosphinate (DTPI) were chosen as collectors with different chemical structures.

EIS was decided as the most appropriate electrochemical method for determining the degree of hydrophobicity of sulphide minerals. By EIS method, amount of collectors adsorbed on the mineral surfaces could be identified.

Key Words: Sulphide minerals, hydrophobicity, EIS, collector adsorption

Advisor: Prof. Dr. Zafir Ekmekçi, Hacettepe University, Mining Engineering Department

SÜLFÜRLÜ MİNERALLERDE HİDROFOBİKLİK DERECESİNİN ELEKTROKİMYASAL YÖNTEMLERLE BELİRLENMESİ

ESRA BAĞCI TEKEŞ

ÖZ

Flotasyonda konsantre olarak alınan değerli mineralin miktarı, mineralin hidrofobiklik derecesi ile ilişkilidir. Talk, grafit, molibdenit gibi bazı mineraller doğal hidrofobikliğe sahiptirler. Bununla birlikte birçok mineral hidrofilik özelliğe sahip olduğu için, yüzeylerini hidrofobik yapmak için toplayıcıya ihtiyaç duyulur. Hidrofobiklik, minerallerin yüzeyinden suyu uzaklaştırma ve hava kabarcığına yapışma eğilimi olarak tanımlanabilir. Minerallerin hidrofobiklik derecelerinin belirlenmesi, flotasyon sürecini gözlemlemek ve değerlendirmek için oldukça önemlidir. Soğurulan toplayıcı miktarıyla hidrofobiklik derecesi arasında bir ilişki vardır.

Bugüne kadar sülfürlü minerallerin hidrofobiklik derecesini ölçmek için çeşitli deneysel yöntemler kullanılmıştır. Temas açısı ölçümleri, kabarcık bağlanma süresi, mikroflotasyon ve spektroskopik yöntemler (UV görünür bölge spektrofotometresi, FTIR, HPLC,ToF-SIMS, vs.) en çok kullanılan yöntemlerdir. Bununla birlikte bu yöntemler nicel veya en fazla yarı nicel ölçümler sağlamaktadırlar. Ayrıca bu yöntemler için özel numune hazırlama gerekliliği ve deneylerin ex-situ yapılması bu yöntemler için birer dezavantajdır.

Bu çalışma sülfürlü minerallerin hidrofobiklik derecesini sülfürlü minerallerin yarı iletken özelliklerini kullanarak elektrokimyasal yöntemler ile ölçmeyi amaçlamaktadır. Sülfürlü minerallerde mineral-toplayıcı etkileşimi elektrokimyasal ve kimyasal reaksiyonlar ile meydana gelmektedir. Bu sayede minerallerin hidrofobiklik dereceleri elektrokimyasal tekniklerle belirlenebilmektedir.

Bu çalışmada açık devre potansiyeli ölçümleri, voltametrik yöntemler, kronoamperometri, ve empedans (EIS) sülfürlü minerallerin hidrofobiklik derecelerinin belirlenmesi amacıyla kullanılmıştır. Sülfürlü mineral olarak kalkopirit ve pirit kullanılmıştır. Toplayıcı olarak ise farklı kimyasal yapılara sahip sodyum iso propil ksantat (SIPX) ve di thiofosfin (DTPI) kullanılmıştır.

EIS yönteminin minerallerin hidrofobiklik derecelerinin belirlenmesinde en uygun elektrokimyasal yöntem olduğuna karar verilmiştir. EIS yöntemi ile yüzeye soğurulan toplayıcı miktarı kantitatif olarak belirlenebilmiştir.

Anahtar Kelimeler: Sülfürlü Mineraller, hidrofobiklik, EIS, toplayıcı soğurumu

Danışman: Prof. Dr. Zafir Ekmekçi, Hacettepe Üniversitesi, Maden Mühendisliği Bölümü

ACKNOWLEDGMENTS

I would like to express my gratitude to the following people for their contribution, both directly and indirectly, to my research work and the writing of this thesis:

First and foremost, I acknowledge my husband Öncü Tekeş and my family for their trust, patience, many support and encouragement.

Special thanks to my supervisor Prof. Dr. Zafir Ekmekçi for his outstanding supervision, experienced guidance as well as for his encouragement without which this thesis would not have got to this point.

Special thanks to Prof. Dr. Kadir Pekmez and Dr. Metin Can for their support insightful guidance, especially advice and assistance during experimental phase of this thesis.

Hacettepe University, Mining Engineering Department for making this thesis possible. Also all the staff and research assistants especially I would like to acknowledge to Dr. Özlem Bıçak and Dr. İlkay Bengü Çelik for their helps and support. Okan Altun is also thanked for moral support and helps all the time during the thesis whenever I needed.

TUBITAK (The Scientific and Technological Research Council of Turkey) for National PhD fellowship.

I would like also to thank Hacettepe University Research Foundation Unit (Project No:08/01/602004) for their financial support.

AMIRA is especially thanked for their financial support for P9O Project.

TABLE OF CONTENT

Page

TABLE OF FIGURES

Page

LIST OF TABLES

Page

1. INTRODUCTION

Froth flotation is a complex physicochemical process used widely for concentrating minerals. The complex nature of flotation comes from the variety of physical and chemical variables affecting the process. Countless research performed in the last 100 years and advance in several areas of flotation contribute to understand the theory of flotation. The use of advanced surface analytical techniques and instrumentation are still limited to laboratory scale measurements.

Flotation utilizes the differences in surface properties of the minerals for separation. Floatability of minerals changes as a function of mineral properties (particle size, liberation, surface composition, etc.), hydrodynamic conditions in the cell and chemistry of the pulp. For a given hydrodynamic condition and particle size, floatability is proportional to collector coverage. Therefore, adsorption of collector on a mineral surface is the crucial step in flotation and influenced mainly by surface characteristics of the mineral and, composition and concentration of collector. Hence, density of collector adsorption on a particular mineral surface can be accepted as a proxy of chemistry of flotation.

Various experimental techniques have been used to measure collector coverage on mineral surface. Contact angle, bubble induction time, microflotation and spectroscopic methods (UV visible spectroscopy, FTIR, HPLC, ToF-SIMS) are the most commonly used techniques. However, most of these techniques provide qualitative or at most semi-quantitative measurements and require special sample preparation techniques. Electrochemical techniques have also been used to detect adsorption of collectors on sulphide minerals.

Sulphide minerals are semi-conductor. Electrochemical behavior of mineral surfaces effects flotation process in many ways. For instance, surface form of sulphide minerals is dependent on the oxidation potential of the solution that surrounds the mineral surface. Adsorption mechanisms of collectors which are very frequently used in flotation of sulphide minerals such as xanthate and dithiophosphate, are known to be electrochemical. Differences between the open circuit potential of the sulphide in the solution can be deemed an indication that each sulphide mineral have a different electrochemical characteristic. Bearing all

these conditions in mind, it seems possible to determine the amount of collector on surfaces of sulphide minerals, hence their hydrophobicity degrees by electrochemical methods.

Determining the degree of hydrophobicity of minerals is very important for evaluating and optimizing the flotation behavior of sulphide minerals.

In this thesis, the main objective was to identify the most suitable electrochemical method that may quantitatively determine the amount of collectors adsorbed on the surfaces of sulphide minerals.

The second objective was to provide the basis for developing a measurement method for in-situ measurements in flotation plants.

2. LITERATURE REVIEW

2.1. Flotation

Flotation is a physico-chemical enrichment process that separates valuable minerals from waste minerals by using differences in surface properties. Flotation method makes contribution to the development of mining industry by providing the processing of complex ores. Flotation is a selective process that can be used for separating complex ores such as copper-lead-zinc, platinum, nickel, gold hosting sulphides, hematite-cassiterite and malachite-cerussite (Wills, 2006).

The complex nature of flotation is based on the effect of many physical and chemical parameters at the same time. Over a hundred years, many researchers have made investigations in different areas of flotation process and have helped us to understand the flotation nature. Today, advanced surface analysis techniques make it possible to analyse compounds on mineral surfaces and these developments provide understanding of the flotation chemistry in detail.

2.2. Importance of Hydrophobicity in a Flotation Model

Modelling and simulation is the most effective engineering tool to design and optimize a process. Although modelling of complex processes like flotation is very difficult due to the number of variables involved and dynamic nature of the process, a recent model has been derived in JKMRC after many years of research. This separates the flotation cell into two phases, as pulp zone and froth zone, and predicts the flotation performance successfully under constant chemical conditions. The flotability parameter (P) in the model expresses the chemical changes in the pulp zone. In fact, P changes as a function of particle size, degree of liberation and hydrophobicity.

Flotability of minerals changes as a function of mineral properties (particles size, liberation, texture, surface composition etc.), hydrodynamic conditions in the cell and the chemistry of the pulp (Eh, pH, dissolved oxygen concentration, reagent type, and dosage, dissolved ions in the pulp, etc.). The chemical conditions determine surface characteristics of the minerals in terms of hydrophobicity which

is essential to achieve flotation. The hydrophobicity of mineral surface is the crucial step in flotation and influenced mainly by the surface characteristics of the mineral and, the composition and concentration of the collector. Degree of hydrophobicity was measured as surface coverage of collector.

Vianna (2004) investigated flotability by separating it as a function of particle size, liberation and degree of hydrophobicity. This study showed that flotability increased with the increase in the amount of adsorbed collectors on mineral surface and that this was valid for all particle sizes of galena. Degree of hydrophobicity was measured as the surface coverage of collector by using HPLC to determine the amount of collector stripped from the surface of particles reported to the concentrate. Then the surface coverage was calculated for each size fraction by mass balancing of surface area of each size fraction. Moreover, at a fixed particle size and liberation, the flotability (P) was strongly influenced by the balance between hydrophobic and weakly hydrophobic active sites on the particles. In other words, it was shown that the presence of heterogeneous surface in terms of degree of oxidation, surface defect, etc., on particles having the same size and liberation may result in different flotability.

Gorain et. al. (1996, 1997) expressed the flotation rate constant (k) in terms of mineral flotability (P), bubble surface area flux (S_b) generated in the cell and froth recovery (R_f).

$$k = P * S_b * R_f \tag{2.1}$$

Based on equation (2.1), Savassi (1998) developed a flotation model expressing the recovery for a given particle size and the liberation class as a function of flotability (P), bubble surface area flux (S_b), residence time in flotation cell (τ), water recovery (R_w), degree of entrainment (ENT) and froth recovery (R_f).

$$R_{i,j} = \frac{(P_{i,j} S_b \tau R f_i)(1-R_w)+ENT_i R_w}{(1+P_{i,j} S_b \tau R f_i)(1-R_w)+ENT_i R_w} \tag{2.2}$$

In order to use this model, the variables included in it must be measured precisely. Various techniques and methodologies have been developed at JKMRC to measure these parameters. Among these parameters, the one that is most difficult to predict is the flotability of mineral particles (P). The methodology used to predict P is based on standard batch flotation tests performed for the feed, concentrate and tail streams of circuit. P is recalculated according to batch flotation test results.

This ex-situ analysis technique is time consuming to perform in each cell and requires calculations based on some assumptions. Therefore, a fast and reliable technique is required to measure degree of hydrophobicity of floatable minerals at different locations in a flotation circuit.

Sulphide minerals are semi-conductors with varying rest potentials reflecting their electrochemical character. Therefore, tools of electrochemistry, which are improved very fast in parallel with the progress in electronics and computers, are very suitable to develop a fast, reliable, in-situ a relatively low cost technique for hydrophobicity measurement.

2.3 Properties of Sulphide Minerals

The flotation behavior of minerals depends on types of bonds in their structure. Increasing ionic bonding in mineral structure causes an increase in the hydrophilic characters of mineral surfaces and thus the flotation of minerals gets harder as a result of that. Dennen's gradation between ionic and covalent bonding for minerals is shown in Figure 2.1 (Dennen,1959). The chemical bonds in a sulphide are generally ionic, covalent, etc., in various proportions.

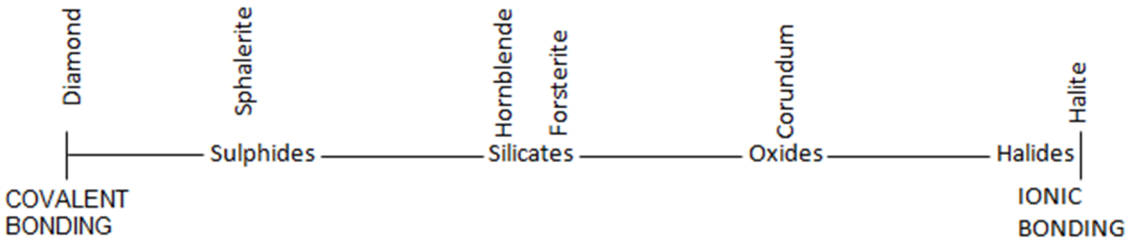

Figure 2.1 Gradation between ionic and covalent bonding. (Dennen,1959)

The sulphides are compounds of sulphur with electropositive metals and can be considered as salts of hydrosulphiric acid (H_2S) or hydrogen polysulphide (H_2S_x). Normal sulphides (M_2S) are formed with H_2S, and polysulphides (M_2S_x) with H_2S_x (Abromov and Audohin,1997).

Depending on the dominant type of chemical bond and physical-chemical properties, the sulphides can be divided into three groups.

1) Sulphides of non-transition metals and transition metals having outer s-electrons

2) Sulphides of transition metals with incomplete d- and f-electron shells

3) Sulphides of transition metals and semimetals with outer s- and p-electrons.

The sulphide minerals are solids distinguished by their variety of crystal structures which are determined by the charge and electron configuration of the ion. The coordination polyhedrons of the metals in the sulphides are primarily tetrahedrons, octahedrons or distorted modifications of these figures.

Polymorphism- the existence of a chemical compound of a given composition in two or more structural forms- is the characteristics of the sulphide minerals (e.g pyrite (cube) and marcasite (Rhomb.), FeS_2 or sphalerite (cube) and wurtzite (Hexagonal) ZnS). As a result of this difference, responses of pyrite and marcasite to adsorption and decomposition change. For example, marcasite has been shown to decompose more readily than pyrite under microwave treatment (Huang and Rowson, 2001). In addition, measurement of mineral potentials in distilled water showed that marcasite (+0.37 Volt) would be oxidized more quickly than pyrite (+0.18 Volt) when it was in contact with a copper electrode (Glembotskii, et al., 1974).

Furthermore, a number of sulphides do not follow Dalton's law in terms of constancy or uniform ratios of their component elements M:S (nonstoichiometry). The limits of nonstoichiometry are observed in the sulphides of iron, lead, copper and other metals. These structures are derived from known crystal structures by ordered substitution (chalcopyrite, $CuFeS_2$, derived from sphalerite by ordered replacement of Zn by Cu and Fe) or distortion (triolite, FeS, is a distorted NiAs-

type). Some rather more unusual structures are also found which involve anion-anion bonding in layer structures (CuS, MoS_2), or metal-metal bonding (in $(Ni,Fe)_9S_8$, pentlandite). Where complex substitutions are involved with uncertainties over site occupancies and valence states as, for example, in the economically important tetrahedrite minerals, $(Cu,Fe,Zn,Hg,Ag,Cd)_{12}(Sb,As)_4S_{13}$, these have now been resolved using spectroscopic methods to supplement conventional X-ray diffraction techniques (Ekmekçi, 2006).

2.4 Electrochemistry of Sulphide Minerals

Sulphide minerals are semiconductors with varying electrochemical properties determined by the type of metal atoms and the crystal structure (metallic or n- or p- type), and their electronic conductivity enables them to act as a source or sink for electrons in coupled electrochemical processes. Since the sulphide minerals behave as an electron receiver and transmitter, electrochemical reactions may occur on their surfaces (Woods,1984).

Reactions occurred on sulphide minerals surfaces can be shown by reactions given below (Guy and Trahar,1985).

$$M_zS \rightarrow zM^{+n} + S^0 + zne^- \quad \text{(acidic media)} \qquad (2.3)$$

$$M_zS + znH_2O \rightarrow zM(OH)_n + S^0 + znH^+ zne^- \quad \text{(neutral/alkali media)} \qquad (2.4)$$

In some cases, oxi-sulphide compounds can be occurred.

$$xM_zS + (zxn + y)H_2O \rightarrow zxM(OH)_n + S_xO^{-2} + (2y + zxn)H^+ + (2y + zxn - 2)e^- \quad (2.5)$$

While the elemental sulphur rich surface such as in reactions (2.3) and (2.4) increases flotability, existence of oxy-sulphur compounds as in reaction (2.5) depresses it. Besides, hydroxide species having stable hydrophilic structure also causes depression of flotation (Guy and Trahar, 1985).

The potential difference across the mineral/solution interface is the important factor in determining the rate of such reactions and hence the flotation behavior exhibited by the mineral. The electrode potential determines the type of electrochemical reaction (oxidation or reduction) that is thermodynamically possible and their kinetics. (Guy and Trahar,1985).

The potential at a solid/liquid interface is determined by the presence of oxidizing and reducing species in solution. In order to monitor redox properties, the potential of an indicator electrode placed in the solution should be measured. Noble metals (usually platinum or gold) are generally used for this purpose because of their high resistance to corrosion.

Eh and E^{o}'s inability to show the pace of the reaction constitutes the main problem faced at thermodynamic qualities. For instance, sulphide ions are supposed to be the oxidation product of sulphide minerals thermodynamically (Pourbaix,1966). However, in flotation, sulphoxide compounds and elemental sulphur occur on the mineral surface since the oxidation reaction of sulphide ions are slow (Chander,1988).

Gardner and Woods (1973) aimed to show the relation between flotation with electrochemical potential and a small pneumatic flotation cell modified so as to control the potential and to take electrochemical measurements in the flotation cell at the same time. In galena flotation, it was observed that the flotation did not occur until the potential between solid and liquid reach a higher (anodic) potential than the one required for PbX_2 formation and for the oxidation of xanthate ion to dixanthogene.

2.4.1 Collectorless Flotation of Sulphide Minerals

Many different theories about natural flotability of sulphide minerals have been proposed by researchers. Fuerstenau (1980) found that sulphide minerals are naturally floatable in the absence of oxygen and Yoon (1981) proposed that the natural flotability of some sulphide minerals is based on their very low solubility.

Some sulphides, such as molybdenite (MoS_2), are naturally floatable under most conditions whereas others are considered to have intrinsic hydrophobic character

in the absence of oxidation (Ekmekçi, 2006). However, under condition of specific pulp potential ranges sulphide minerals display a hydrophobic behavior due to surface self-oxidation (Hu, 2009). Finkelstein et. al. (1975), considered that the natural flotability of sulphide minerals occurred as a result of formation of elemental sulphur on mineral surface and the thickness of elemental sulphur layer increase the flotability of sulphide minerals.

Sulphide lattice ions are expected to be weakly hydrated and do not interact strongly with water molecules. The sulphide minerals are thermodynamically unstable and moderately oxidizing conditions lead to formation of elemental sulphur (in atomic form, S^o, and in S_8 form), polysulphides or metal-deficient sulphur layer which make the surface hydrophobic (Chander, 1991; Gardner and Woods, 1979; Heyes and Trahar, 1977; Smart, 1991; Ekmekçi and Demirel; 1997).

The reasons for flotability of sulphide minerals in the absence of collectors may vary from mineral to mineral. In most cases, the flotation behavior depends on the nature of the surface which might be readily altered by electrochemical reactions.

Oxygen has an important role in natural hydrophobicity of sulphide minerals. Oxygen is always present in flotation pulps and acts as an electron acceptor. The oxidation reaction producing elemental sulphur is schematically illustrated in Figure 2.2. The anodic and cathodic reaction sites may co-exist on one surface or they can occur through galvanic interaction of two minerals having different rest potentials. As it is illustrated in Figure 2.2, presence of oxygen or any type of electron acceptor is essential. However, increasing activity of oxygen in the solution will shift the mixed potential to higher values at which dissolved metal ions and elemental sulphur are further oxidized into form of metal oxy-hydroxide and sulphoxy compounds. Thus, collectorless flotation can only occur under moderately oxidizing conditions where elemental sulphur and polysulphides are stable.

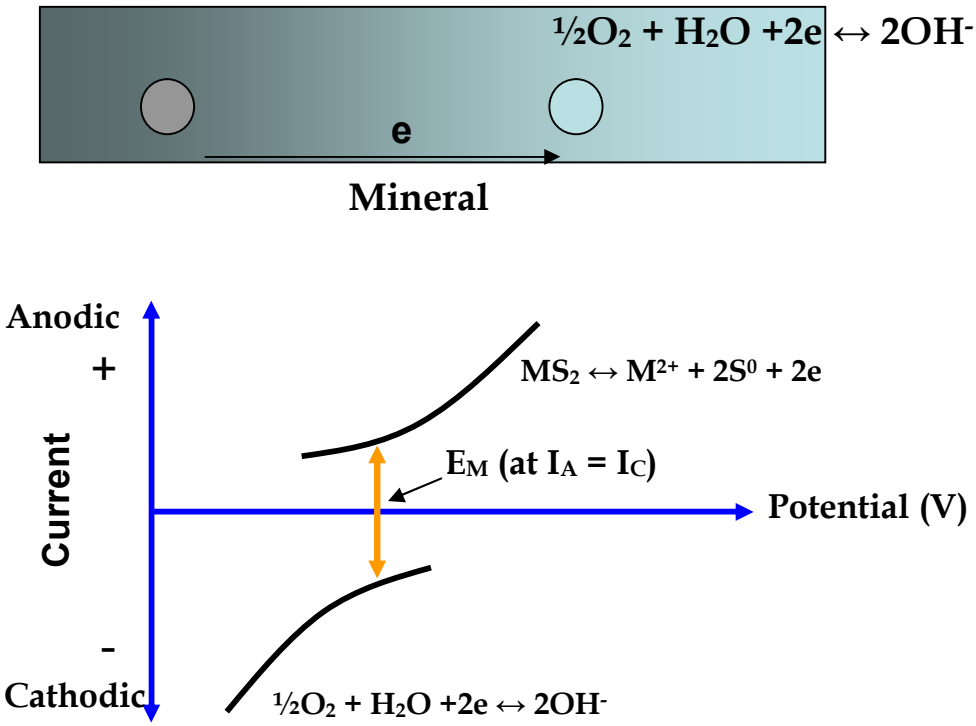

Figure 2.2. Schematic representation of electrochemical mechanism of elemental sulphur formation.

The following electrochemical reactions have been proposed by Gardner and Woods (1979) for chalcopyrite;

In acidic solutions,

$CuFeS_2 \leftrightarrow CuS + Fe^{2+} + S^{o} + 2e^{-}$ $E^{o}= 0.293$ Volt (2.6)

$Eh= 0.293 + 0.0296 \log(Fe^{2+})$

In neutral and alkaline solutions,

$CuFeS_2 + 3H_2O \leftrightarrow CuS + Fe(OH)_3 + So + 3H^{+} + 3e^{-}$ $E^{o}= 0.548$ Volt (2.7)

$Eh= 0.548 – 0.0592pH$

These reactions are anodic reactions and they are dependent on the electrochemical potential of the solution. Therefore, collectorless flotation of chalcopyrite could only be observed at potentials greater than reversible potentials (Eh) of reactions (2.6) and (2.7), where hydrophobic elemental sulphur forms at the surface.

2.4.2 Collector Interaction (Hydrophobicity and Flotability)

Hydrophobicity defines the ability of the mineral surface to repel water. Thus, mineral particles attach to the air bubble.

Hydrophobicity develops with the collector adsorbed on the mineral surface. It would be better to mention the concept of mixed potential before mentioning the adsorption of collector on the mineral surface.

2.4.2.1 Concept of mixed potential

The equilibrium state is rarely achieved in flotation. The measured potential remains constant as long as the reactions proceed at constant rates. The introduction of reduced or oxidized forms of a reagent or an increase in the solution mixing changes the rate of the reactions and causes a drift in the potential value. Therefore, the potential measured by the indicator electrode is not a reversible reaction of one specific couple but rather a “mixed potential”. Mixed potential is the generic term for a potential measured in a complex system.

A mixed potential arises when there are two (or more) redox couples present in the system and they are not in equilibrium.

$$E^0_{\mathrm{Re}\,d_1/Ox_1} + \frac{RT}{n_1 F}\ln\frac{[Ox_1]}{[\mathrm{Re}\,d_1]} \neq E^0_{\mathrm{Re}\,d_2/Ox_2} + \frac{RT}{n_2 F}\ln\frac{[Ox_2]}{[\mathrm{Re}\,d_2]} \qquad (2.8)$$

Thus, the overall redox potential in the solution is not represented by a unique Eh value, but rather it is represented by two potentials (Figure 2.3). When an indicator

electrode is introduced into the solution, its electrons can exchange with two separate redox couples and the measured potential will reach a value, lying between the reversible potentials of the two couples where the component anodic and cathodic processes proceed at equal and opposite rates, as illustrated in Figure 2.3.

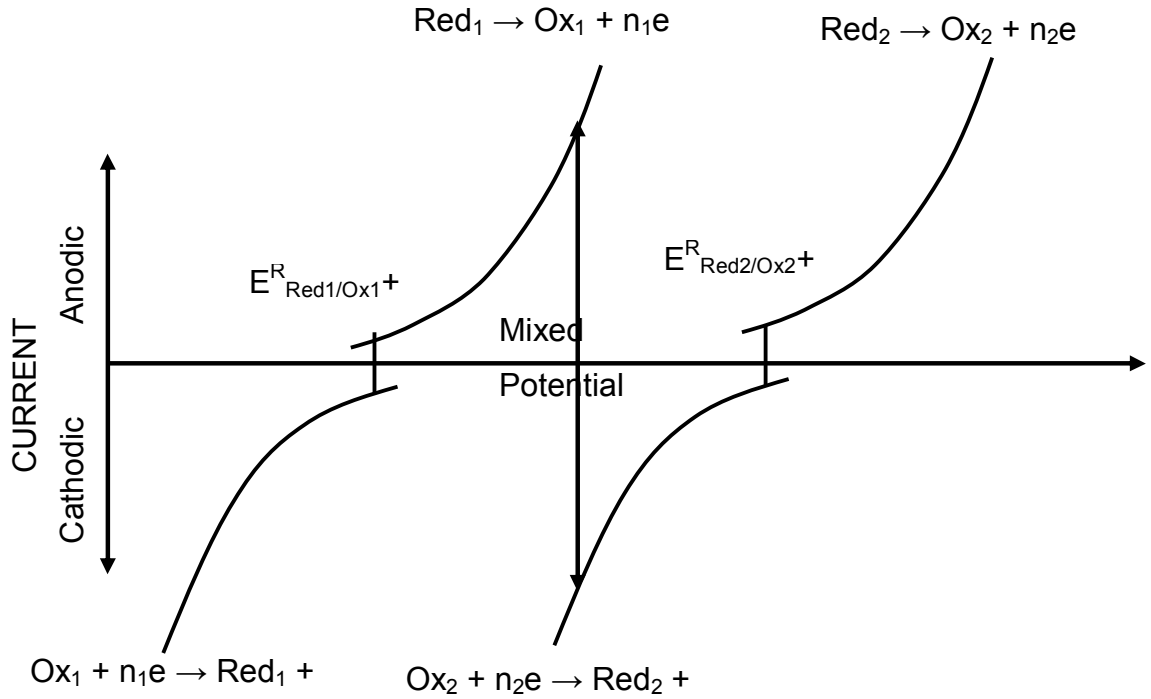

Figure 2.3. Schematic representation of a mixed potential system (Rand and Woods, 1984).

The mixed-potential model demonstrates the importance of electrode potential in flotation systems. The mixed potential or open circuit potential of an electrode provides information to determine the identity of the reactions that take place at the mineral surface and the rates of these processes.

Hydrophobicity of mineral surface is directly proportional to the amount of collectors adsorbed on the surface. Hydrophobicity increases as the amount of adsorbed collectors increase (Figure 2.4).

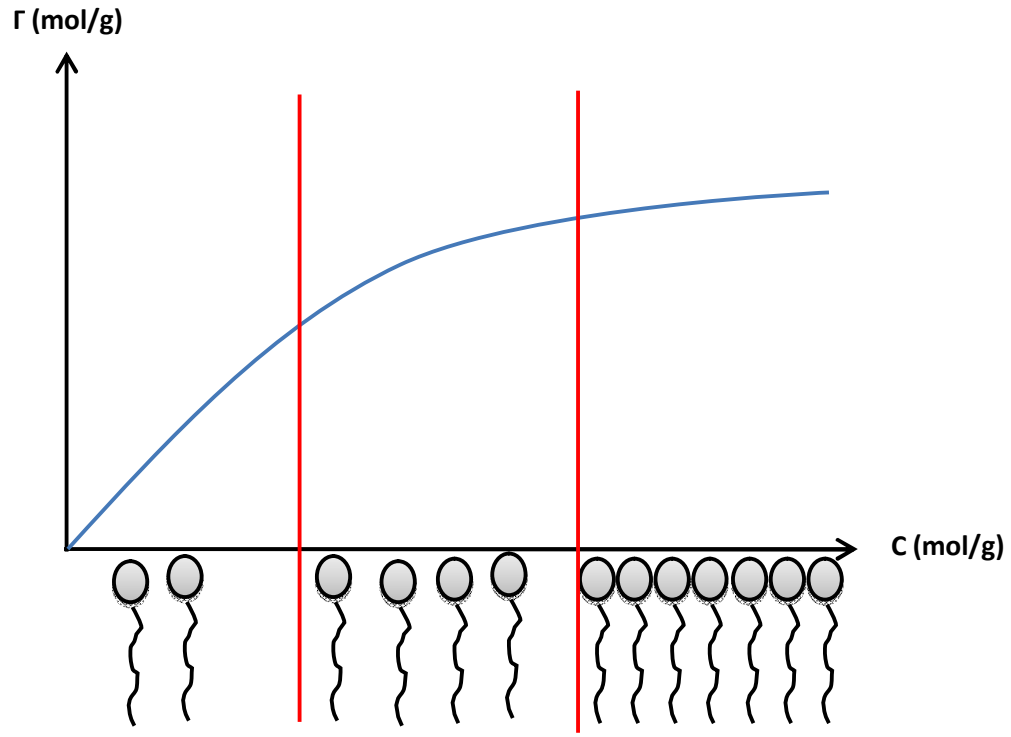

Figure 2.4. Schematic representation of collector dosage/adsorption amount relationship

Collector adsorption mechanisms are explained below.

i) Ion Exchange Theory

There is a strong correlation between adsorption of xanthates and the solubility of the heavy-metal xanthates. It has been considered that the collector is adsorbed by ion exchange mechanism between hydroxide ions at the surface and collector ion in the bulk phase owing to the higher stability of metal-collector species (Gaudin, 1932; Wark and Cox, 1934). Schematic representation of the ion exchange mechanism is illustrated as follows:

$$MS\begin{matrix}H^+\\OH^-\end{matrix} + X^-_{(aq)} \rightleftharpoons MS\begin{matrix}H^+\\X^-\end{matrix} + OH^-_{(aq)} \qquad (2.9)$$

With this theory, Taggart explained the stoichiometric balance between the sulphate, carbonate, thiosulphate and thionate ions dissolved from the galena

surface into the solution and the xanthate ions adsorbed on the galena surface. Inception of oxidation on galena surface depends on the amount of lead compounds that may be displaced with xanthate ions.

The relationship between the hydroxide ion concentration and collector ion concentration in a flotation pulp is quantified by the so-called Barsky relation.

$$\frac{[X^-]}{[OH^-]} = cons. \qquad (2.10)$$

ii) Chemical Reaction Theory

Taggart (1930) related the adsorption of collectors on sulphide minerals to the chemical reactions between the reagent and the particle affected (Taggart et al., 1930). This theory is different from the ion exchange theory. Taggart's theory is based on the relationship between the equilibrium of metal ions (M^+) and anions (A^-) of the mineral (MA) and, the equilibrium between metal ions and collector ions (represented by xanthate, X^-) of metal xanthate (MX) in solution. This relationship can be represented by an ordinary chemical reaction, in which solid metal xanthate is formed by exchange reaction with the mineral, yielding anions to the solution, with an equilibrium constant shown.

$MS_{(s)} = M^+_{(aq)} + A^-_{(aq)}$ (2.11)

$MX_{(s)} = M^+_{(aq)} + X^-_{(aq)}$ (2.12)

$MA_{(s)} + X^-_{(aq)} = MX_{(s)} + A^-_{(aq)}$ (2.13)

$K_{MA} = [M^+]\,[A^-]$ solubility product of the mineral, (2.14)

and

$K_{MX} = [M^+]\,[X^-]$ solubility product of metal-xanthate (2.15)

Then the overall equilibrium constant for the overall reaction should be

$$K = \frac{K_{MA}}{K_{MX}} \qquad (2.16)$$

The results of infrared spectroscopy (Leja, 1982) and microcalorimetry (Mellgren, 1966) studies performed on galena-xanthate system have shown that the uptake of xanthate by oxidized galena occurs by the chemical exchange reaction of forming lead-xanthate.

iii) Electrochemical Theory

In the model proposed by Salamy and Nixon (1953), the interaction between collector and oxygen at the mineral surface takes place by separate electrochemical reactions which proceed simultaneously. The anodic oxidation reaction can occur in several ways. The electrons evolved from these anodic reactions are transferred to the mineral and these are returned to the solution phase by cathodic reduction of oxygen.

Wark's adsorption model would be given by the following anodic process

$$X^- \rightarrow X_{ads} + e^- \qquad (2.17)$$

Taggart's chemical mechanism would involve an anodic process as shown in reaction (2.18).

$$MS + 2X^- + 4H_2O \rightarrow MX_2 + SO_4^{2-} + 8H^+ + 8e^- \qquad (2.18)$$

This reaction could proceed either in single stage or via separate processes occurring subsequently. Oxidation of sulphide at the surface to sulphate could

occur on exposure of the mineral to atmosphere, as in the case of galena. If following reaction considered first,

$PbS_{(s)} + 2O_{2(g)} \rightarrow PbSO_4$ $K = 10^{124}$ (2.19)

with the following equilibrium expression,

$$\frac{[PbSO_4]}{[PbS][P_{O_2}]^2} = 10^{124} \quad (2.20)$$

where $[PbSO_4] = 1$

$[PbS] = 1$ Therefore, $P_{O_2} = 10^{-62}$ atm.

The partial pressure of oxygen in the air is 0.2 atm >> 10^{-62} atm, thus oxidation of galena occurs to thiosulphate or sulphate. In this case, adsorption of collector follows the processes shown in reaction (2.21) and (2.22) subsequently.

$MS + 4H_2O \rightarrow MSO_4 + 8H^+ + 8e^-$ (Anodic reaction) (2.21)

$O_2 + 2H_2O + 4e^- \rightarrow 4OH^-$ (Cathodic reaction) (2.22)

$4X^- + O_2 + 2H_2O \rightarrow 4X_2 + 4OH^-$ (2.23)

However, in the case of grinding in a reducing environment and absence of oxygen, the sulphide at the surface will not be oxidized and the process shown in reactions (2.24) and (2.25) will be valid.

$$2X^- + MS + 4H_2O \rightarrow MX_2 + SO_4^{2-} + 8H^+ + 8e^- \text{ (Anodic reaction)} \quad (2.24)$$

$$O_2 + 2H_2O + 4e^- \rightarrow 4OH^- \text{ (Cathodic reaction)} \quad (2.25)$$

The third anodic process is oxidation of the thiol collector to its dithiolate as in the following anodic reaction,

$$2X^- \rightarrow X_2 + 2e^- \quad (2.26)$$

The dithiolate is formed on an unaltered sulphide surface, or on a surface which has previously chemisorbed the collector or reacted to form a metal collector compound. All these anodic reactions are dependent on the pulp potential. Therefore, the potential determines the identity of the reactions that take place at the mineral surface and the rates of these processes.

A typical example of potential dependence of sulphide mineral flotation in the presence of a thiol collector is given in Figure 2.5. Figure 2.5 shows the results of chalcocite (Cu_2S) flotation with ethyl xanthate at pH=8 and 11 (Heyes and Trahar, 1979). The potential has been controlled by addition of dithionite as reducing agent or hypoclorite as oxidizing agent to the solution. The potential of the beginning of flotation is independent of pH and close to that found for commencement of chemisorption of xanthate on this mineral (reaction 2.27).

$$Cu_2S + X^- \rightarrow CuS + CuX + e^- \qquad E^0 = -0.234 \text{ V} \quad (2.27)$$

Flotation is inhibited at high potentials at pH=11 but not at pH=8. This is attributed to the oxidation of the surface xanthate to copper oxide by the following reaction:

$$CuX + H_2O \rightarrow CuO + X^- + 2H^+ + e^- \quad (2.28)$$

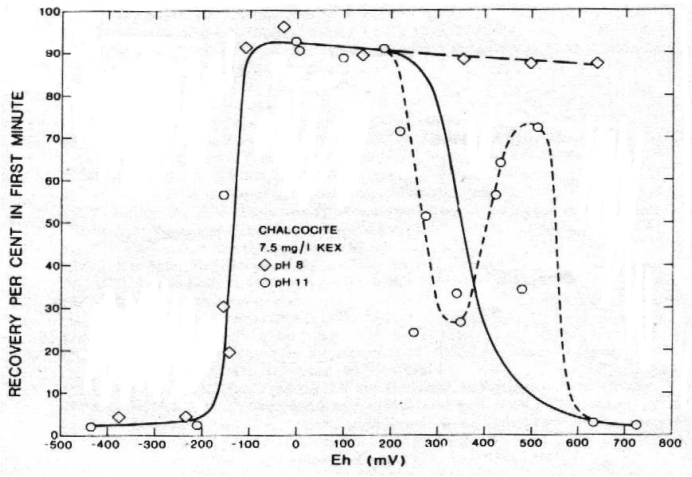

Figure 2.5. The flotation response of chalcocite (Cu_2S) at pH 8 and 11 as a function of potential (Heyes and Trahar, 1979).

2.5. Methods to Determine Degree of Hydrophobicity

2.5.1 Analytical Methods

For determining the adsorption density on mineral surface, devices such as UV, FTIR, Raman spectroscopy, HPLC, XPS are used. Those devices can provide detailed information on mineral surface and the structure of compounds adsorbed on surface.

The following two methods are used for determining the amount of collectors adsorbed on mineral surface.

1. Determining the collector concentration remained in the solution (Residual analysis method)
2. Determining the collector concentration by extracting the collector adsorbed on mineral surface.

2.5.1.1 UV Visible Spectroscopy

For investigating the surface characteristics of sulphide minerals, UV visible spectroscopy is used alone or together with electrochemical methods. UV visible spectroscopy is quite useful particularly when an extraordinary increase in the

current occurs through oxidation of minerals, other than the collector in the solution. (Buckley and Woods, 1997).

Tolley et al. (1996), conducted a potentiostatic adsorption test by using a modified Hallimond Tube (Figure 2.7) in pH 9.2 buffer solution. Potassium ethyl xanthate (KEX) was used as a collector and by utilizing a potenstiostate potential was applied on the mineral bed fitted on glass frit for 20 minutes for each potential. During the experiment, the solution has been pumped continuously down to glass frit that supports the mineral base (through the UV spectrophotometer) and thus the measurement was taken.

Walker et al. (1984), used a microflotation- electrochemical cell connected to a fast scan UV spectrometer. Fast scan UV spectrometer is able to scan at 200-800 nm range in one second. Solution was pumped from the cell to the UV at 60-70 ml/sec. Thus, any compound formed on the packed bed at measurable amount could be determined between 2 to 4 seconds. During the experiment, the solution amount that was circulated between the cuvette and pump was 12-13 ml.

Woods (1994) investigated the correlation between copper electrode and ethyl xanthate by UV and FTIR spectroscopies. Xanthate was observed to disappear from the solution at the potential that it was absorbed on copper electrode which was previously determined by experiments. Besides, xanthate was observed to reappear in the solution when the potential was returned at more negative values. This showed that the absorption of xanthate was reversible at -0.55 -0.19 mV potential at which the experiment was conducted (Figure 2.6).

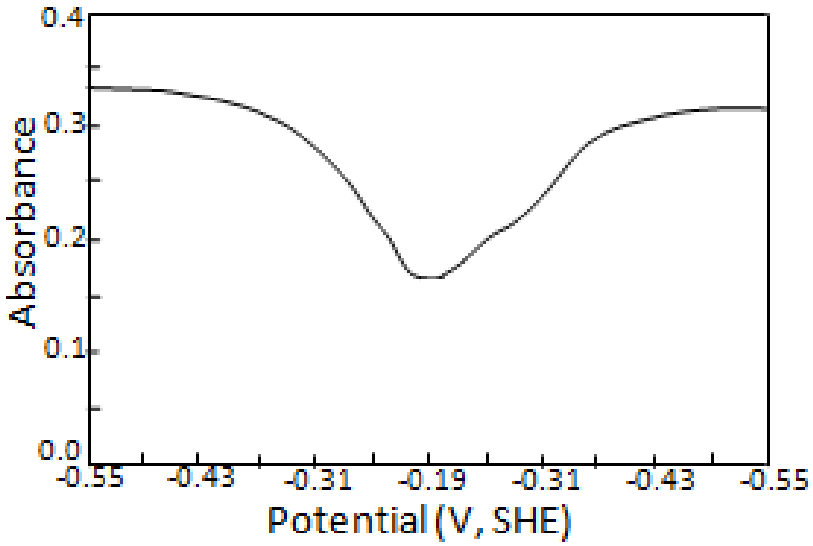

Figure 2.6. Absorbance at 301 nm of a pH 9.2 solution in the presence of 2x10-5 M ethyl xanthate. The potential was held at -0.55 V for 2 min and then a triangular potential cycle at 1mV/s-1 was applied between -0.55 V and -0.19 V.

2.5.1.2. Fourier Transform Infrared Spectroscopy (FTIR)

Infrared spectroscopy provides broad information about sulphide formations on the surface and the chemical structure of compounds adsorbed on mineral surface. FTIR is particularly useful when an additional increase in the current occur not only due to absorption but also to other processes at interface. This technique is also used for determining simultaneous formation of two different compounds. For example, Woods et al. (1995) showed that the adsorption of xanthate on gold electrode occurred just below the reversible potential of xanthate/dixanthogen pair.

2.5.1.3. Raman Spectroscopy

Raman spectra are acquired by irradiating a sample with a powerful laser source of visible or near-IR monochromatic radiation. During irradiation, the spectrum of the scattered radiation is measured at some angle (often 90") with a suitable spectrometer. An important advantage of Raman spectroscopy over IR lies in water being a quite useful solvent (Skoog, 2007).

Vermaak et al. (2005) performed electrochemical studies for investigating Pd-Bi-Te interaction with ethyl xanthate. Raman spectroscopy showed that xanthate coexisted with dixanthogen. As a result of this study, formation of dixanthogen was proved when the surface was polarized at anodic range. Usage of Raman spectroscopy at electrochemical studies provided quite valuable information about the surface. Controlling surface potential while the liquid face is circulating enabled the investigation of different compounds at different potentials. Raman spectroscopy showed that the xanthate was transformed into dixanthogen at high anodic currents.

Hope et. al. (2003) used spectroelectrochemical methods for observing interaction between sulphide minerals and collectors. SERS (Surface Enhanced Raman Scattering) helped explaining collector adsorption on electrochemically controlled surface. SERS studies were carried out with different kind of collectors. Adsorption for each collector has occurred by the formation of metal-sulphide bonds through electron transfer.

2.5.1.4 X-ray Photoelectron Spectroscopy (XPS)

Velásquez et. al. (2001) used analytical techniques along with electrochemical techniques in order to investigate the surface of natural chalcocite (Cu_2S) which was modified electrochemically. The results showed that oxidation of chalcocite in an alkaline medium results in a modified morphology and chemical composition of the surface. The usage of analytical techniques (SEM,EDX and XPS) and electrochemical techniques (CV and EIS) together provide an opportunity to relate changes on the surface at different potential values.

Miller et al (2006) investigated the hydrophobicity of pyrite at low potential range in nitrogen environment at the presence of potassium amyl xanthate (PAX) at pH 4.5 and 9.2. Pyrite was polarized in air and nitrogen environment and pyrite spectrum was taken by V6 Scientific 220i XL Electron Spectrometer which has a monochromatize Al K_α X-ray source. Species formed on surface was determined by using the X-ray Photoelectron Spectroscopy handbook. (Mauler et al., 1995)

2.5.1.5. Atomic Force Microscopy (AFM)

Miller (2006) used Nanoscope III Electrochemical Atomic Force Microscope (ECAFM). In his experiments, a liquid AFM cell which enables control on sample surface potential by a potenstiostat was used. ECAFM can function through conventional three electrodes method and can perform many electrochemical methods such as potential control and cyclic voltammetry. Thus, it may be possible to simultaneously determine the compounds formed on surface while electrochemical reactions continue. In that study of Miller et al, pyrite was used as working electrode and it was determined that pyrite oxidized to ferric hydroxide at 125 mV. After adjusting the potential, images have been taken by AFM at different times. (initially, between 0-20 minutes and then after 20 minutes). Scanning speed was 5 Hz. It took 40 seconds to capture a 10X10 μm image.

2.5.2. Microflotation

Microflotation does not involve bubble phase. Thus, the results can be directly evaluated as hydrophobicity of minerals. Experiments are carried out mostly with pure minerals and approximately 2 grams of those minerals are used. In microflotation studies, sometimes ore is used instead of the pure mineral and in this case, 2 grams of sample might not represent the ore as a whole. This constitutes the main disadvantage of microflotation tests.

Tolley et al (1996) has used modified Hallimond Tube to investigate flotation chemistry of oxidized chalcocite. By the modified Hallimond Tube, flotability, open circuit potential and AC impedance can be measured at the same time. In the experiment, 2 grams of sample and $1x10^{-7}$ M KEX was used. Mineral bed was conditioned with collector for 10 minutes and was floated by air bubble without the use of frother. Chalcocite was floated for 2 minutes in order to determine its flotability. Volume of floating part amount was determined by measuring the height of the mineral base. Floating sample was then turned back to mineral bed and the experiment was repeated by gradually increasing KEX concentration up to $5x10^{-3}$ M.

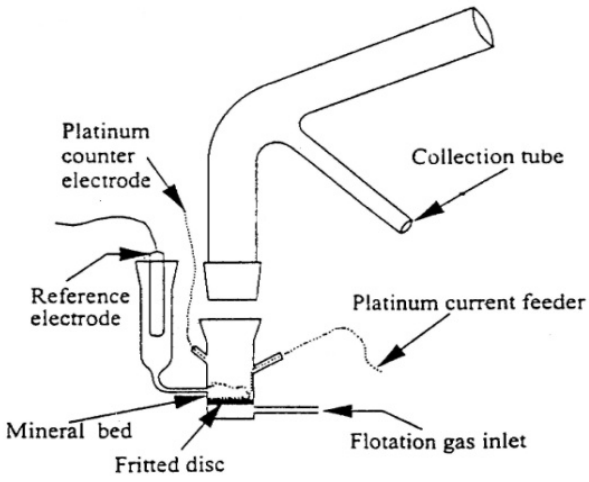

Figure 2.7. Modified Hallimond Tube

Walker et al (1984), used a modified microflotation cell for investigating low grade complex sulphide minerals. In order to establish a correlation between flotation behavior of minerals and reactions occurred on surface, mineral bed was used as the working electrode and microflotation experiments were carried out. During the experiments, solution concentration was monitored by a fast scan UV. Figure 2.8 shows the microflotation-electrochemistry cell used in the said study.

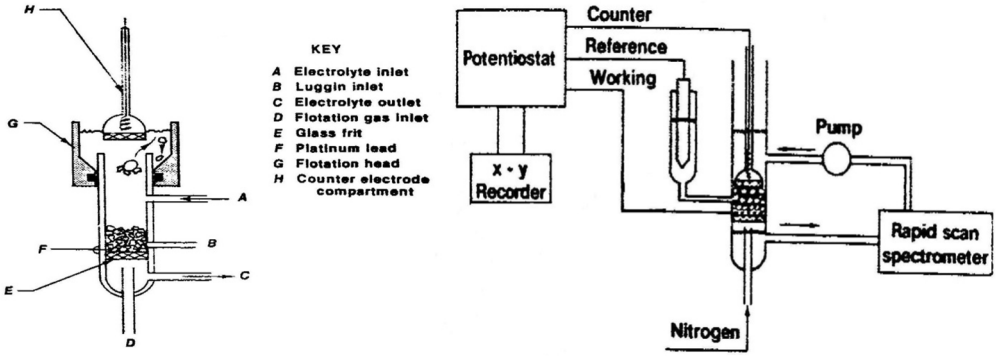

Figure 2.8. Microflotation-electrochemistry cell (Walker et. al., 1984) and spektroelectrochemical experiment mechanism

Experiment mechanism is shown in Figure 2.8. Mineral base potential is provided by a potanstiostat and electrolyte is continuously circulated in UV spectrometer.

Guo and Yen (2002) investigated pulp potential and flotability of chalcopyrite. Microflotation, UV and contact angle measurements were taken in order to observe the effect of potential that was outwardly applied on natural and synthetic chalcopyrite in potassium amyl xanthate (PAX) solution. Flotation, in the absence and presence of collector, was used for determining floatable potential range of chalcopyrite under potential control at pH 10.

Dixanthogen form increases together with increased potential, however it rapidly decreases after a certain potential (Figure 2.9).

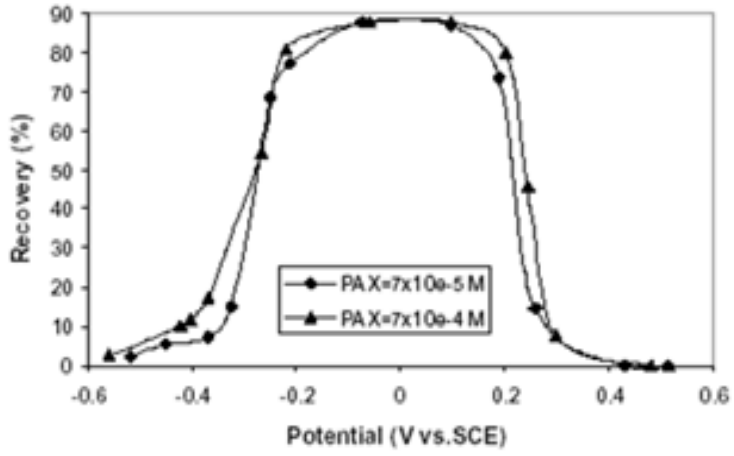

Figure 2.9. Flotability of natural chalcopyrite with PAX at pH 10.

2.5.3. Contact Angle Measurements

Angle between solid-liquid and gas phases is called the contact angle and it is generally measured through liquid phase. Contact angle is accepted as a measure of hydrophobicity. It is known from the previous experiments that when the amount of collector adsorbed on surface increases, the contact angle, hence hydrophobicity degree of mineral surface increases.

Correlation between surface tension and contact angle can be determined by Young equation,

$$\gamma_{SG} = \gamma_{SL} + \gamma_{LG} \cos\theta \qquad (2.29)$$

Young's equation is valid in ideal conditions where solid-liquid and gas phases are in equilibrium and there is no gravity effect (Johnson,1959). In real flotation conditions, it is impossible to establish a direct connection between dynamic and turbulence conditions where mineral particle and bubble adhere through collision. Real surfaces are heterogeneous and rough. Contact angle, measured on natural surface, display hysteresis. Contact angle results measured at roughness surface does not display real situation.

Vermaak et al. (2005) investigated the interaction between ethyl xanthate and Pd-Bi-Te by contact angle, electrochemical and Raman Spectroscopy measurements. Contact angle measurements were made in a modified electrochemical cell having two parallel windows. The electrochemical cell was inserted into goniometer. In that experiment, contact angles at different potential were measured. Pd-Bi-Te electrode was conditioned for 5 minutes at each potential and then by generating nitrogen bubble on surface, contact angle was measured from both direction. It was observed that as potential increased in anodic direction, contact angle increased dramatically. Maximum contact angle obtained was 63^{o}.

Guo and Yen (2002) also used contact angle measurements for investigating flotability of chalcopyrite. Guo and Yen measured contact angles at different potentials. In those experiments, xanthate solution at two different concentrations ($7x10^{-4}$ M ve $7x10^{-5}$ M PAX) was tested. Decreasing PAX concentration caused a decrease in contact angle on chalcophrite surface and it was observed that potential ranges that contact angle occur straiten.

2.5.4 Bubble Induction Time

Besides thermodynamic conditions, froth flotation depends on many factors such as physical and mechanical characteristics of liquid film thickness, hydrodynamics of water/mineral suspensions and attachment of mineral particles to bubbles (Leja,1982). Adhesion of mineral particles to bubbles is the most important requirement for the success of flotation (Fuerstenau, 1980). For mineral particle interaction, liquid film should thin and rupture before a strong bond is established between mineral and the gas phase. Interfacial forces control stability of the liquid

film between bubble and mineral. Three forces affect stability of the liquid film. These are van der Waal's dispersion force (P_{vdW}), electrical double layer interaction (P_e) and solvation layer (P_s) (Derjaguin, 1961).

$$P = P_{vdW} + P_e + P_s \tag{2.30}$$

If P<0, then liquid film is not stable. Time required for thinning of the liquid film to a critical thickness and its eventual rupture is called bubble induction time.

Yordan and Yoon (1985) measured bubble induction time required for bubble-particle contact in the quartz-dodecylammonium chloride system at different pH's. It was observed that when bubble induction time is at lowest pH, flotation efficiency is at its highest (Figure 2.10).

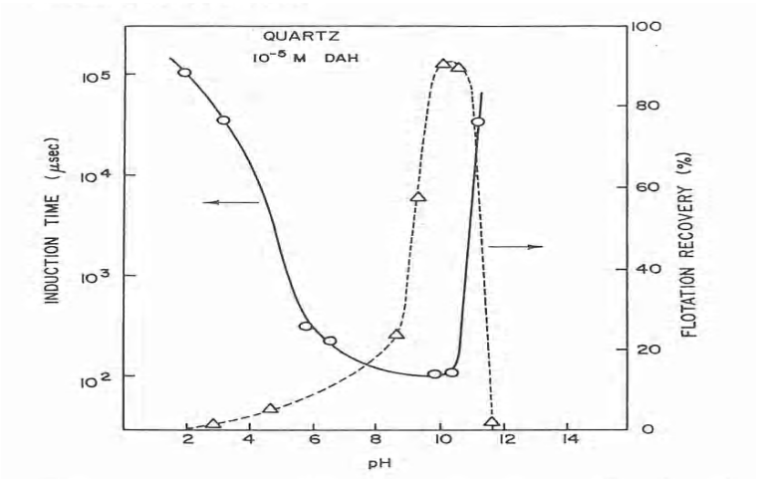

Figure 2.10. Bubble induction time results for quartz-dodecylammonium chloride system at different pH's.

Bubble induction time is a function of chemistry and hydrodynamic of the system and thus it provides information about the kinetics of the system. In this respect, it can be said about flotation behavior of minerals that it provides far more reliable information than the contact angle. However, bubble induction time for an identical

mineral is two times more in experiments conducted with flat plate than in the ones conducted with powder sample. (Sutherland and Wark,1955). For this reason, bubble induction time experiments can only be used to roughly compare wettability and to make a general evaluation on flotation behavior.

2.5.5 Electrochemical Methods

Electrochemical behavior of mineral surfaces affects flotation in many ways. Surface form of sulphide minerals depends on the oxidation potential of solution that surrounds the surface and absorption mechanism of collectors widely used for flotation of sulphide minerals such as xanthate, dithiphosphate (DTP) and dithiophosphinate (DTPI) is known to be electrochemical or electrochemical/chemical. Also, precipitation of metals to mineral surface in the pulp affects oxidation potential.

Electrode potential determines the kind of the reactions (oxidation and reduction) thermodynamically possible on mineral surface as well as the kinetics of this reaction. A chemical material's quantity that reacts with electrode is proportional to electric current passing through the cell. According to Faraday's Laws, chemical and electrochemical change (N mole material formation) depends on the electric load (Q) passing through the electrochemical reaction.

$$Oxidation + ne^{-} \rightarrow Reduction \tag{2.31}$$

$$N = \frac{Q}{neL_{AV}} \quad N = \frac{Q}{nF} \tag{2.32}$$

Adsorption of collectors to sulphide minerals occur according to Frumkin isotherm. As collector concentration increases, the amount of collector adsorbed on mineral surface also increases. Adsorption of more collectors to the surface causes an increase in the current. Information about the degree of hydrophobicity of minerals may be obtained surface by investigating increase of current value.

Electrochemical methods used in the literature so far are as follows:

1. Open Circuit Potential
2. Cyclic Voltammetry
3. Chronoamperometry
4. Electrochemical Impedance Spectroscopy

2.5.5.1 Open Circuit Potential

If the measurement is taken when no current passes through the mineral electrode, then the measured potential is called the open circuit potential of the mineral. Mineral electrode potential is measured against the reference electrode. It is possible to get information about the system by comparing the measured open circuit potential with equilibrium potentials obtained in thermodynamic data at different conditions.

Allison et. al. (1972) measured the rest potentials of various sulphide minerals in the presence of ethyl xanthate to estimate the type of surface species on the surface using equilibrium potentials of the reactions of metal xanthate or dixanthogen formation (Table 2.1). Dixanthogen (X_2) is formed when the rest potential is high, metal xanthate (MX) is formed when the potential is moderate, and no collector species is identified when the potential is low.

$$X_2 + 2e^- \rightarrow 2X^- \quad E^0 = 0.13 \text{ V } (6.25 \times 10^{-4} \text{ M KEX , pH=7}) \qquad (2.33)$$

In other words, anodic reactions occur if the open circuit potential is above the equilibrium potential of reaction (2.33). The reverse situation exists for cathodic process. For a cathodic process to take place; the rest potential must be below the equilibrium potential for this process (Ekmekçi, 2006).

Table 2.1. Rest potentials and products of interactions of ethyl xanthate with sulphide minerals (Allison 1972)

Mineral	Product	Rest potential after 10 min vs.N.H.E
Sphalerite	NPI	-0.15
Stibnite	NPI	-0.125
Realgar	NPI	-0.12
Orpiment	NPI	-0.1
Antimonite	NPI	-0.09
Cinnabar	NPI	-0.05
Galena	MX	0.06
Bornite	MX	0.06
Chalcocite	NPI	0.06
Covellite	X_2	0.05
Chalcopyrite	X_2	0.14
Alabandite	X_2	0.15
Molybdenite	X_2	0.16
Pyrrhotite	X_2	0.21
Pyrite	X_2	0.22
Arsenopyrite	X_2	0.22

Potential for $X_2 + 2e^- \rightarrow 2X^-$ at 6.25×10^{-4} M KEX and pH=7 is 0.13 V

Goold and Finkelstein (1972) conducted similar experiments with other thiol reagents, viz., sodium diethyl dithiocarbamate (DTC), dithiophosphate (DTP) and mercaptobenzothiazole 5 (MBT). Formation of dithiolates was observed when the rest potential of the sulphide mineral was above reversible potential for thiol and its dithiolate.

2.5.5.2 Cyclic Voltammetry

In cyclic voltammetry method, current between a working electrode and a counter electrode is measured against the voltage applied that is changed in time in terms of value. The graph drawn for showing applied potential against the measured current values is called voltamogram (Yıldız, A., vd., 1997). It is determined that if the region that the current is increasing is anodic, an anodic reaction, if contrary, a cathodic reaction occurs on mineral surface. Amount of the current transfer between the working electrode and the counter electrode (platinum plate) shows the size of reaction occurred on mineral surface, while electron flow direction shows the characteristic (anodic or cathodic) of the reaction. Reaction is anodic when electron flow direction is from mineral to platinum, while it is cathodic on the contrary. Cyclic voltammograms show that the reactions on mineral surface and the potential value they occurred.

Mechanisms of surface oxidation and adsorption of flotation reagents was studied for all of sulphide minerals, particularly pyrite, galena and chalcopyrite by using cyclic voltammetry (Woods,1972, Chander et.al,1993, Güler et.al.,2005). Most of the surface reactions in sulphide mineral systems are in the form of irreversible or quasi-irreversible reactions. Therefore, careful analysis of the voltammograms is required for characterization of the surface species, elucidate the reactions and postulate adsorption mechanisms of flotation reagents.

Valdiviezo et al (2003) investigated the adsorption of isopropyl xanthate ions to arsenopyrite (FeAsS) surface by using voltammeter and open circuit potential methods at pH 6. Experiments were conducted in nitrogen environment by using a three electrode system. Pieces of -38μ arsenopyrite embedded in carbon paste, graphite electrode and saturated calomel electrode was used as working electrode, counter electrode and reference electrode respectively. Cyclic voltammeter studies were conducted at pH 6, at three different xanthate concentrations (0 M, 10^{-4} M and 10^{-3} M). As shown in Figure 2.11, xanthate peak was obtained at 10^{-4} M and 10^{-3} M xanthate concentrations. Amount of current increases as the amount of collectors adsorbed increases.

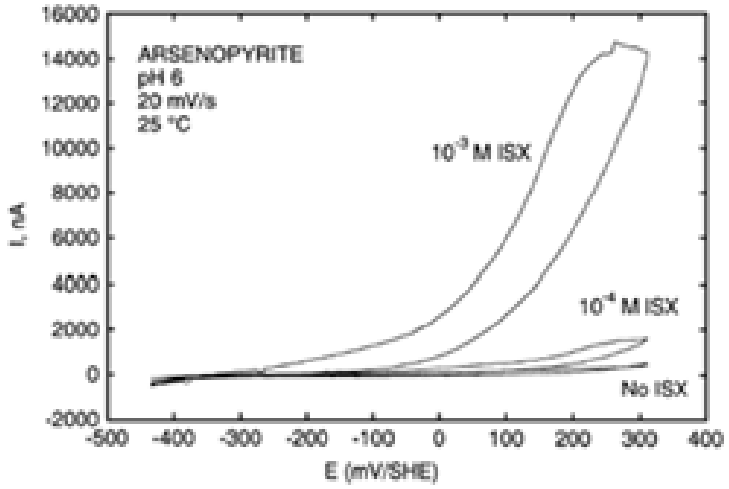

Figure 2.11. Arsenopyrite electrode in 0 M, 10^{-4} M ve 10^{-3} M sodium iso propyl xanthate solution, pH 6.

Measurements of cyclic voltammetry, open circuit potential and contact angle have been made for investigating the interaction of sodium di iso buthyl dithiophosphinate (DTPI) with galena and pyrite and the role of redox potential at hydrophobic characteristics of mineral surface in an alkali environment (pH 9) in the presence of a collector (Pecina et al., 2006). Experiments were conducted in the absence and presence of 10^{-3} M DTPI. Voltammograms were conducted at pH 9 in nitrogen environment. Figure 2.12 shows galena voltammogram taken in the presence of DTPI. A new peak beginning at 30 mV has been formed when collector added. This is the peak where $Pb(DTPI)_2$ occurs. Figure 2.13 also shows pyrite voltammogram taken in the presence of DTPI. A1 peak shows that pyrite interacts with DTPI. Electrochemical process occurred is being thought of as the oxidation of DTPI (dimmer formation). The fact that the iron compounds enter into a hydrolyze reaction (hydroxide formation) instead of forming iron-DTPI supports that condition.

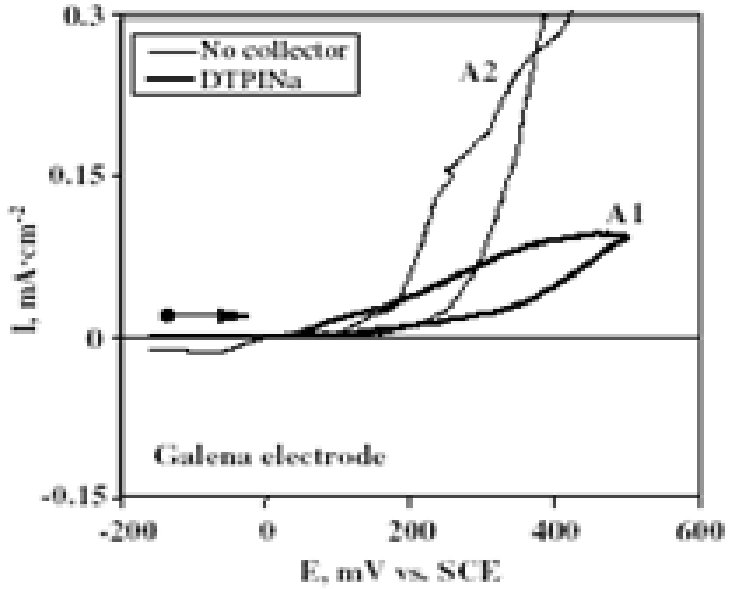

Figure 2.12. Galena voltammogram in the absence and presence of DTPI, pH 9 (10^{-2} M $NaNO_3$), 20 mV/sec

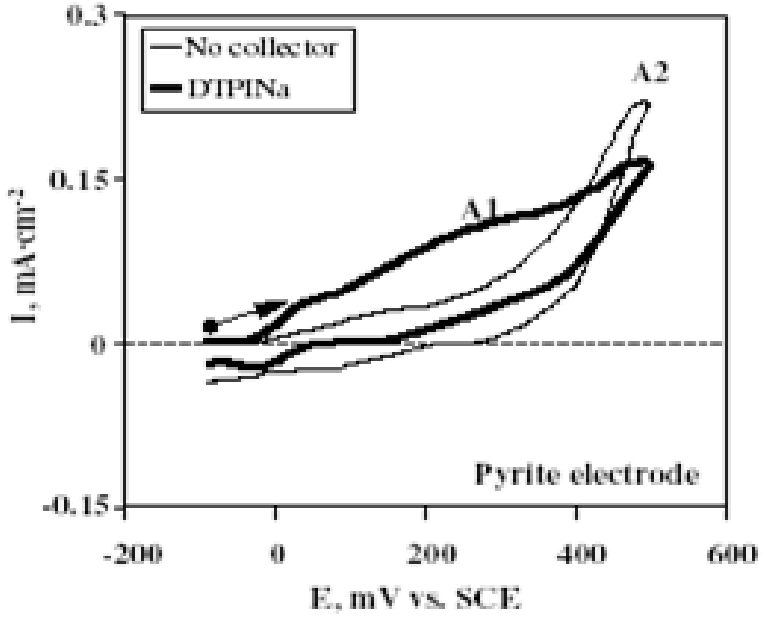

Figure 2.13. Pyrite voltammogram in the absence and presence of DTPI, pH 9 (10^{-2} M $NaNO_3$), 20 mV/sec

2.5.5.3 Chronoamperometry

Chronoamperometry involves stepping the potential of the working electrode from a value at which no Faradic reaction occurs to a potential at which the surface concentration of the electroactive species is effectively zero (Figure 2.14a). A stationary working electrode and unstirred solution are used. The resulting current-time dependence is monitored. As mass transport under these conditions is solely by diffusion, the current-time curve reflects the change in the concentration gradient in the vicinity of the electrode surface (Figure 2.14b). This involves gradual expansion of the diffusion layer with depletion of the reactant (Figure 2.14c). This behavior is expressed by Cottrel equation (2.34) (Bard,1980; Wang,2000).

$$i(t) = \frac{nFACD^{1/2}}{\pi^{1/2} t^{1/2}} = kt^{-1/2} \qquad (2.34)$$

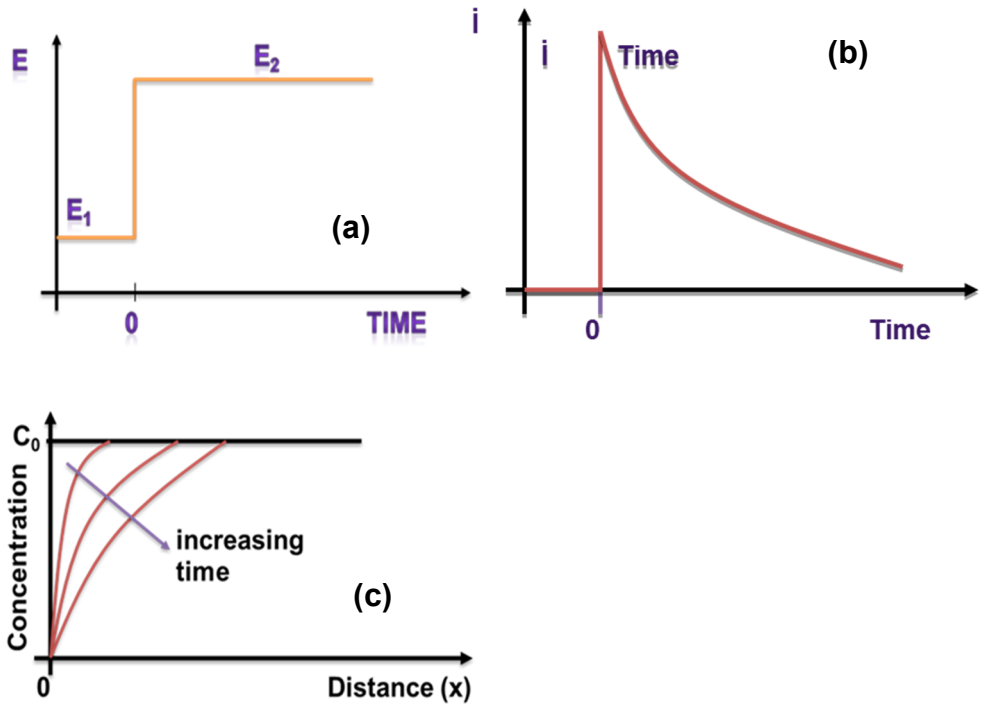

Figure 2.14. Chronoamperometry experiment: a) potential-time waveform; b) resulting current-time response; c) change of concentration profiles.

Chronoamperometry is usually employed to measure diffusion coefficient of electroactive species, surface area of working electrode and investigate mechanism of electrode process, such as adsorption and desorption of flotation reagents.

Oxidation/reduction behavior of pyrite was investigated by using chronoamperometry technique (Mendriatta, 2000). In these experiments the surface of pyrite electrode was fractured in the cell to create fresh surface. Prior to fracture the electrode was held at these potentials for 15 minutes to stabilize the residual currents. Following fracture, a spike was observed in chronoamperometry curves (Figure 2.15). Anodic (positive) currents indicate that pyrite undergoes oxidation after fracture and cathodic (negative) currents suggest that pyrite undergoes reduction. As expected more positive potentials caused an increase in oxidizing currents and more negative potentials caused an increase in reduction currents. There is a unique potential where no oxidation or reduction currents form after fracture. At this potential the newly formed pyrite surface is non-reactive and stable.

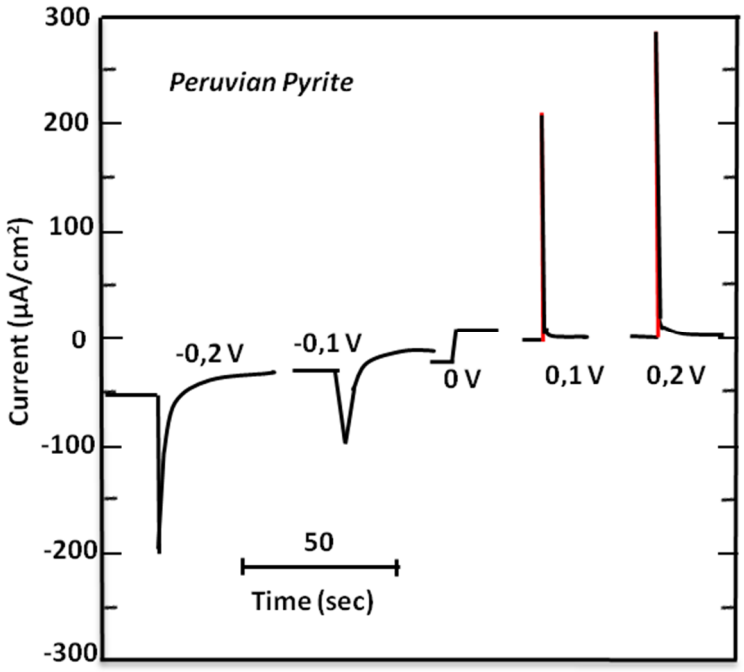

Figure 2.15. Chronoamperometry of pyrite fractured freshly under different applied potentials (Mendriatta,2000).

Tao et al (2003) also used the same technique to investigate oxidation and reduction behavior of five different pyrite samples of different origin.

2.4.5.2 Electrical Impedance Measurements

Impedance measurement is one of the suitable techniques for in- situ investigation of solid/liquid buffer surface. This technique measures surface resistance against electric current passing through the surface as well as the surface resistance dependent on diffusion of ionic charge conductors.

Analysis of experimental data of EIS provides information about physical and chemical process present in the electrode/electrolyte interface, such as charge transfer resistance, which is related to the faradaic current flowing across the interface, and the Warburg impedance, which is related to the diffusion controlled migration (Velasquez,1997).

The electrochemical system can be modelled as resistors, capacitors and inductors (Silverman,1986; Venter,2008). Electrical equivalent circuits (Figure 2.16) are designed and modified until the model circuit fits the test system. Theoretically obtained model does not fully reflect the characteristics mineral surface physically; however reliable data that show change on surface can still be obtained.

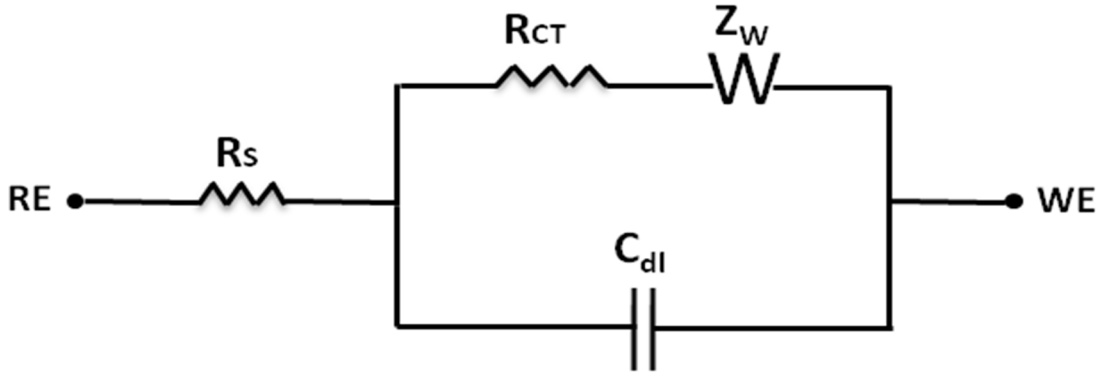

Figure 2.16. An equivalent circuit for an electrochemical cell

Tolley et al (1996) investigated flotation of sulphide minerals by using electrochemical techniques and modified Hallimond Tube. Significant changes were observed in impedance spectrum of fresh grounded chalcocite after addition of ethyl xanthate (Figure 2.17). A quite large increase in Rt value was observed. An increase in flotability of chalcocite is seen as resistance against the current passing through the surface increases. This shows that the xanthate forms a passive layer on chalcocite surface in EX solution and the increase in Rt ve Rp shows that oxidation occurs on chalcocite surface. An increase in the resistance of that passive layer is seen as the oxidation period increases.

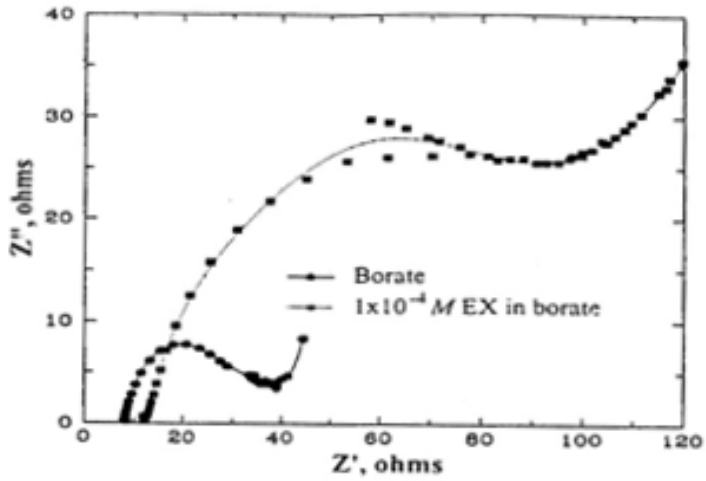

Figure 2.17. Nyquist curve obtained by impedance measurements of chalcocite in 0.05 M borate solution

Velasquez et. al. (1998) investigated chalcopyrite ($CuFeS_2$) obtained from the “El Teniente” mine by electrochemical impedance spectroscopy (EIS) in an alkaline solution for different oxidation potentials. For values lower than 0.4 V vs. SCE, a Randles equivalent circuit model can be used to represent surface modification. However, after 0.4 V vs. SCE surface layer model must be used. Changes were occurred due to the initial formation of a layer of Fe_2O_3 and the inner layer of CuO and Fe_2O_3.

3. MATERIALS AND METHODS

3.1. Fabricating Electrodes

Three different types of electrodes were used in the experiments, namely pure specimen mineral electrode, particle electrode and combined (two minerals) electrode. Pure mineral specimens were supplied from Ward's Natural Science Company.

3.1.1. Pure Specimen Mineral Electrodes

Mineral electrodes are fabricated by using mineral sections of rectangular or cylinder shape cut from high purity specimens. Chalcopyrite, pyrite and galena electrodes were fabricated in order to use electrochemical experiments. Figure 3.1 shows the schematic representation of mineral particle electrodes.

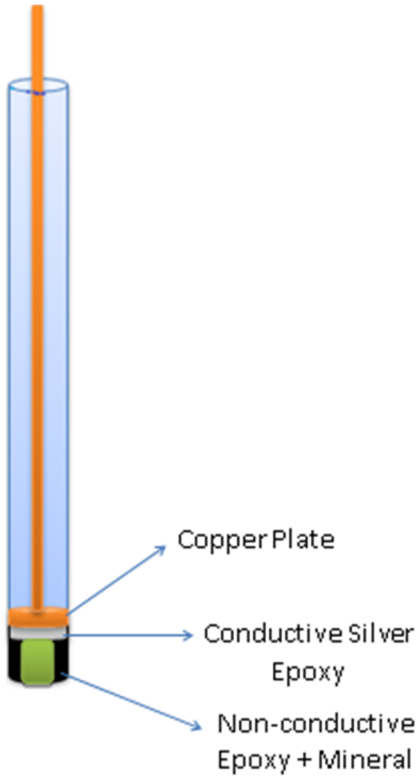

Figure 3.1. Schematic representation of mineral particle electrodes

3.1.2. Particle Electrodes

To fabricate mineral pellet, mineral particles and graphite was mixed in the ratio of 2:1. Graphite powder is used as the conductive matrix in the electrode, as the interaction between collectors and graphite is negligible. A conductive binder is also added to the mixture to increase the strength of the pellet. The mixture was pressed in a die of 14 mm diameter under 200 kN pressure. A cylinder shaped sample of about 15 mm height was produced and copper wire was pasted to the electrode via conductive silver epoxy Figure (3.2a).

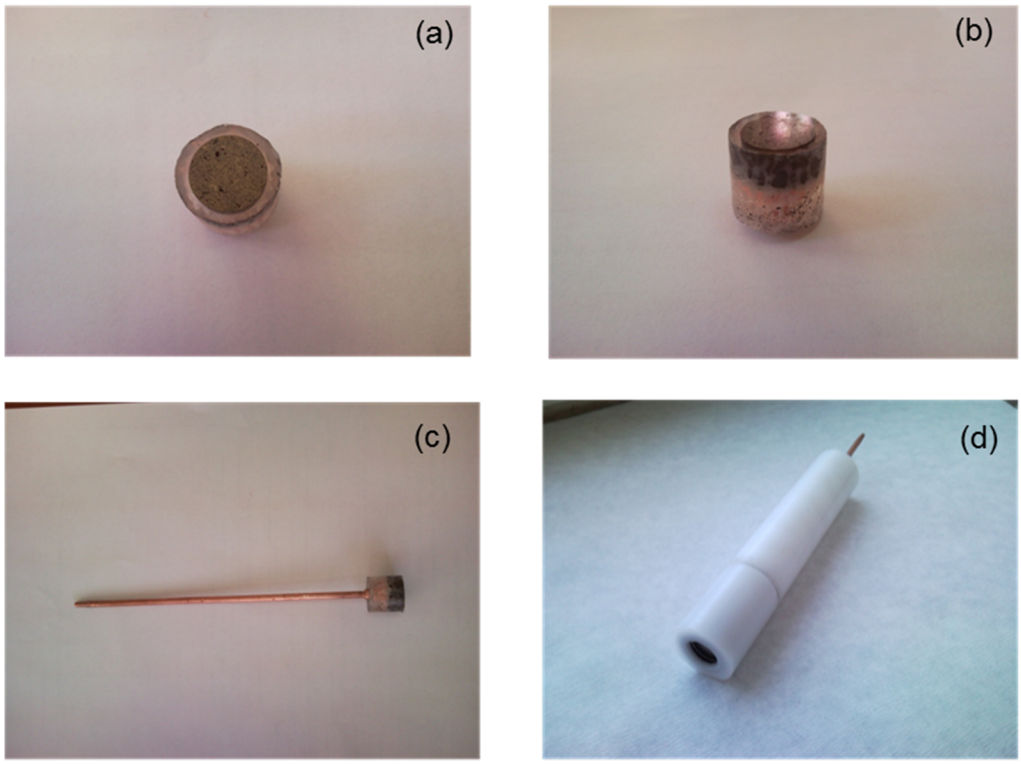

Figure 3.2. Mineral electrode fabricated using particles.

A copper wire is screwed to the mineral electrode section whenever electrochemical measurements were performed (Figure 3.2c). The pellet section can be removed before or after the measurements for mineralogical and surface characterizations. The pellet and the copper wire are mounted in a Teflon tube as shown in Figure (3.2d).

With this design, surface of the electrode can be polished for mineralogical analysis to determine the mineral distribution, their surface area and liberation state. Photo of the chalcopyrite mineral electrode of -20+9 µm size fraction is shown in Figure 3,3. Chalcopyrite particles mounted in graphite matrix are clearly identified and their surface area, which is required for calculation of density of collector adsorption, can be measured easily.

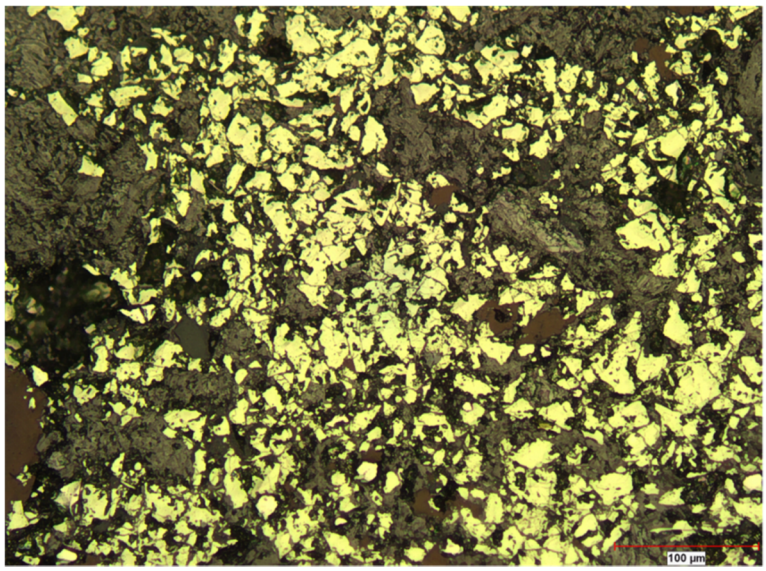

Figure 3.3. Photo of polished surface of the chalcopyrite electrode (-20+9 µm).

3.1.3. Composite Electrodes

Mineral electrodes were fabricated by using chalcopyrite and pyrite sections of different surface areas, as shown in Figure 3.4. Seven electrodes with different surface area ratios were prepared: Cp (100%), Cp(90%)/Py(10%), Cp(80%)/Py(20%), Cp(70%)/Py(30%), Cp(50%)/Py(50%), Cp(30%)/Py(70%), Py (100%). These electrodes are considered to simulate the electrochemical behavior of liberated and composite particles.

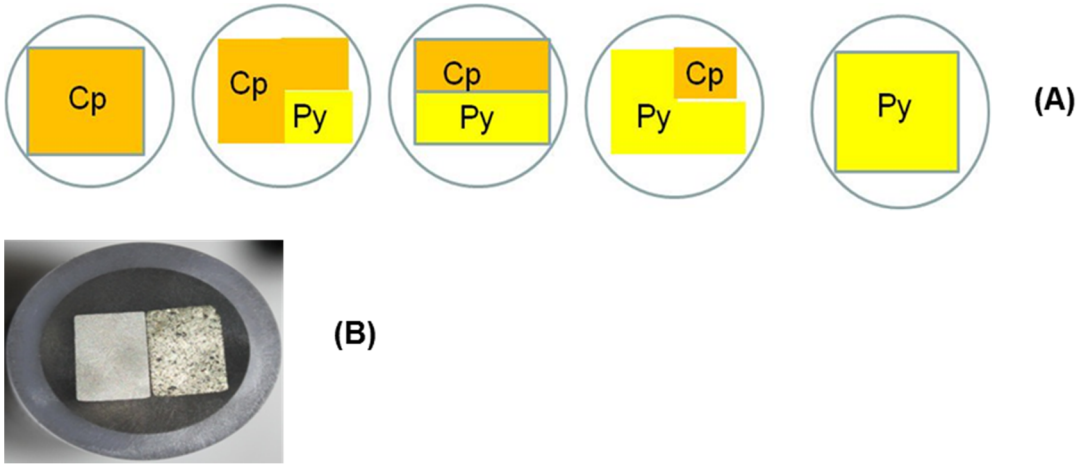

Figure 3.4. (A): Schematic representation of the Cp/Py mixture electrodes. (B): photograph of the Cp(50):Py(50) mixture electrode

3.2 Collectors

Sodium isopropyl xanthate (SIPX) and Sodium diisobutyl dithiophosphinate (DTPI) were used as collectors. DTPI (AEROPHINE 3418A) was supplied from the Cyctec Technology Co. The chemical formulas of collectors were illustrated in Figure 3.5.

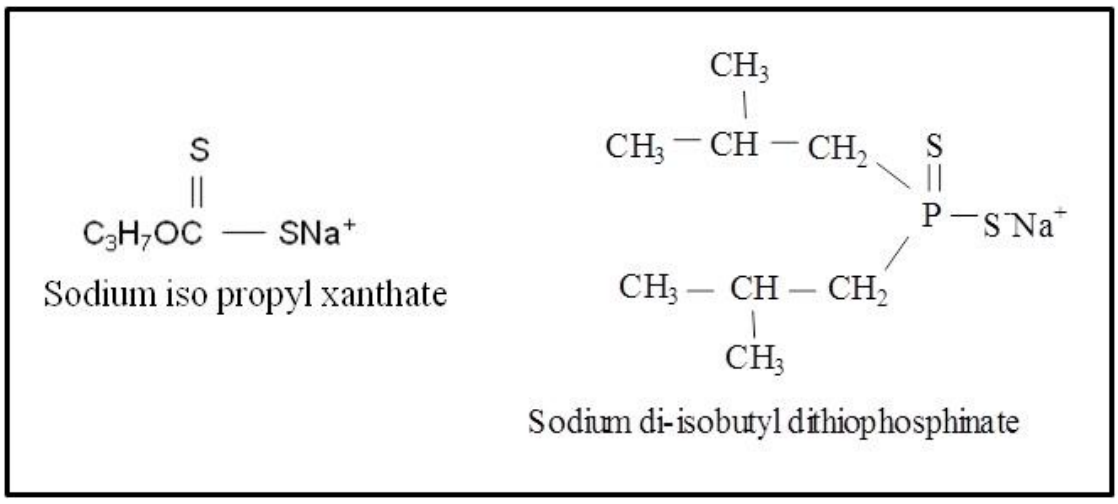

Figure 3.5. Chemical formula of collectors

3.3 Electrochemical Methods

3.3.1. Open Circuit Potential Measurements

Open circuit potential measurements of chalcopyrite, pyrite, galena and platinum electrodes were performed in solutions of pH 9.2 and 11, in the presence of different concentrations of sodium iso-propyl xanthate (SIPX) and sodium di-isobutyl dithiophosphinate (DTPI). The measurement was started in the absence of the collector, and the addition of the lowest dosage (10^{-5} M) of the collector was introduced after a 5 minute stabilisation period. Following a 5 minute measurement period, additional collector was introduced to increase the total dosage incrementally to 10^{-2} M. The measurements were performed in the absence of dissolved oxygen and any other dissolved ions (such as Cu^{2+}, Fe^{2+}, Fe^{3+}, Ca^{2+}, $S_xO_y^{-2}$, SO_3^{-2}, SO_4^{-2}, etc.) which exist in a typical flotation pulp.

3.3.2. Cathodic Stripping Measurements

Cathodic stripping measurements include cathodic stripping voltammetry, differential pulse voltammetry and chronoamperometry methods. This measurement involves the anodic deposition of xanthate, which is followed by stripping through the negative potential scan. According to Faraday's Law, the amount of chemical or electrochemical change in an electrochemical reaction is related to the electrical charge passed through it. The current density, or more precisely, the total charge passed during the cathodic stripping of the collector molecules, gives the required quantitative information about the surface coverage of the collector.

The experiments were performed using chalcopyrite, galena and pyrite electrodes in the presence of different concentrations of both SIPX and DTPI. The electrodes were conditioned for 5 minutes in the open air, in the presence of different concentrations of the collector, and then rinsed with distilled water and transferred into an electrochemical cell for the cathodic stripping experiment.

3.3.3. Electrical Impedance Spectroscopy (EIS)

Electrochemical Impedance Spectroscopy (EIS) measures resistance and conductance of an electrical double layer, as a function of an applied frequency on the mineral surface. The adsorption of the collector molecules on the mineral surfaces changes the form of the electrical double layer, which can be monitored by the measurement of both resistance and capacitance values.

3.3.3.1. Influence of the polarization potential

The adsorption of thiol collectors, particularly xanthate type collectors, occurs at moderately oxidizing pulp potentials, indicating the importance of the surface potential of the minerals in flotation. Consequently, experiments were carried out to investigate whether the changes in composition of the surface layer of chalcopyrite can be detected by EIS or not. Pure specimen chalcopyrite electrode was used. The Chalcopyrite electrode was conditioned for 10 minutes in pH 9.2 buffer solution in the absence and presence of collector. $1x10^{-3}$ M SIPX was used as collector. EIS measurement was performed between the frequency values of 10^{5} – 10^{-3} Hz. DC potential was changed for each experiment from -500 mV to 300 mV. The AC voltage was 7 mV and was kept constant in all of the experiments.

3.3.3.2. Prediction of collector adsorption using EIS

Three sulphide minerals, chalcopyrite, galena and pyrite, and two collectors with different chemical characteristics were used in these tests. The experimental set-up was designed to simulate plant scale measurements, i.e. electrodes were conditioned in the pulp and EIS measurement was taken in a separate electrochemical cell (Figure 3.6). In each experiment, 0.25 g of sample and mineral electrode were conditioned for 10 minutes in a 20 ml solution of collector. The solution was then filtered rapidly using a vacuum filter and the filtrate was analyzed with SHIMADZU Multi-spec-1501 UV Spectrophotometer to determine the residual collector concentration. The characteristic peaks for SIPX were found at 301 nm and 228 nm, while DTPI gave only one characteristic peak at 228 nm. ε constants for each peak were determined separately using the following equation:

$$ABS = \varepsilon \times C \quad (3.1)$$

Both capacitance and resistance values can be used to determine the adsorption of the collector. In this section, resistance values were taken into account. Surface coverage of the collector is directly proportional to the change in the resistance of the electrode surface. The resistance value measured in the absence of the collector was taken as the reference point for zero surface coverage of the collector, and the adsorption was related to the difference between the reading at a given collector dosage and that at zero collector addition.

$$Zreal = Zreal_i - Zreal_0 \quad (3.2.)$$

Where;

$Zreal_i$: resistance measured in the presence of concentration i of the collector.

$Zreal_0$: resistance measured in the absence of the collector.

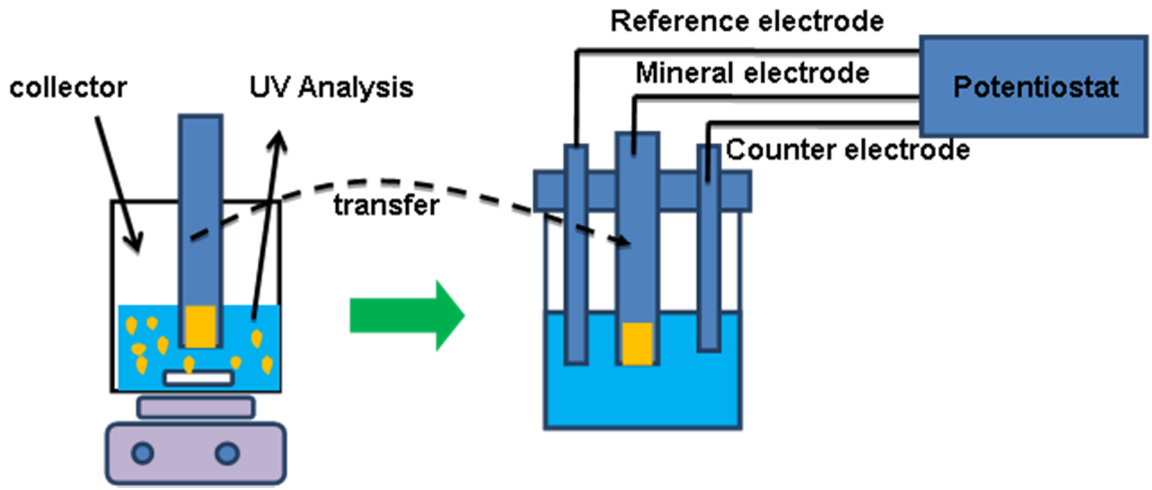

Figure 3.6. Experimental set up of adsorption experiments

The mineral electrode potential was set to 300 mV during the 10 minute conditioning period, but the DC potential was set to OCP during EIS measurement, so as not to change the surface condition during measurement. EIS

measurement was performed between the frequency values of 10^5 – 10^{-3} Hz. The AC voltage was 7 mV and was kept constant in all of the experiments.

3.3.4. Composite Particles

3.3.4.1. Cyclic Voltammetry

Cyclic voltammetry experiments were performed to investigate galvanic interaction mechanism on composite particle surface. These experiments were performed using a conventional three electrode electrochemical cell. A saturated calomel electrode, a platinum plate electrode and a mineral electrode were used as reference, counter and working electrodes respectively.

Two different collectors, sodium iso prophyl xanthate (SIPX) and di iso buthyl dithiophosphinate (DTPI), having different chemical and adsorption characteristics were used in the experiments. The experiments were performed at pH 9.2 using buffer solution of 0.05 M sodium tetra borate. Before each experiment, high purity nitrogen gas was bubbled through the solution in the electrochemical cell for 15 minutes to remove dissolved oxygen. Surface of the mineral electrode was regenerated by using 500 grit silicon carbide paper. Then, the surface of the mineral electrode was cleaned in ultrasonic bath for 1 minute to remove any kind of contaminants prior to the CV experiment and transferred to the cell immediately after washing. Scan rate was determined as 20 mV/sec and all measurements were taken as three cycles.

All the potentials reported in this work were converted to the standard hydrogen electrode (SHE) scale by adding 245 mV to the SCE readings.

3.3.4.2. Electrochemical ımpedance Spectroscopy

EIS measurements of composite electrode were performed in pH 9.2 buffer solution. Electrode surface was cleaned before every experiment by using 500 # SiC paper and placed immediately into electrochemical cell. The frequency range was set to 100000-0.01 Hz and the amplitude value was taken 7 mV rms.

Experiments were carried out in absence and presence of two different collectors. Sodium iso prophyl xanthate (SIPX) and di iso buthyl dithiophosphinate (DTPI) were used in the experiments having different chemical and adsorption characteristics. Electrode was conditioned for five minutes before experiments. Each condition was repeated at least three times for reproducibility.

3.4 Batch Flotation Tests

3.3.5. Preliminary Flotation Tests

Both pure specimen mineral electrode and particle electrode were tested. Pure chalcopyrite specimen and pure chalcopyrite particles (-106 µm) were used as a working electrode. Two different conditioning methods and two different impedance measurements were tested. 100 g/t DTPI was used as a collector. Experimental setup is given in Figure 3.7.

Conditioning Methods:

- Electrodes conditioned in pulp cell and 300 mV (SHE) polarization potential was applied during condition period for 10 minutes.
- Electrode surface was cleaned chemically at -500 mV (SHE) in EC Cell (pH 9.2 buffer solution), then conditioned in pulp cell without polarization for 10 minutes.

Impedance Measurements:

- Measurements were taken in EC Cell
- Measurements were taken in Pulp Cell

The brief information about conditions are given below in Table 3.1

Table 3.1. Preliminary Laboratory Test Results

Electrodes	Conditioning Method	Impedance Measurement Method
Chalcopyrite Specimen Electrode	Polarization (300 mV, SHE) 10 minutes (in pulp)	In EC Cell (pH 9.2 buffer solution)
Chalcopyrite Particle Electrode	Surface Cleaning (-500 mV, SHE) 5 minutes in EC Cell	In Pulp Cell - Çayeli Ore (%33 w)

Figure 3.7. Experimental set up of pulp experiments

3.3.5.2. Batch flotation Tests

Batch flotation experiments were performed in two phases as impedance measurements and flotation experiments. The working electrode was submerged into the flotation cell and conditioned together with the pulp for 3 minutes. Then the

flotation continued, while the electrode taken from the cell for impedance measurement. The Çayeli Cu-Zn sulphide ore was used in laboratory test and the same ore was also used in batch flotation experiments.

Conditioning and Impedance Measurement Procedure

After adding collector in the flotation cell, working electrode was submerged into this cell together with calomel and reference electrodes and it was polarized at 300 mV (SHE) while it was conditioned with the collector for 3 minutes. After conditioning, the electrodes were then placed into the EC cell. During the measurement, DC Volt, amplitude and frequency range were set to open circuit potential, 10 mV and 10000- 0.01 Hz respectively.

The working electrode was electrochemically cleaned in EC cell for 5 minutes at -500 mV (SHE). Then, the electrode was conditioned without polarization, in flotation cell with the collector. Subsequently, the electrode was taken back to pH 9.2 solution. During the measurement, DC Volt, amplitude and frequency range were set to open circuit potential, 10 mV and 10000- 0.01 Hz respectively.

The pulp in the batch flotation cell was pumped into the pulp cell by a peristaltic pump and the collector was supposed to be reached to the cell after two minutes. Then, the working electrode was placed into the pulp cell and polarized at 300 mV for 3 minutes. Impedance measurement was taken in the pulp cell.

Flotation Procedure

The flotation tests were performed using Çayeli Cu-Zn sulphide ore. 1.15 kg of sample was ground to 80% -36 µm at 60% pulp density. The ground material was then the transferred into a 3 lt cell and the pulp volume was adjusted to 30% w/w density by water addition. The flotation tests were performed in a modified Leed flotation cell at 1200 rpm and 3 lt/min air flow rate. A di-isobutyl dithiophosphinate type collector (Aerophine 3418A) was used in the experiments at pH 11.5, at collector dosages of 30, 50 and 100 g/t. Two stages of cleaning were applied to the rougher concentrate to obtain a final concentrate of 25 % Cu grade. The majority of the minerals in the final concentrate were assumed to be recovered

mainly by true flotation. Therefore, the surface coverage of the collector, as measured by EIS, can be related to the flotation recovery. In the EIS measurements, a chalcopyrite mineral electrode was used. Conditioning of the electrode was performed in the cell and the impedance measurement was taken in the electrochemical cell. Experimental set up was given in Figure 3.8.

Figure 3.8. Picture of experimental set up of flotation tests

4. RESULTS

4.1. Open Circuit Measurements (OCP)

The OCP measurements of galena, chalcopyrite, pyrite and platinum in the presence of the different concentrations of SIPX at pH 9.2 are illustrated in Figure 4.1. The results showed that the OCP values of all the electrodes decreased gradually as a function of increasing collector concentration.

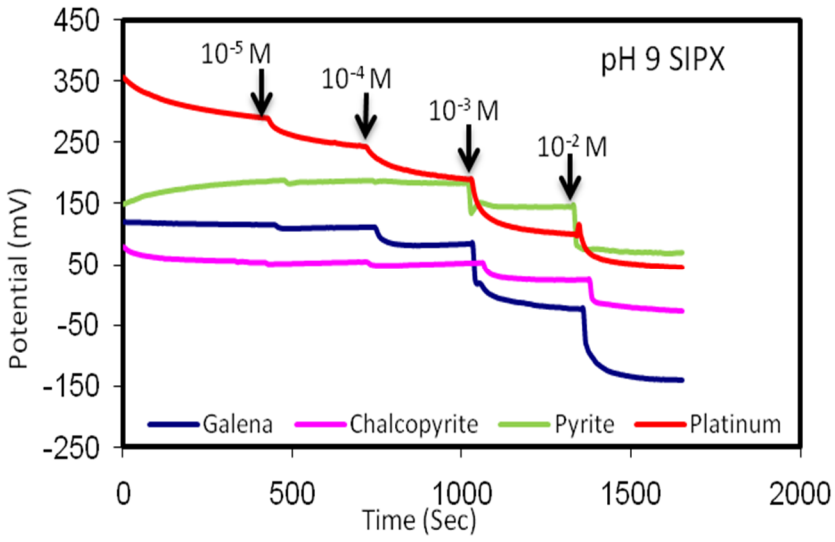

Figure 4.1. Open Circuit Potential measurements at pH 9.2 and various concentrations of SIPX.

It is very well known that the adsorption of xanthate occurs through various anodic reactions, depending on the structure of the mineral surface:

$$X^- \rightarrow X_{ads} + e^- \quad (4.1)$$

$$2X^- \rightarrow X_2 + 2e^- \quad (4.2)$$

$$MS + 2X^- \rightarrow MX_2 + S^0 + 2e^- \quad (4.3)$$

$$MS + 2X^- + 4H_2O \rightarrow MX_2 + SO_4^{2-} + 8H^+ + 8e^- \quad (4.4)$$

Therefore, the adsorption of the collector resulted in a decrease in open circuit potential due to the flow of electrons towards the mineral phase. In order to demonstrate the relationship between the collector addition and the OCP values, the absolute change in OCP was calculated by subtracting the potential readings in the absence of the collector from those done in the presence of the collector.

$$|\Delta E| = E_2 - E_1 \qquad (4.5)$$

where

E_2=open circuit potential in the presence of the collector
E_1 =open circuit potential in the absence of the collector

The greater the decrease in the OCP, the more collectors was adsorbed at the surface. The absolute differences of the OCP measurements, upon the addition of the collector, are illustrated in Figure 4.2 as a function of the collector dosage. The highest difference was observed with the platinum and the galena electrodes, indicating more collector adsorption. The differences at the low collector dosages, those at which flotation plants are usually operated, were negligible, but at collector dosages greater than 10^{-4} M, the change in ΔE was almost linear, as a function of the SIPX concentration.

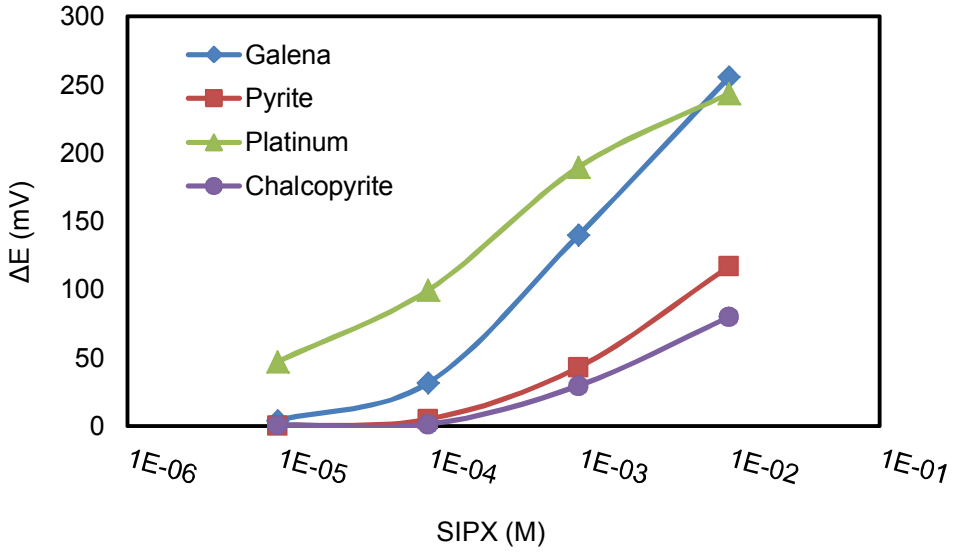

Figure 4.2. The absolute differences in the OCP of various electrodes as a function of the SIPX concentration.

Similar tests were performed with sodium di-isobutyl dithiophosphinate (DTPI) as the collector (Figure 4.3). There was no change in the response of the electrodes at low collector dosages and some very small reductions were noted with the platinum and the galena when compared to the trends observed with the SIPX. This was attributed to the differences in the adsorption mechanisms of SIPX and DTPI on sulphide minerals. While SIPX is adsorbed through an electrochemical reaction, DTPI adsorption is observed in the form of an electrochemical-chemical reaction [1](Guler, et al., 2004).

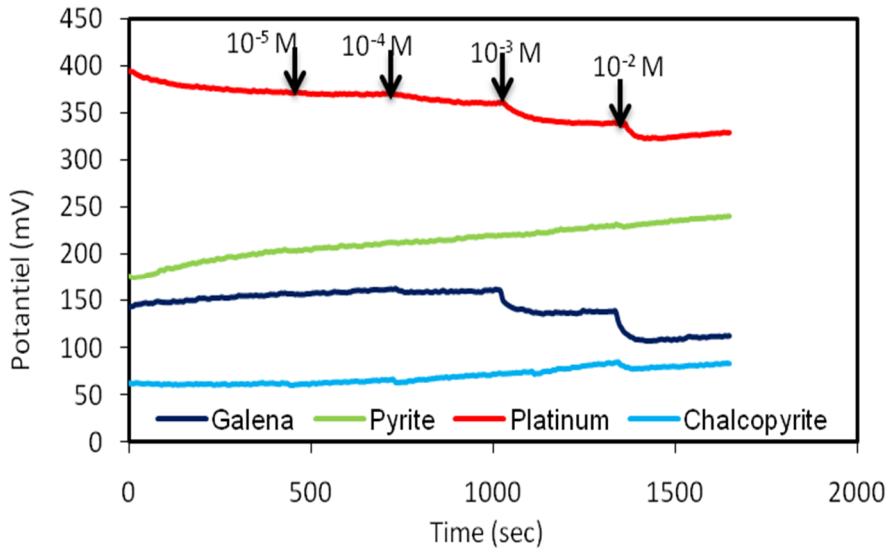

Figure 4.3. Open Circuit Potential measurements at pH 9.2 and various concentrations of DTPI.

Similar measurements were taken at pH 11 with both SIPX and DTPI. However, there was no meaningful response of the electrodes to the addition of the collectors at this pH (Figure 4.4). This was attributed to less dimer formation and lower surface coverage of the collectors at the mineral surface. However, it must be noted that the flotation of chalcopyrite is performed at this pH with high recoveries. Therefore, rest potential measurements can be an indicator of the

[1] A chemical step is a step where there is no electron transfer either to or from the electrode. Such a step does not of itself produce a charge flow into or out of the electrode and thus is not directly observable by an external measuring circuit. It may however influence the charge flow because of other steps in the mechanism which can be detected indirectly. The chemical step is not influenced directly by the electrode potential. An electrochemical step, on the other hand, involves electron flow to and from the electrode, and as such produces a flow of charge which can be monitored by the external measuring circuit.

most suitable electrochemical conditions for maximum recovery, though not of the amount of surface coverage of the collector in flotation.

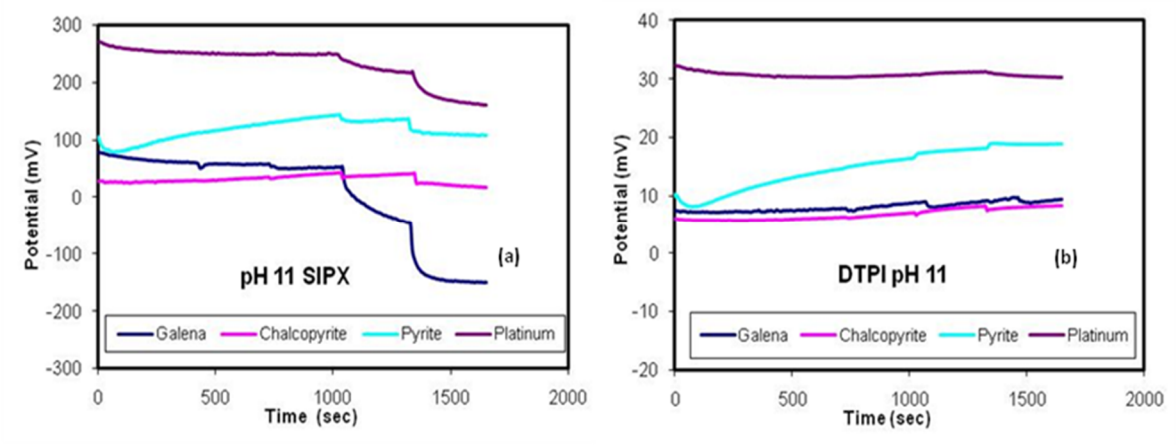

Figure 4.4. OCP measurements in pH 11 and various concentrations of DTPI and SIPX

4.2. Cathodic Stripping Measurements

The adsorption of collectors on the sulphide minerals is considered to occur through both an electrochemical and chemical mechanism. Similarly, the desorption of the collector from the mineral surface should also be electrochemical in nature. In these experiments, the mineral electrodes were conditioned in the presence of the collector at various dosages and potentials. Next, the adsorbed collector was stripped from the surface at cathodic potentials to determine the density of the collector adsorption (Figure 4.5). Three different techniques were employed for this purpose: voltammetry, differential pulse voltammetry and chronoamperometry.

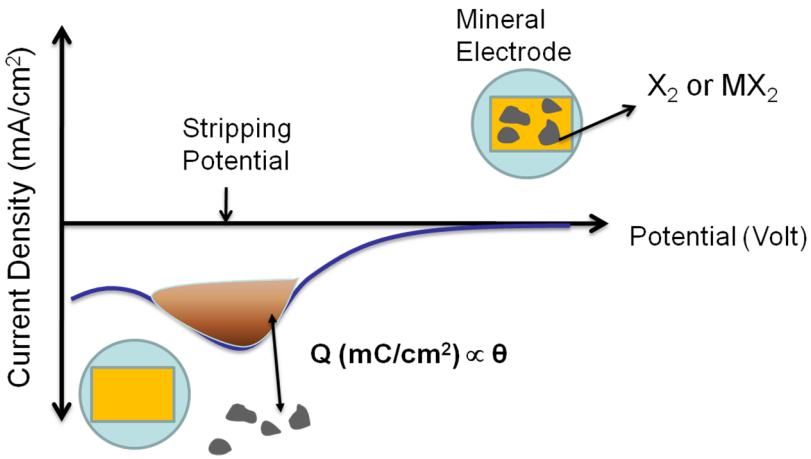

Figure 4.5. Schematic illustration of the cathodic stripping of the collectors.

4.2.1 Cathodic Stripping Voltammetry

The results of the cathodic stripping voltammetry experiments of chalcopyrite are given in Figures 4.6 and 4.7 for SIPX and DTPI respectively.

No cathodic peak was observed in the range studied, when the surface of chalcopyrite was free of the oxidised species. However, after the addition of the collector, a cathodic peak appeared at about -350 mV showing a reduction of the collector species at the surface. Similar responses were obtained with both SIPX (Figure 4.6) and DTPI (Figure 4.7). The current density of the reduction peak would be expected to increase with increasing collector concentration in the solution as the surface coverage of the collector is increased. However, contrary to the results reported in the literature, the current intensity of the reduction peak decreased with an increase of the collector concentration. This was attributed to multilayer adsorption of the collector, which increased the effect of mass transport i.e. the diffusion of the reduced collector ions away from the electrode surface during the cathodic scan. In addition to that finding, no difference could be detected between the 10^{-5} M and 10^{-4} M dosages.

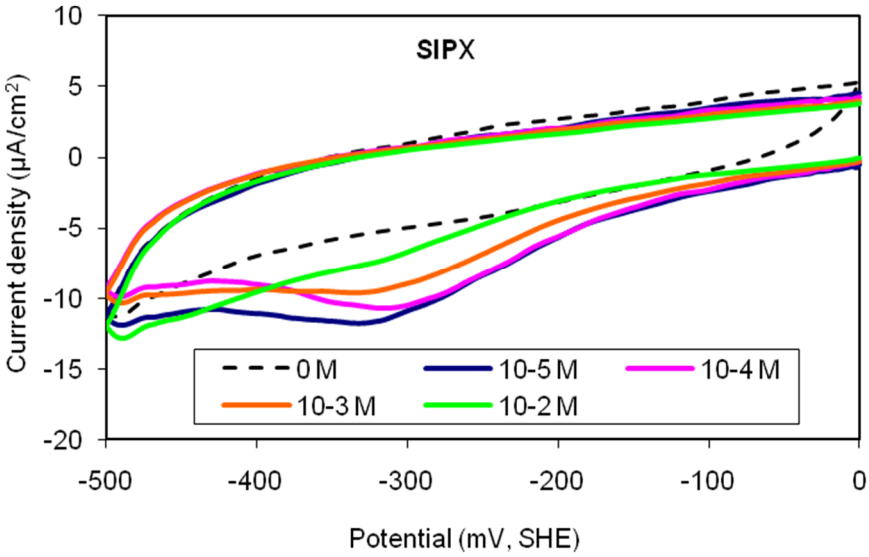

Figure 4.6. Cathodic stripping voltammetry of chalcopyrite in the presence of different concentrations of SIPX.

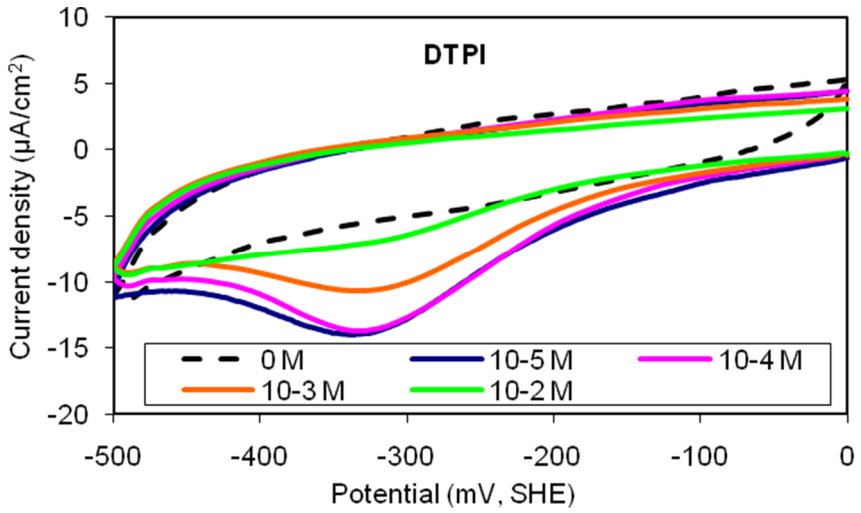

Figure 4.7. Cathodic stripping voltammetry of chalcopyrite in the presence of different concentrations of DTPI.

In the case of pyrite, the reduction peak of xanthate shifted towards the anodic values by 50 mV (Figure 4.8). In spite of that it was quite plausible to relate the current density of these peaks solely to the reduction of the xanthate species. A

distinguishable cathodic peak was only observed with a very high collector dosage.

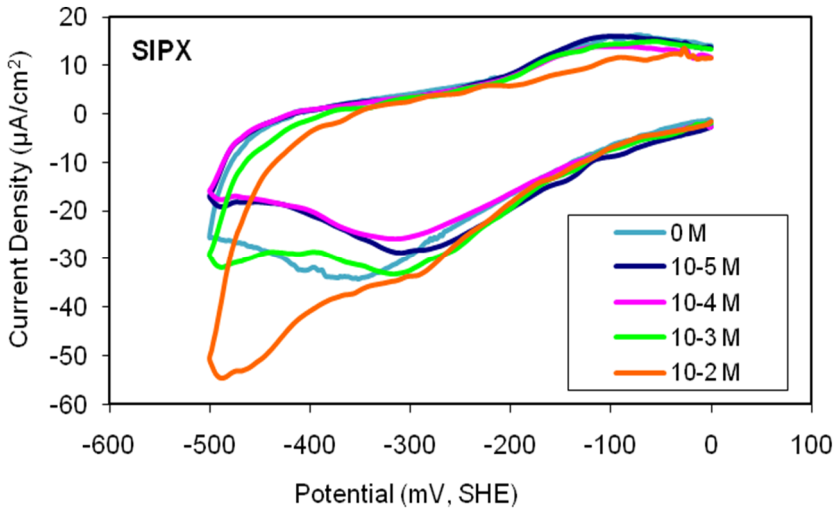

Figure 4.8. Cathodic stripping voltammograms of pyrite in the presence of different concentrations of SIPX.

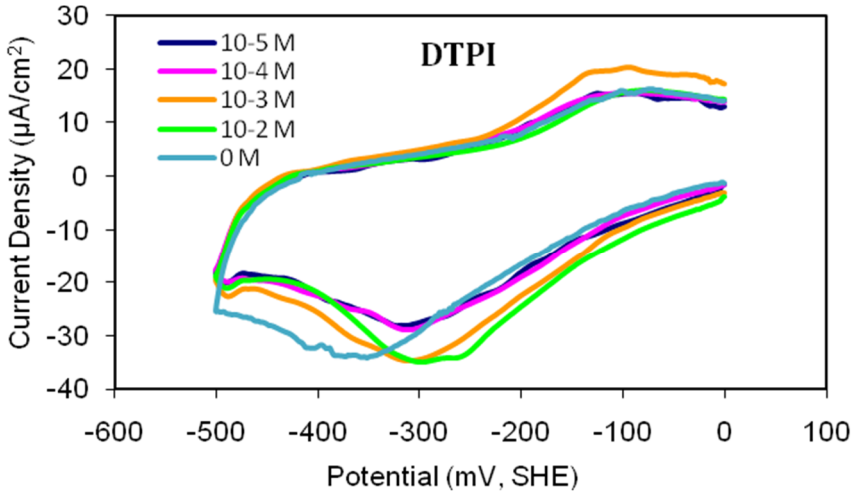

Figure 4.9. Cathodic stripping voltammograms of pyrite in the presence of different concentrations of DTPI.

In the case of DTPI, no collector adsorption was expected on the pyrite surface. The current intensities of the cathodic peaks were almost the same for all concentrations tested (Figure 4.9). This correlates well with the previous observations, as DTPI does not adsorb on the pyrite.

4.2.2. Differential Pulse Voltammetry (DPV)

This technique is extremely useful for measuring trace levels of organic and inorganic species adsorbed at the electrode surface. It is applied to measure the differences in adsorption at low collector dosages. Figure 4.10 shows that DPV is very successful at low collector dosages and the difference between the 10^{-5} M and 10^{-4} M SIPX dosages could be measured. However, the trend of variation in the current density was the same as that observed with cathodic stripping voltammetry. The current density decreased at higher dosages of the collector. This was attributed to the multilayer adsorption of the collector and to a lower rate of diffusion, which resulted in an electrochemically passive layer. By using rotating disc electrodes, dynamic voltammetry may be useful in removing the reduced species from the surface and in observing the Faradic process at work.

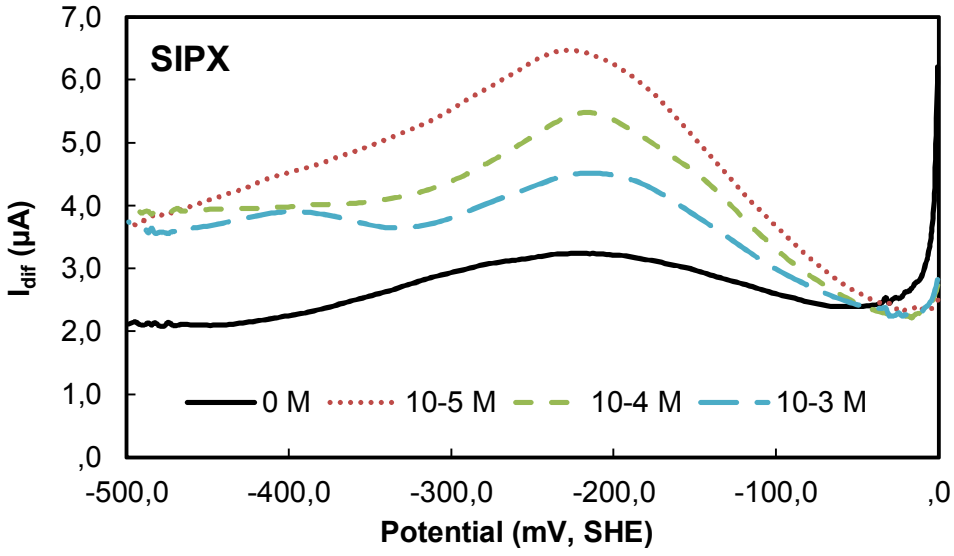

Figure 4.10 Differential pulse voltammetry of chalcopyrite in the presence of different SIPX concentrations.

Similar experiments were performed with galena and the results are illustrated in Figure 4.11. As a base line, a straight horizontal line was obtained in the absence of the collector. When 10^{-5} M SIPX was added into the solution, a small desorption peak was observed at the 150 mV potential. This peak corresponds to the desorption of the chemisorbed xanthate species at the low collector concentration. At the higher concentration (10^{-4} M), the current of the peak increased. However, when the concentration was increased to 10^{-3} M, the potential of the peak shifted to more negative values (-350 mV), possibly due to the reduction of dixanthogen which can form easily at high collector concentrations. The current intensity of the same peak increased considerably at a 10^{-2} M SIPX.

The results of the experiments performed with the galena electrode in the presence of DTPI are given in Figure 4.12. No noticeable peak could be obtained with DTPI. This was probably due to the differences in the adsorption mechanisms of SIPX and DTPI on galena. Adsorption of DTPI is observed in the form of surface passivation rather than a new peak formation. Therefore, in the given potential range, no reduction peak was observed on galena, which means that the surface is covered with the adsorbed collector species even at reducing potentials. Moreover, the electrochemical techniques, based on the measurement of the current intensity of the collector reduction peak, seem to be ineffective with collectors like DTPI.

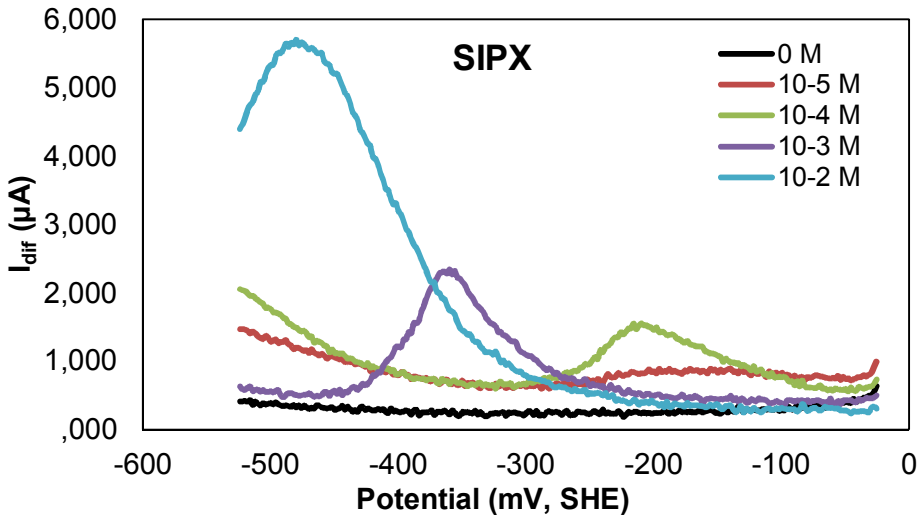

Figure 4.11. Differential pulse voltammetry of galena in the presence of different SIPX concentrations.

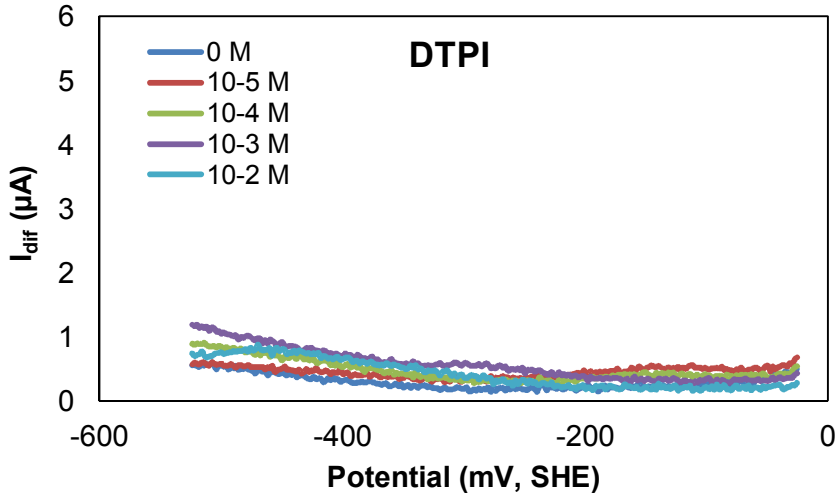

Figure 4.12. Differential pulse voltammetry of galena in the presence of different DTPI concentrations.

4.2.3. Chronoamperometry

This technique involves the stepping of the potential of the working electrode from a potential at which no Faradic reaction occurs to a potential at which the surface concentration of the collector is effectively zero. The resulting current-time dependence is monitored. Mass transport under these conditions is by diffusion and the current-time curve reflects the change in the concentration gradient in the vicinity of the surface (Figure 2.14). This involves a gradual expansion of the diffusion layer associated with the depletion of the reactant, i.e. the collector in this case.

The resulting current is measured as a function of time for the various dosages of the collector addition. Integration of the current density gives the total charge passed due to collector adsorption. The potential was set to the peak of the collector reduction (i.e. -300 mV for chalcopyrite) and the variation in the reduction current was measured as a function of time.

Before starting the chronoamperometry experiments, cyclic voltammetry of chalcopyrite was performed at different anodic switching potentials, to determine the formation and decomposition potentials of SIPX at the surface of the chalcopyrite electrode. The results showed clearly that the decomposition potential

of copper xanthate and dixanthogen was about -300 mV potential (Figure 4.13).Subsequently, chronoamperometry experiments were performed at different set potentials to confirm the required potential for desorption of xanthate from the surface. In the first part, the formation of copper xanthate occurred. This was achieved by using different set potentials as indicated in the legend (Figure 4.14). In the second part, the potential value was changed to the xanthate desorption potential and the resultant current-time curves were recorded. The area under the current-time curves was calculated, and reported as the charge density due to xanthate desorption. The relationship between the applied potentials for adsorption and the difference in the charge density is given in Figure 4.15a. The results showed that the density of collector coverage increased at the adsorption stage when the applied potential was increased to 400 mV.

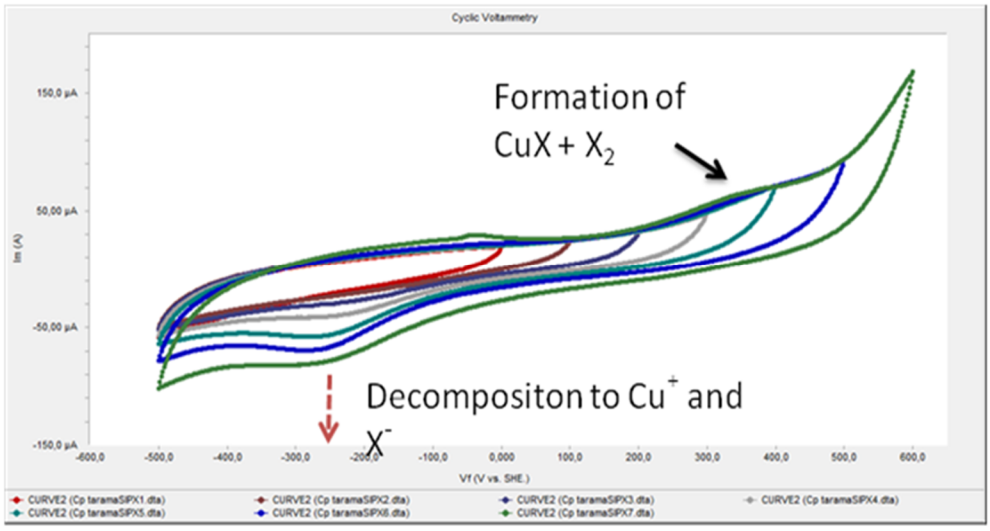

Figure 4.13. Cyclic voltammetry experiments at different anodic switching potentials in pH 9.2 and $1x10^{-3}$M SIPX

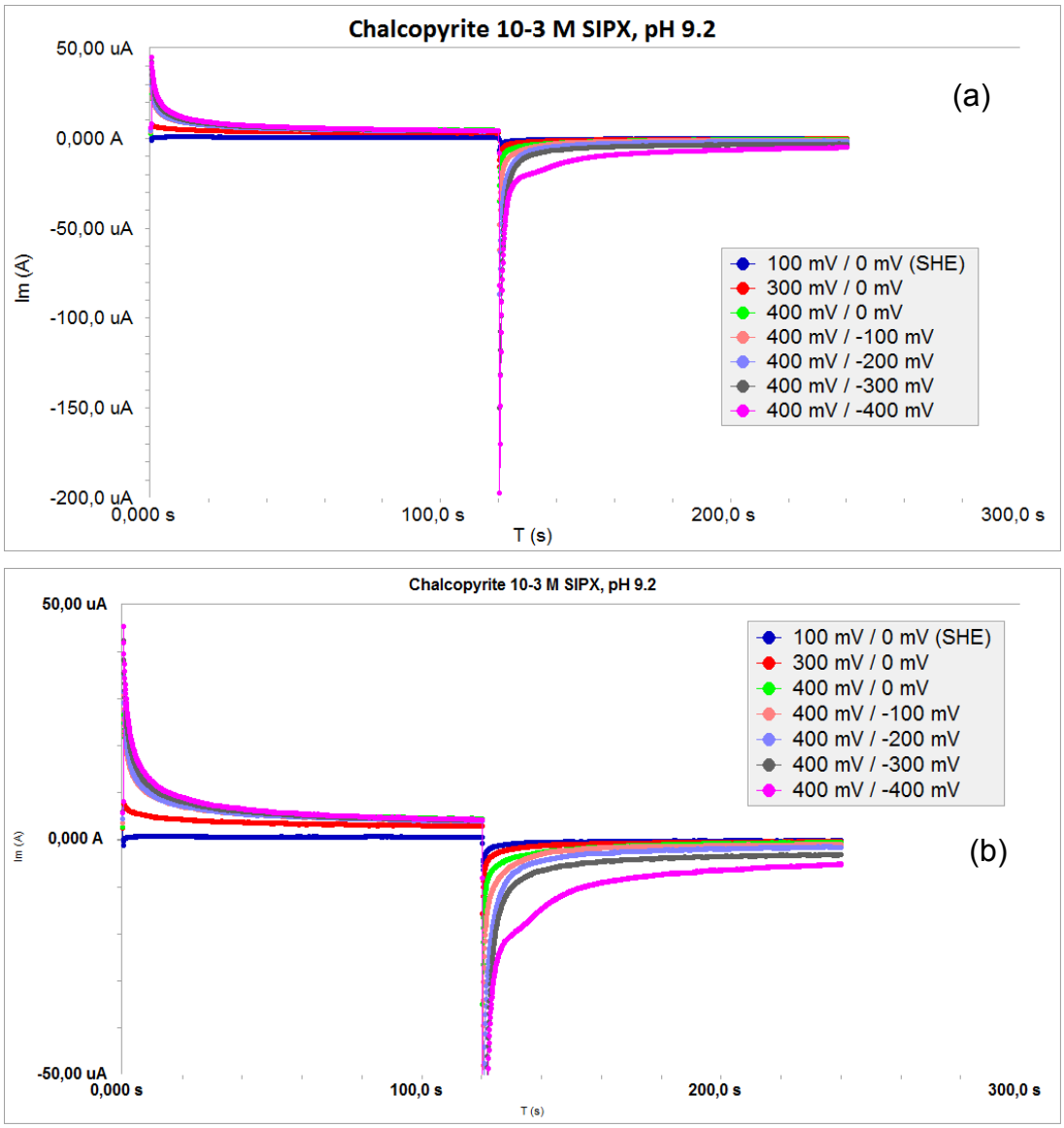

Figure 4.14. Chronoamperometry measurements at different adsorption and desorption potentials for chalcopyrite at pH 9.2 and 10^{-3} M SIPX.

Figure 4.15b shows the charge difference between the adsorption at 400 mV and the desorption at different set potentials. As shown in the figure, the collector could not be removed from the chalcopyrite surface at 0 mV potential, since the charge difference is almost equal to the adsorption charge. However, as the values of desorption potential were decreased to more negative values, the charge difference decreased and became zero at -300 mV, which is the desorption potential observed with the cyclic voltammetry of chalcopyrite (Figure 4.13). At higher negative potentials, the charge difference became negative, indicating the desorption of the collector from the mineral surface.

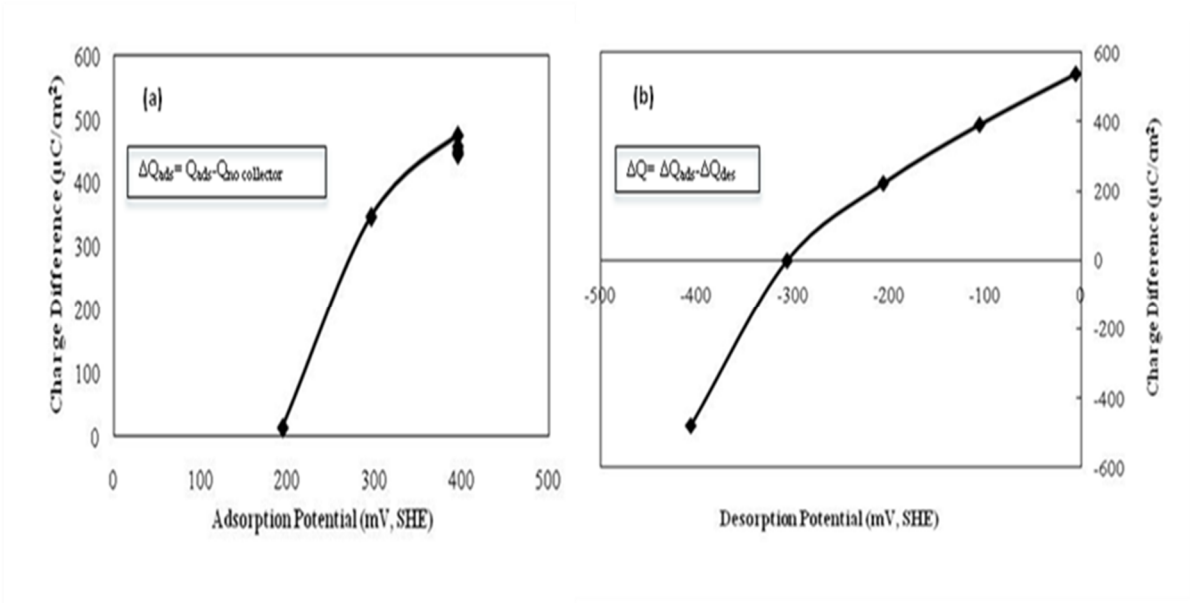

Figure 4.15. The relationships *b*etween (a) applied potentials for adsorption and the difference in the charge density and (b) the charge difference between the adsorption at 400 mV and the desorption at different set potentials.

Similar experiments were performed with the galena electrode in the presence of both SIPX and DTPI. After the adsorption of the collector, linear sweep voltammetry was performed to determine the required desorption potential for SIPX and DTPI (Figure 4.16). The voltammograms showed clearly the desorption potential for both collectors, which was about -600 mV. The set potential for the galena electrode was therefore adjusted to -650 mV; slightly below the peak potential. In addition, the difference between the current density of the curves for SIPX and DTPI is very large. This was attributed to the differences in the adsorption mechanisms of these collectors, as explained previously.

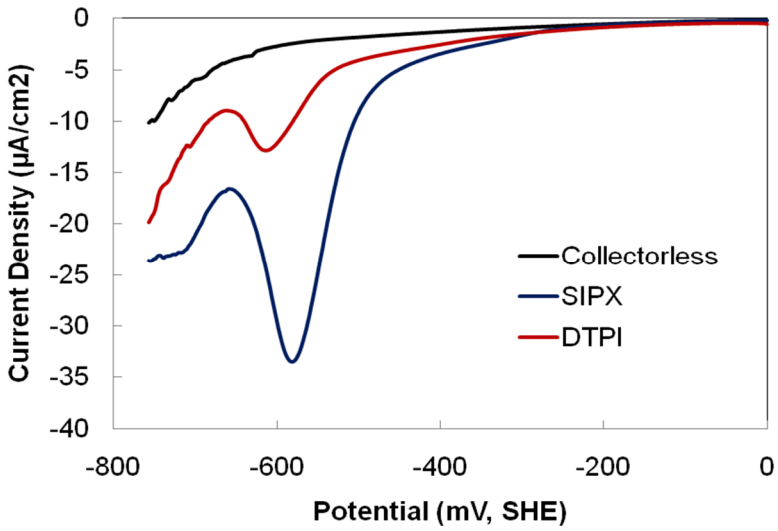

Figure 4.16. Voltammetry of the galena electrode in the absence and presence of collectors (pH 9.2, 10^{-3}M DTPI, 10^{-3}M SIPX).

The charge densities measured in the desorption potential were plotted as a function of the collector concentration in Figure 4.17. Similar responses were obtained with chalcopyrite and galena in the presence of SIPX. The negative charge density resulting from the desorption of the collector increased with higher collector dosages, indicating a higher density of collector adsorption on the mineral surfaces.

However, the decrease in the charge density was considerably lower with DTPI compared to SIPX. This was attributed to the different adsorption mechanism of DTPI, which involves electrochemical-chemical (EC) reactions. Hence, the electrochemical response with DTPI was considerably lower than that of xanthate and almost negligible at low concentrations.

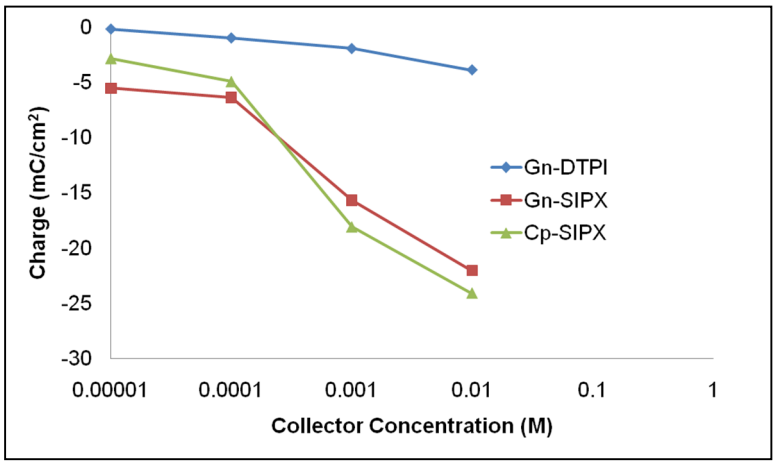

Figure 4.17. The relationship between the charge density and the collector concentration at desorption potential (pH 9.2, 10^{-3} M SIPX, 10^{-3} M DTPI).

4.3 Electrochemical Impedance Spectroscopy (EIS)

When an electrode is placed in an electrolyte, an electrical double layer forms due to the rearrangement of the charges, ions and dipoles at the electrode/electrolyte interface. The double layer represents two charged layers: the electrode surface, and the layer consisting of hydrated ions, i.e. the Helmholtz Plane (Figure 4.18).

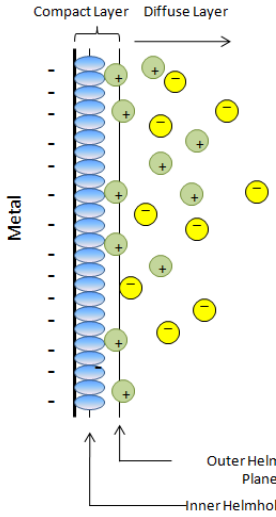

Figure 4.18. Schematic of electrical double layer.

The electrode surface and the Helmholtz Plane are assumed to have equal and opposite charges, maintaining the electrical neutrality. Hence, the electrical double layer is simulated by a capacitor model. The basic characteristic of such a capacitor is its electrical capacitance, which can be measured by various electrochemical techniques. Double layer capacitance (C_{DL}) measurements can provide information on the adsorption, desorption, film formation and degradation of organic coatings.

Electrochemical Impedance Spectroscopy (EIS) is a very versatile electrochemical tool to characterize the intrinsic electrical properties of any material and its interface. The basis of EIS is the analysis of the impedance (resistance of alternating current) of the observed system when subjected to the applied frequency and exciting signal. This analysis provides quantitative information about the conductance, the dielectric coefficient and the static properties of the interfaces of a system, as well as its dynamic change due to adsorption or charge-transfer-phenomena.

Since the sulphide minerals are semiconductors, their surface characteristics are influenced by two types of processes: Faradaic and non-Faradaic. Faradaic processes involve the transfer of charge across the interface causing either oxidation or reduction. Non-Faradaic processes do not involve charge transfer but instead develop resistance to the transfer of electrons due to polarization. Such a resistance is known as charge transfer (R_{CT}), or polarization (R_P) resistance. Therefore, an electrode-solution interface consists of a parallel combination of charge transfer resistance (R_{CT}), double layer capacitance (C_{DL}) and also the solution resistance and capacitances present in an electrochemical system. This is independent of the mechanism of collector adsorption, albeit chemical or electrochemical. Consequently, the changes in the resistance and conductance of the electrical double should be able to be related to the adsorption of the collector, as this adsorption should result in an electrochemically passive layer which increases the resistance and decreases the conductance.

4.3.1 Influence of the Polarization Potential

The influence of polarization potential was investigated using chalcopyrite in the presence and absence of SIPX (Figures 4.19 and 4.20). The Nyquist plot of the EIS results, performed in the absence of SIPX, showed that the changes in composition of the surface layer of chalcopyrite can be detected by EIS. Resistivity of the surface increased at low potentials due to the formation of sulphur based species. At high potentials, on the other hand, the formation of metal hydroxyl species (such as $Fe(OH)_3$, $Cu(OH)_2$, etc.) increased the conductance (higher Z_{imag}) of the surface.

The adsorption of SIPX on chalcopyrite was distinguished clearly at polarization potentials of 200 mV and 300 mV (Figure 4.20). It is well known that xanthate adsorption occurs through electrochemical reactions which require anodic electrode potentials higher than the reversible potential of an xanthate oxidation reaction. This means that xanthate does not adsorb at potentials lower than approximately 0 mV. Therefore, the lowest resistivity (highest Z_{real} values) should have been observed at -500 mV, but they were, in fact, at 100 mV (Figure 4.20). As was shown in Figure 4.19, the form of the surface species changed depending on the polarization potential in the absence of the collector. Therefore, in order to avoid misinterpretation of the data, a comparison should be done of the resistance and conductance values, taken at the same polarization potentials.

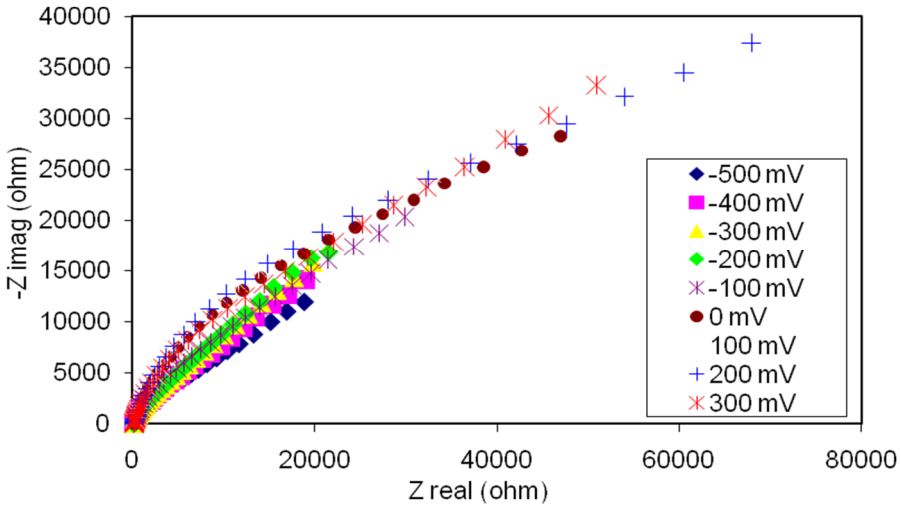

Figure 4.19. Nyquist plots for chalcopyrite at various polarization potentials in the absence of SIPX.

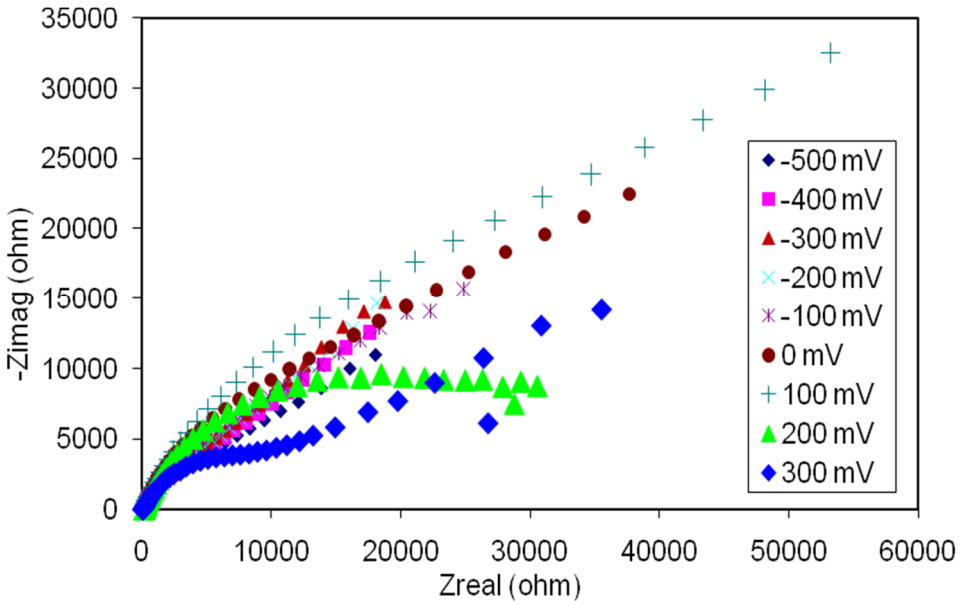

Figure 4.20. Nyquist plots for chalcopyrite at various polarization potentials in the presence of 10^{-3} M SIPX.

Figure 4.21, showing the comparison of the Nyquist plots of the chalcopyrite electrode at the same polarization potential, indicates clearly the required potential for SIPX adsorption. While the curves in the presence and absence of SIPX overlap at reducing potentials, there was a clear difference at potentials higher than 0 mV, showing that the adsorption of SIPX increased gradually at higher potentials.

After completing the experiments investigating the use and accuracy of the EIS technique to determine the adsorption of collectors, combined adsorption-EIS measurement experiments were performed to quantify the collector adsorption and to establish the relationship between the surface coverage of the collector and the EIS readings of resistivity and conductance.

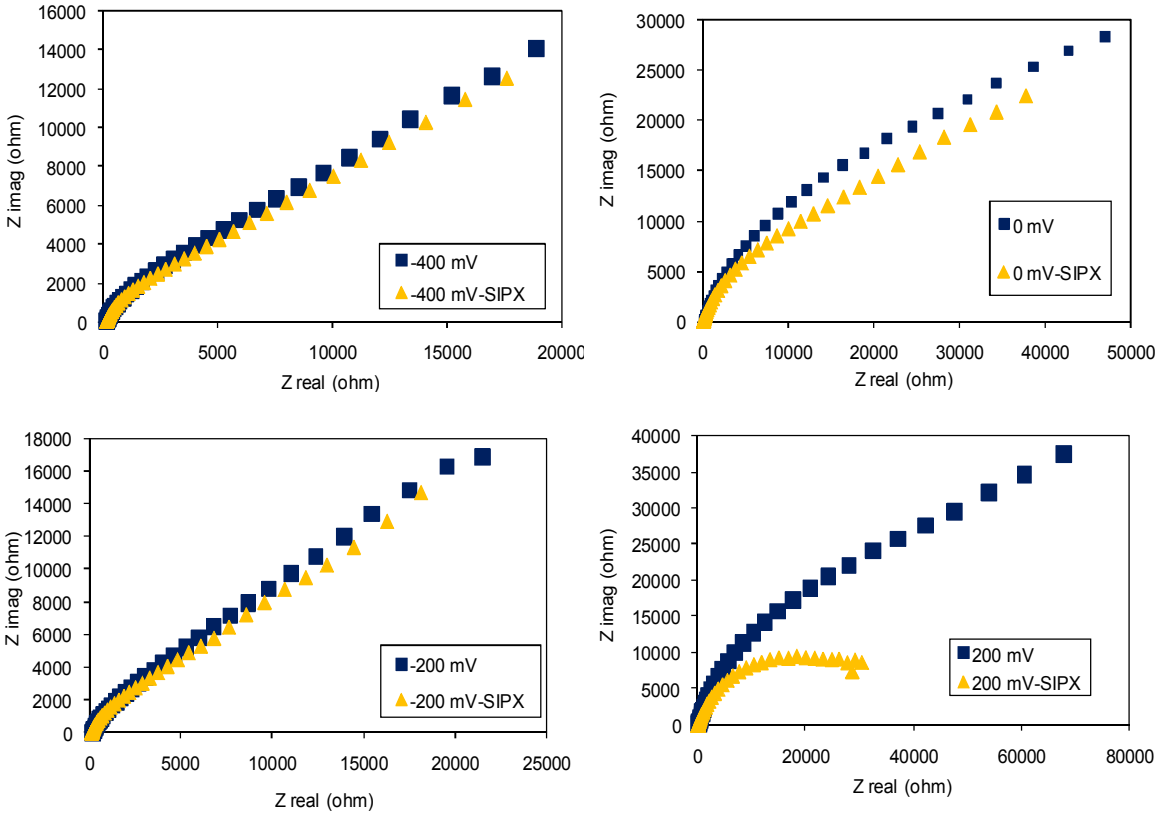

Figure 4.21. Nyquist plots for chalcopyrite at different polarization potentials in the absence and presence of 10^{-3} M SIPX.

4.3.2. Prediction of Collector Adsorption Using EIS

As was discussed in the previous section, the adsorption of the collector was achieved at potentials higher than 0 mV, indicating slightly oxidizing potentials. In this section, the results of experiments performed at a 300 mV polarization potential are presented.

4.3.2.1. Chalcopyrite

4.3.2.1.1. Adsorption of Sodium Isopropyl Xanthate (SIPX)

The EIS spectra of the chalcopyrite electrode in the presence of different concentrations of SIPX are illustrated in Figure 4.22 and Figure 4.23, referencing the Nyquist and Bode plots respectively. The addition of SIPX decreased the

capacitance (i.e. increased resistance) of the electrode surface as a function of the collector dosage.

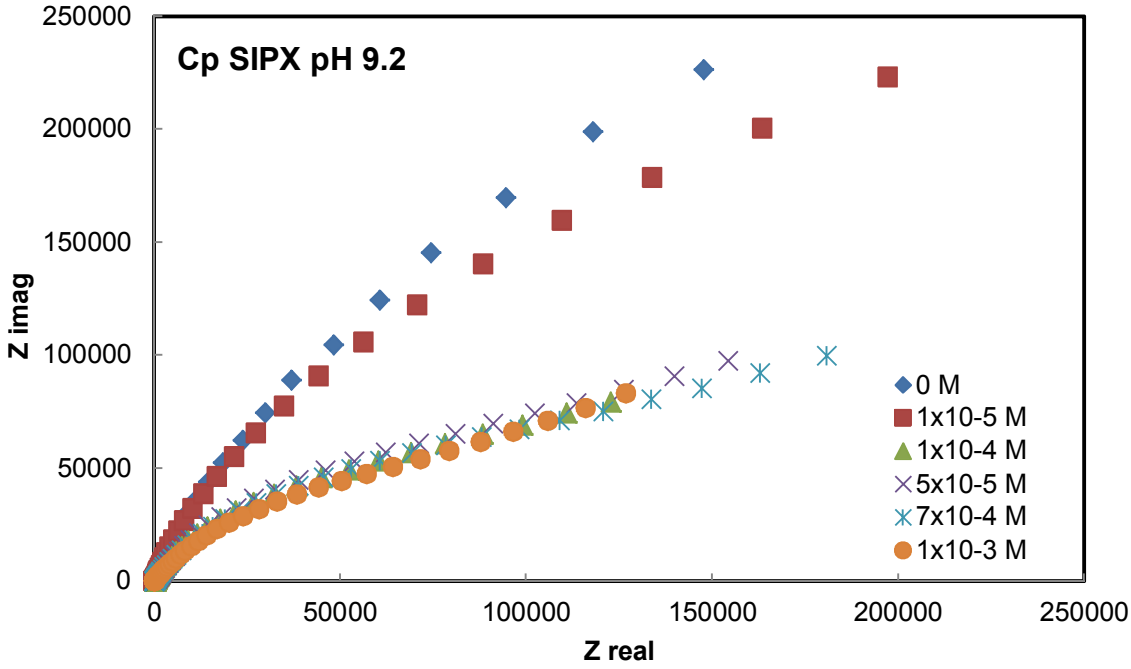

Figure 4.22. Nyquist plot of the impedance spectra of chalcopyrite in the presence of different concentrations of SIPX.

In the Bode plot, variations in the Z_{real} and phase angle were plotted as a function of applied frequency. The differences in the resistivity (Z_{real}) were clearly observed in the medium frequency range (i.e. between 1 Hz and 10 Hz). The maximum value of the phase angle was observed in this region. In the presence of low collector dosages, the maximum phase angle of the experiments was almost the same, but at excess dosages (i.e. $1x10^{-3}$ M) it shifted towards a higher frequency range. This was obviously due to the changes in the structure of the double layer. This observation suggests that a different model may be required to fit the data at low and high collector dosages.

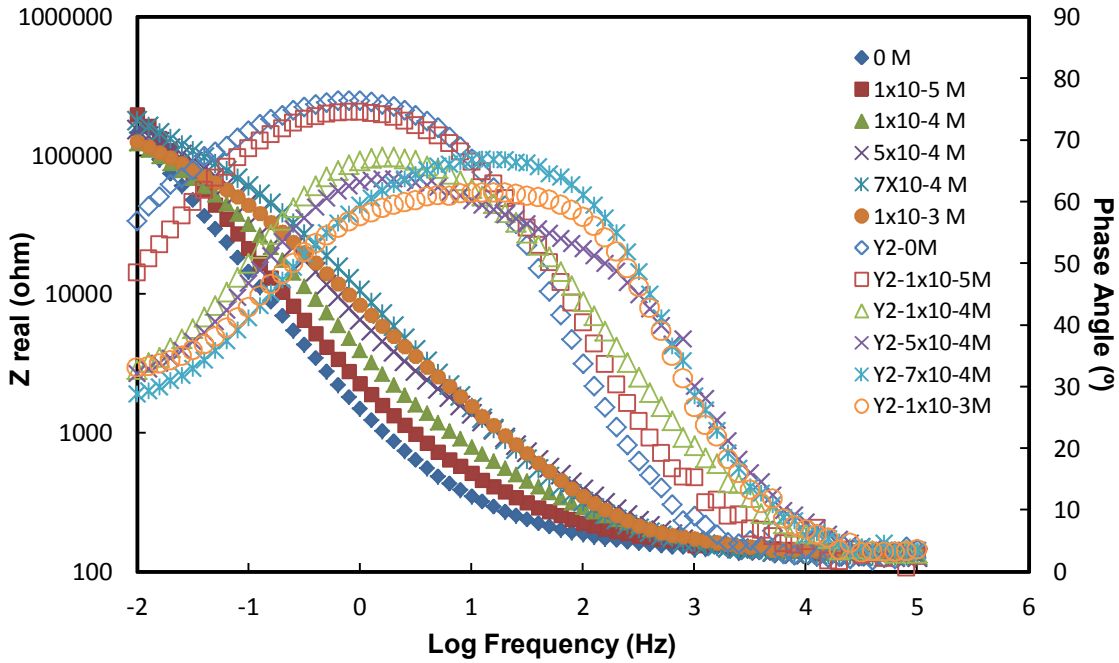

Figure 4.23. Impedance and phase angle plots as a function of applied frequency for chalcopyrite in the presence of different concentrations of SIPX.

The relationship between the collector adsorption (surface coverage) and the EIS results are illustrated in Figure 4.24. The Z_{real} values measured at 1 Hz are plotted in this graph. The relationship between the resistance and density of the collector adsorption was almost linear at low dosages of the collector, where the adsorption process is mainly Faradaic, i.e. based on electron transfer. At high dosages, where multilayer collector coverage is observed, the process becomes diffusion controlled and the measured resistance values shift from a linear trend. In addition to the surface coverage of the collector, detailed analysis of the impedance data gives valuable information about the adsorption mechanism and the form of the adsorbed layer at the surface.

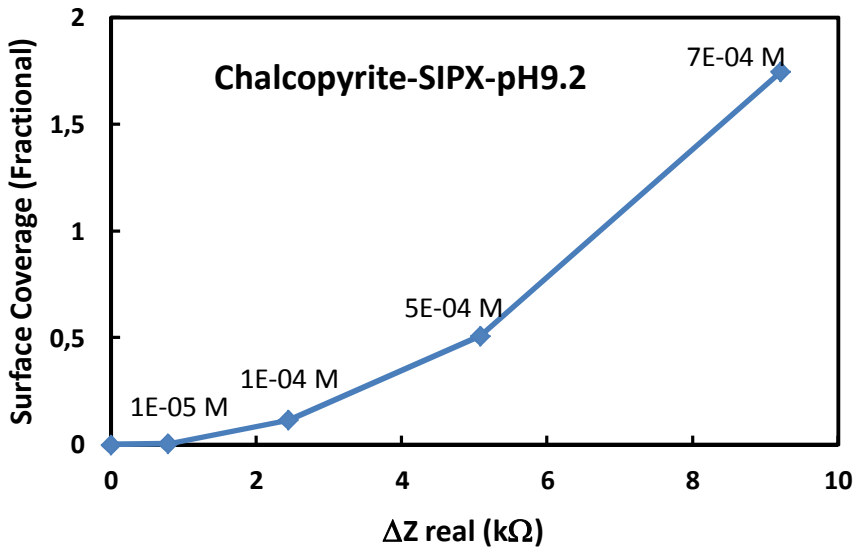

Figure 4.24. The relationship between surface coverage of SIPX and the change in resistance of the electrical double layer at pH 9.2. (Labels show the concentration of the collector in the solution)

4.3.2.1.2. Adsorption of Sodium Di-isobutyl Dithiophosphinate (DTPI)

Similar experiments were performed using DTPI as the collector. Previous electrochemical experiments (voltammetry and chronoamperometry) showed that the mechanism of DTPI adsorption is different from that of SIPX. DTPI is adsorbed through the EC mechanism and therefore fewer electrons are involved in the adsorption process.

The results of EIS experiments are illustrated in Figures 4.25 and 4.26, using Nyquist and Bode plots respectively. Figure 4.26 shows clearly that the capacitance of the electrode surface decreased gradually as the DTPI concentration was increased gradually to 10^{-3} M. The maximum of the phase angle was observed at about 1 Hz frequency (Figure 4.26) which was the same for all of the dosages used in the experiments. Therefore, the measured Z_{real} values at 1 Hz can be correlated to the surface coverage of the collector.

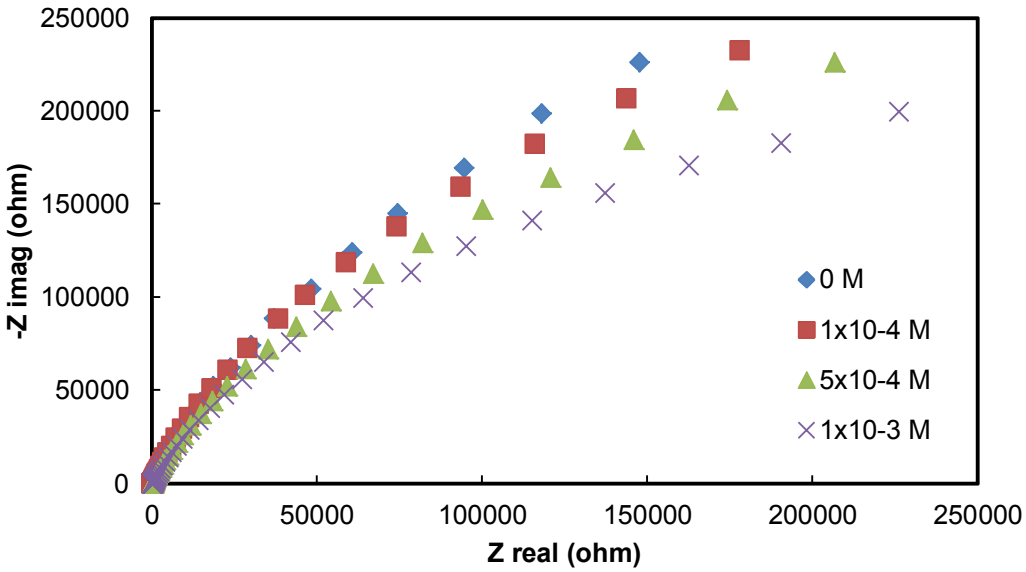

Figure 4.25. Nyquist plot of the impedance spectra of chalcopyrite in the presence of different concentrations of DTPI.

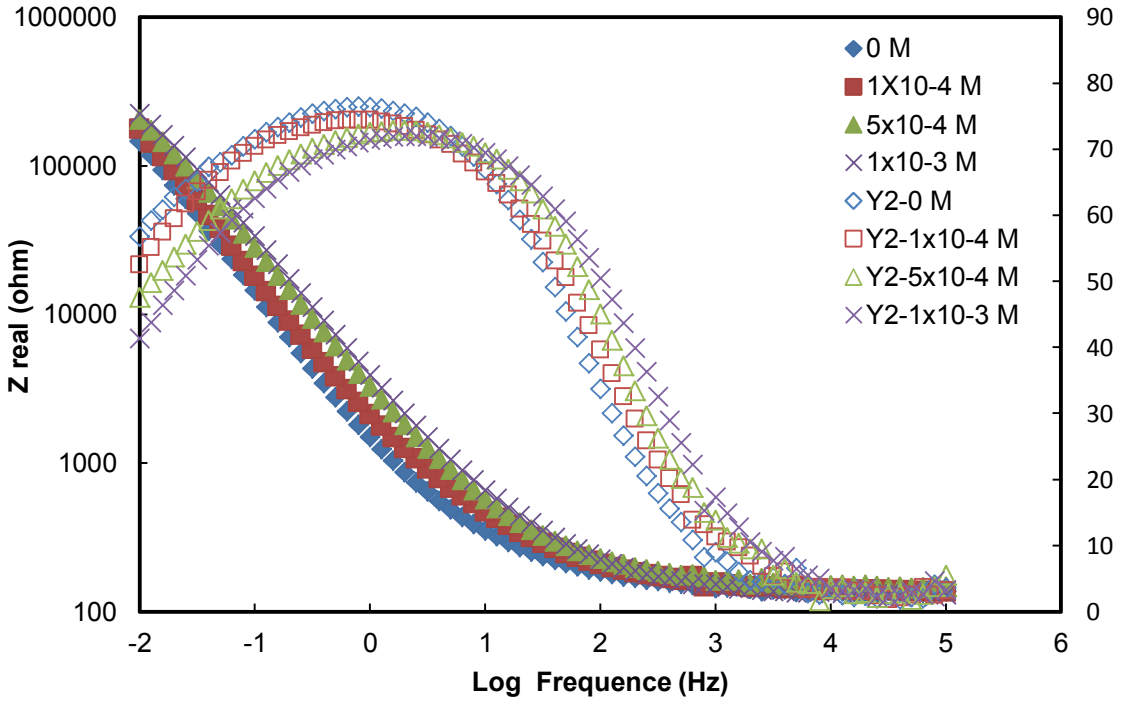

Figure 4.26. Impedance and phase angle plots as a function of applied frequency for chalcopyrite in the presence of different concentrations of DTPI.

Figure 4.27 shows that the surface coverage of DTPI on the chalcopyrite electrode, in other words the degree of hydrophobicity of chalcopyrite, can be predicted using Z_{real} values as measured by impedance spectroscopy. There is an almost linear relationship between the ΔZ_{real} measured at 1 Hz (at maximum of phase angle) and the amount of collector adsorbed on the chalcopyrite surface.

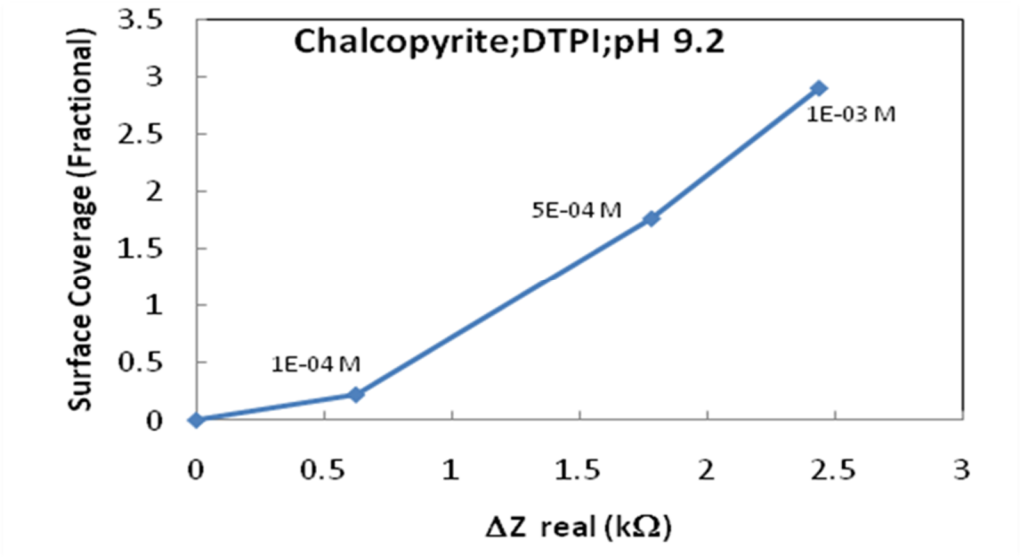

Figure 4.27. The relationship between the surface coverage of DTPI and the change in resistance of the electrical double layer at pH 9.2. (Labels show the concentration of the collector in solution)

4.3.2.1.3. Effect of pH

The flotation of sulphide minerals is usually performed in strongly alkaline solutions to depress pyrite. The EIS method was therefore tested at pH 11 using both SIPX and DTPI. Both the adsorption and EIS experiments were performed at pH 11, in order to preserve the form of the adsorbed collector species in the electrochemical cell. The results obtained with SIPX and DTPI are illustrated in Figures 4.28 and 4.29, respectively.

Surface coverage was below monolayer coverage, even at 10^{-4} M dosages, with both collector types. When the concentration was increased to 10^{-3} M, a multilayer collector coverage was observed. The increase in the resistance was well correlated with the increase in the surface coverage of the collector. These results

showed clearly that the EIS method works well, even with strongly alkaline pH values.

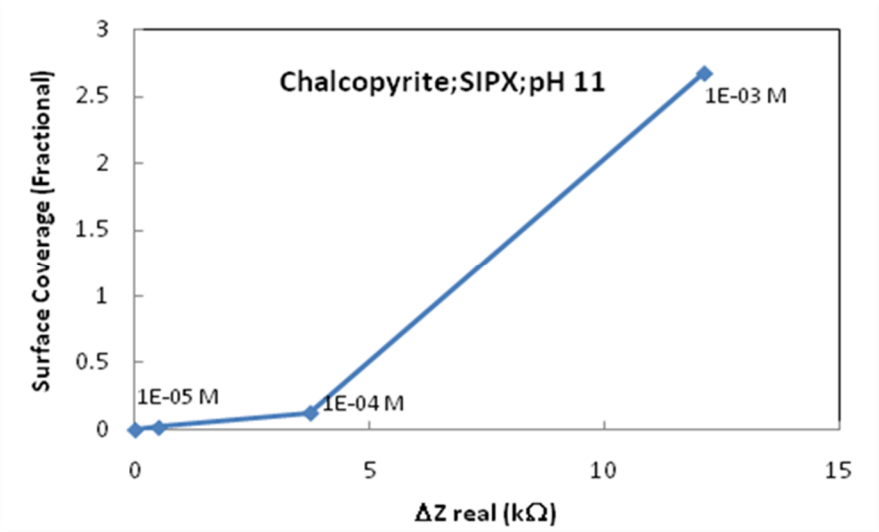

Figure 4.28. The relationship between the surface coverage of SIPX and the change in resistance at pH 11.

The adsorption of xanthate on chalcopyrite follows the Barsky relationship which indicates that OH^- / X^- ion concentrations are inversely proportional. A comparison of Figures 4.28 and 4.29 shows that the adsorption of DTPI is higher than SIPX at pH 11. For both collector types, it was possible to determine the collector adsorption at high pH values using EIS.

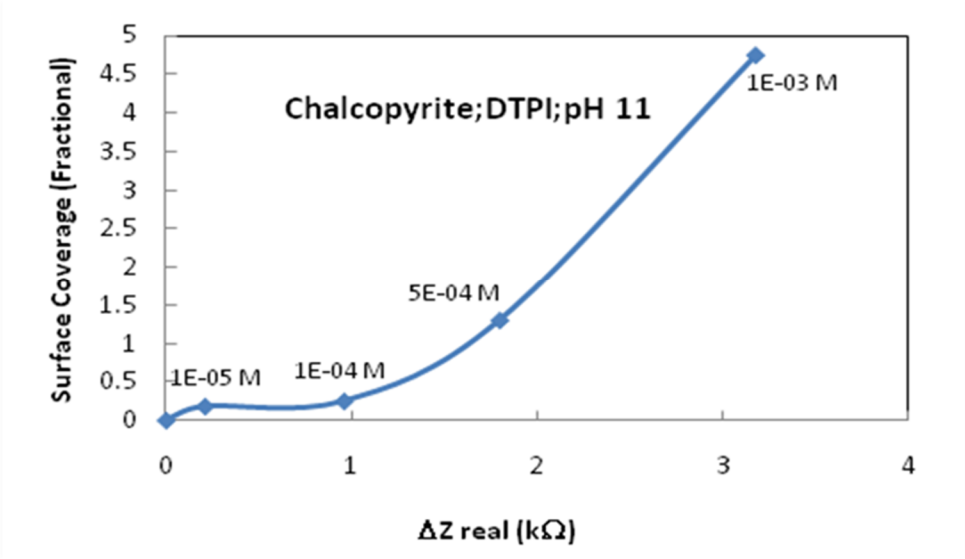

Figure 4.29. The relationship between the surface coverage of DTPI and the change in resistance a pH 11.

4.3.2.2. Galena

Galena has different surface characteristics and flotation behavior than chalcopyrite. The EIS method was used to determine the adsorption of both xanthate and dithiophosphinate type collectors on a galena electrode. The experiments for galena were performed only at pH 9.2, as depression is observed at high pH values due to the formation of stable and hydrophilic plumbite species ($HPbO^{2-}$).

4.3.2.2.1. Adsorption of SIPX

The adsorption-EIS experiments were performed at five different collector concentrations between $5x10^{-6}$ M and $1x10^{-3}$ M. The results of the EIS experiments are given in Figures 4.30 and 4.31 in the form of Nyquist and Bode plots, respectively. The results show that the resistance of the mineral surface increased proportionally with the collector dosage. The trend of the phase angle as a function of the applied frequency was found to be different from that of chalcopyrite (Figure 4.23). The maximum phase angle was observed at a frequency of about 10 Hz for most of the experiments. Therefore, the resistance values recorded at 10 Hz were taken into account.

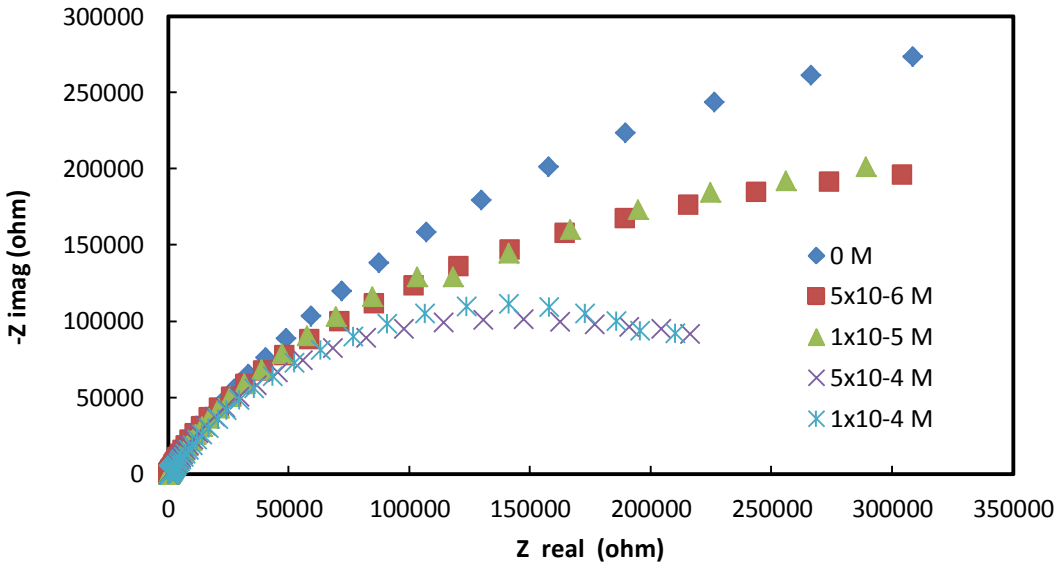

Figure 4.30. Nyquist plot of the impedance spectra of galena in the presence of different concentrations of SIPX.

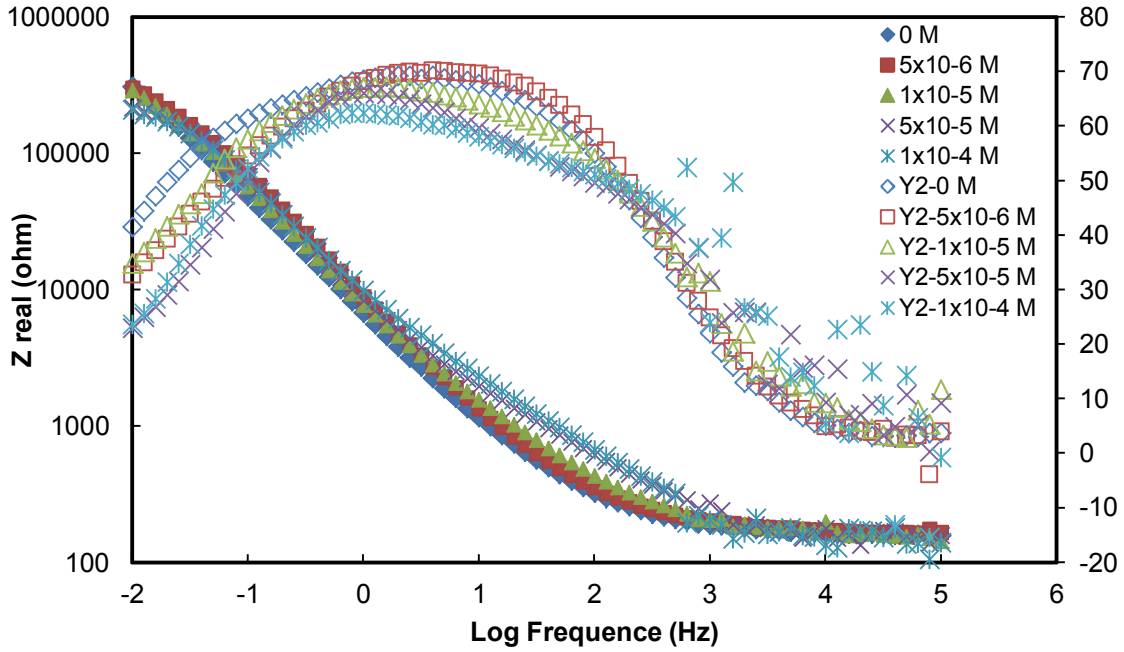

Figure 4.31. Impedance and phase angle plots as a function of applied frequency for galena in the presence of different concentrations of SIPX.

The relationship between the surface coverage of SIPX at low concentrations and the change in resistance at 10 Hz is illustrated in Figure 4.32a. The surface coverage increased linearly with the increase in the resistance. This was possibly due to the low surface coverage (less than a monolayer) under these conditions. When multilayer coverage of the collector was achieved at high concentrations (Figure 4,32b), the trend between the surface coverage and resistance approached an exponential form.

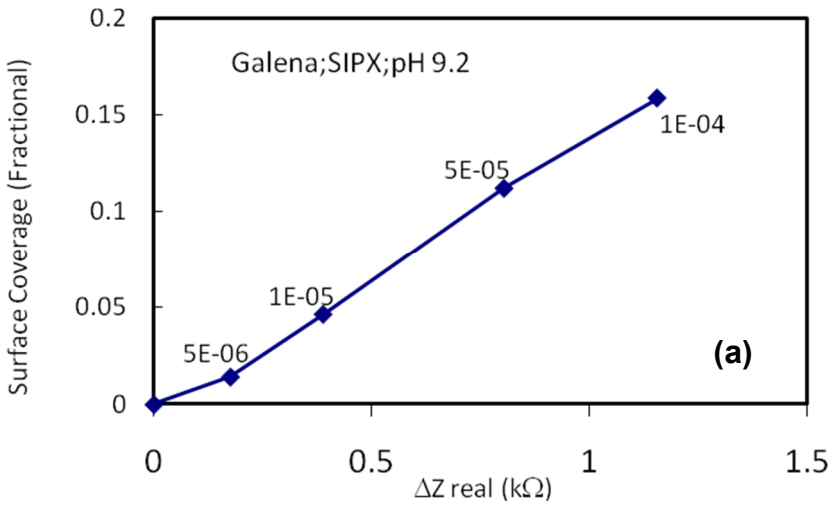

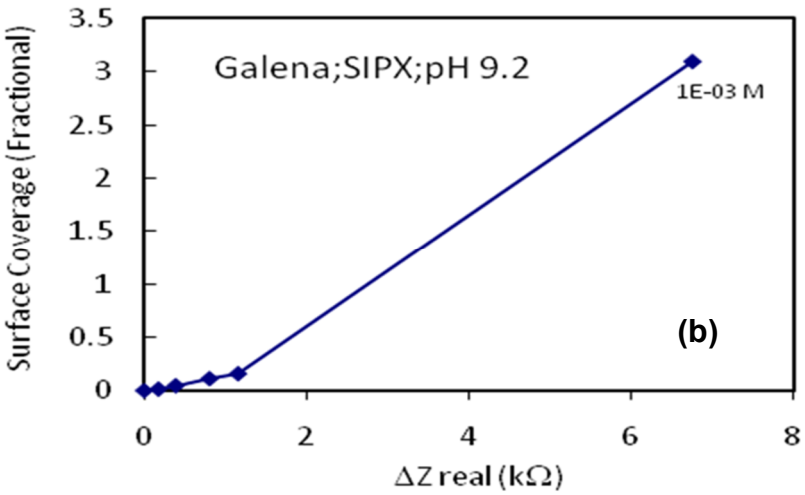

Figure 4.32 (a). The relationship between collector coverage of SIPX and the change in resistance measured at a frequency of 10Hz . (b) Effect of high SIPX concentration on the surface coverage and the change in resistance measured at a frequency of 10Hz

4.3.2.2.2. Adsorption of DTPI

DTPI is also known to be a selective collector for galena, and is used mostly in the flotation of galena from sphalerite. Hence, in addition to SIPX, adsorption tests were also performed with DTPI. The Nyquist and Bode graphs of the EIS measurements of galena in the presence of DTPI are given in Figures 4.33 and 4.34.

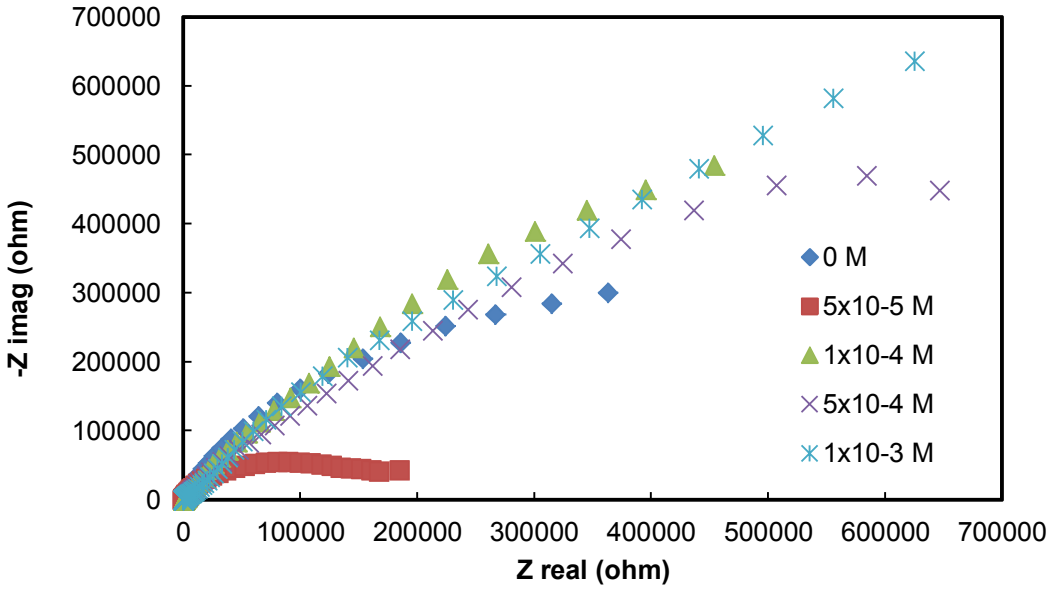

Figure 4.33. Nyquist plot of impedance spectra of galena in the presence of different concentrations of DTPI.

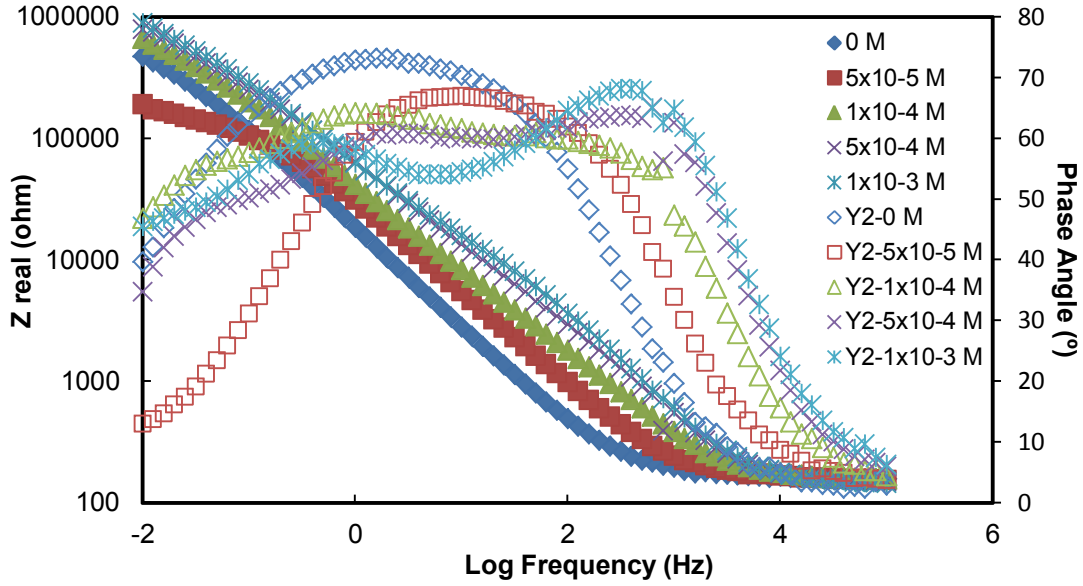

Figure 4.34. Impedance and phase angle plots as a function of applied frequency for galena in the presence of different concentrations of DTPI.

The results of the adsorption-EIS experiments performed in the presence of various concentrations of DTPI are given in Figure 4.35. The relationship between the surface coverage and resistance is of an exponential form due to multilayer

surface coverage. The results of the experiments performed for galena, both with SIPX and DTPI, showed that the adsorption of the collector can be predicted by measuring the resistance using the EIS method.

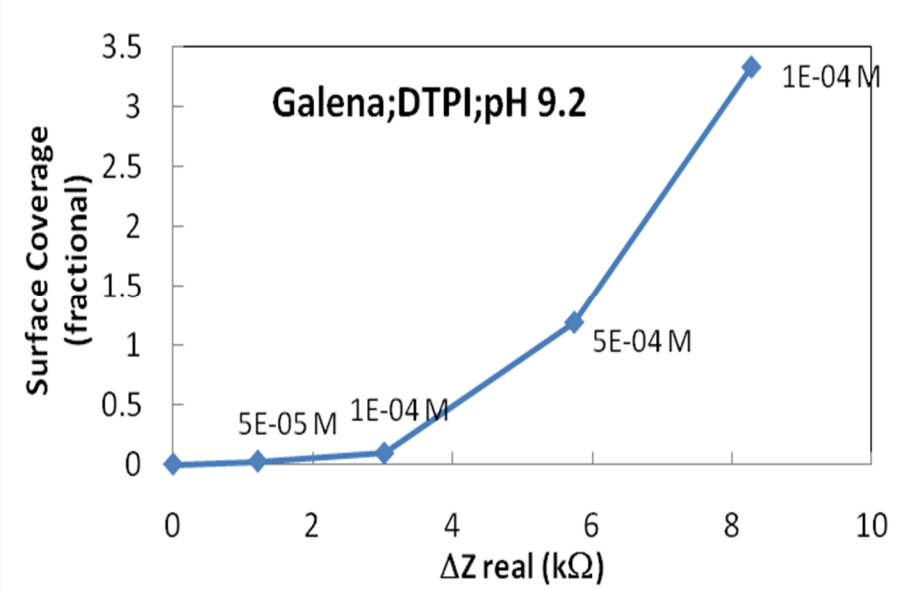

Figure 4.35. The relationship between the surface coverage of DTPI and the change in resistance measured at a frequency of 10Hz.

4.3.2.3. Pyrite

Pyrite, the common sulphide gangue mineral, was chosen as the third mineral in the experimental program. Both the surface characteristics and the flotation behavior of pyrite are considerably different from chalcopyrite and galena, therefore the adsorption of the collector on pyrite surface is expected to display different behavior. The experimental conditions were the same as those applied on chalcopyrite and galena.

4.3.2.3.1 Adsorption of SIPX

The adsorption of SIPX on the pyrite electrode could be observed only at high concentrations both in the adsorption experiments and EIS measurements. The relationship between the surface coverage and the concentration of SIPX in the solution is given in Figure 4.36. The fractional surface coverage of the collector increased to only 0.15 at SIPX concentrations as high as 10^{-4} M. There was no

adsorption at low concentrations. In parallel to the results of the adsorption experiments, the change in resistance was also negligible at these concentrations (Figure 4.37,Figure 4.38).

The maximum phase angle value was observed at about 1 Hz frequency and therefore the Z_{real} values at this frequency were taken into account. The relationship between the surface coverage of SIPX and the surface resistance is given in Figure 4.39. The increase in the surface coverage was proportional to the increase in the resistance value. The EIS was also capable of determining SIPX adsorption on the pyrite surface.

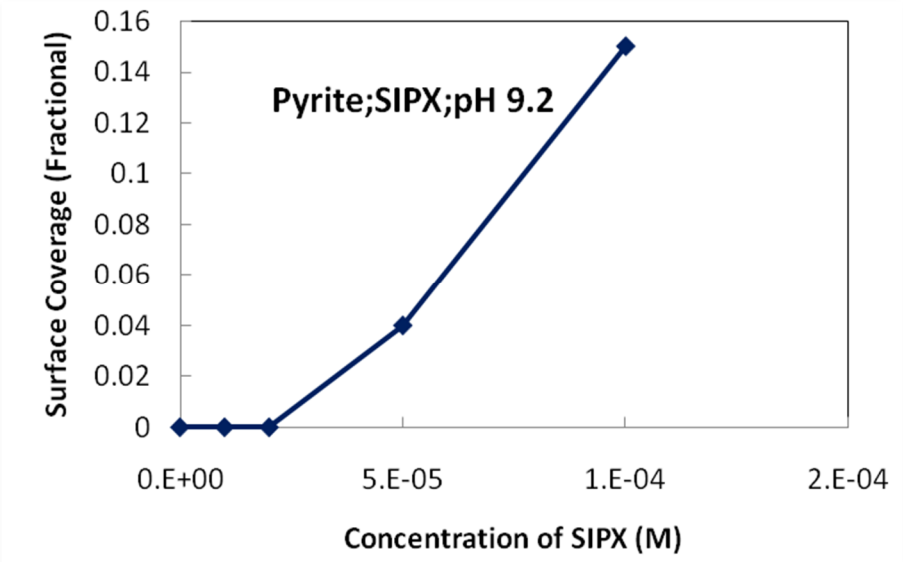

Figure 4.36. The relationship between the concentration of SIPX in solution and the surface coverage on the pyrite surface.

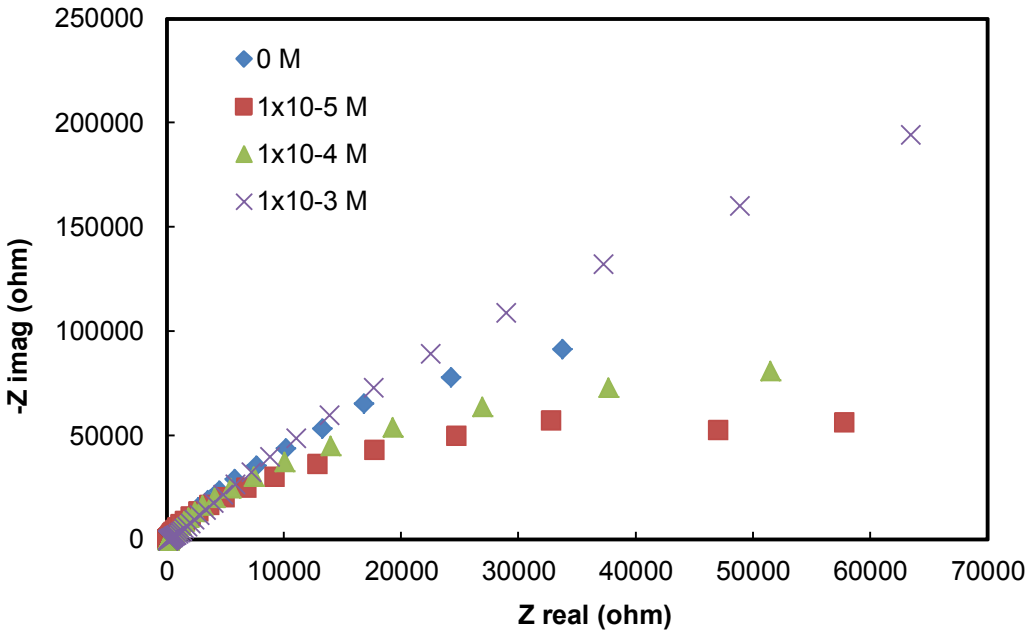

Figure 4.37. Nyquist plot of impedance spectra of pyrite in the presence of different concentrations of SIPX.

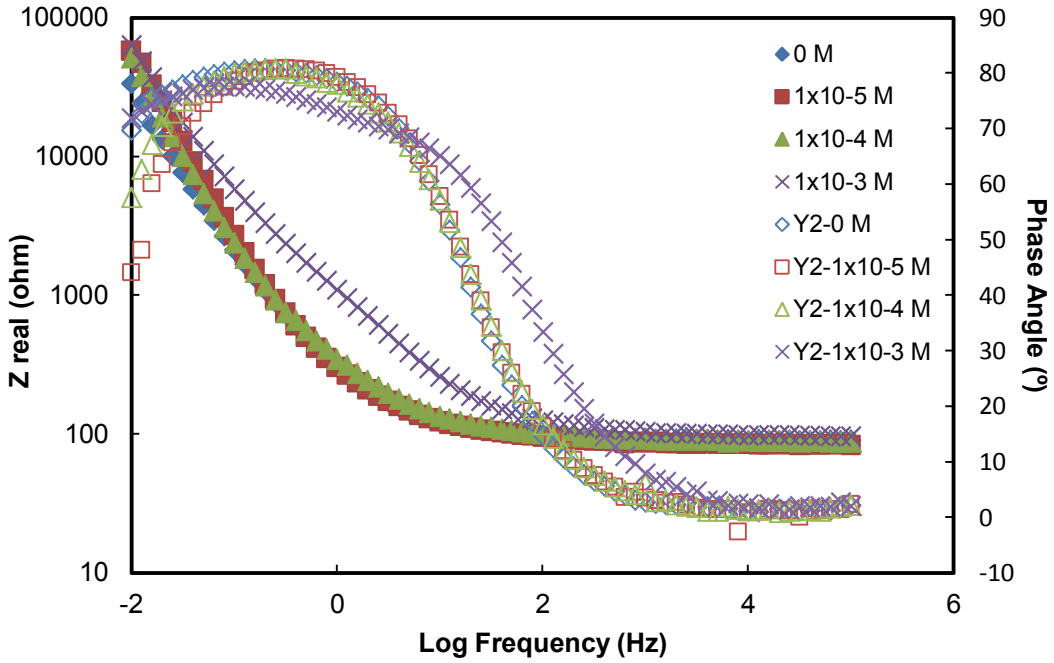

Figure 4.38. Bode plot of impedance spectra of pyrite in the presence of different concentrations of SIPX.

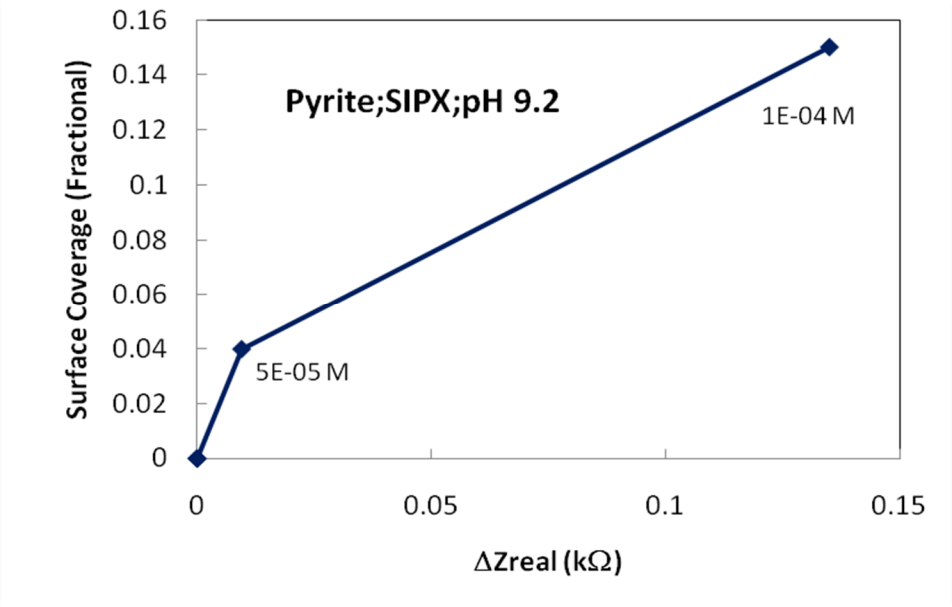

Figure 4.39. Surface coverage of SIPX on pyrite as a function of change of Z_{real} measured at a frequency of 1 Hz.

4.3.2.3.2. Adsorption of DTPI

Similar experiments were performed in the presence of DTPI. The adsorption of DTPI on pyrite was not anticipated, but it is well known from electrochemical research work in the literature that DTPI can be adsorbed on pyrite in $DTPI^0$ form at high concentrations. In parallel to the previous research work, DTPI adsorption was observed on pyrite at concentrations higher than $1x10^{-4}$ M (Figure 4.40).

The results of EIS measurements are illustrated in Figures 4.41 and 4.42 in Nyquist and Bode formats respectively. The variations in phase angle as a function of applied frequency (Figure 4.42) showed that the maximum angle was obtained at slightly lower than a 1 Hz frequency. In the same figure, Z_{real} values are also plotted vs frequency. Very small changes in the Z_{real} values were observed, even at very high concentrations of DTPI, indicating a very low surface coverage of the collector.

The results of the adsorption experiments were found to be in parallel with the impedance measurements (Figure 4.43). The change in the Z_{real} value was negligible at concentrations lower than $1x10^{-4}$ M. This was due to the very low surface coverage of the collector on the surface of pyrite. Because, unlike galena

(Figure 4.35) and chalcopyrite (Figure 4.29), the surface coverage of DTPI on pyrite was only about 0.1 even at $1x10^{-4}$ M concentration.

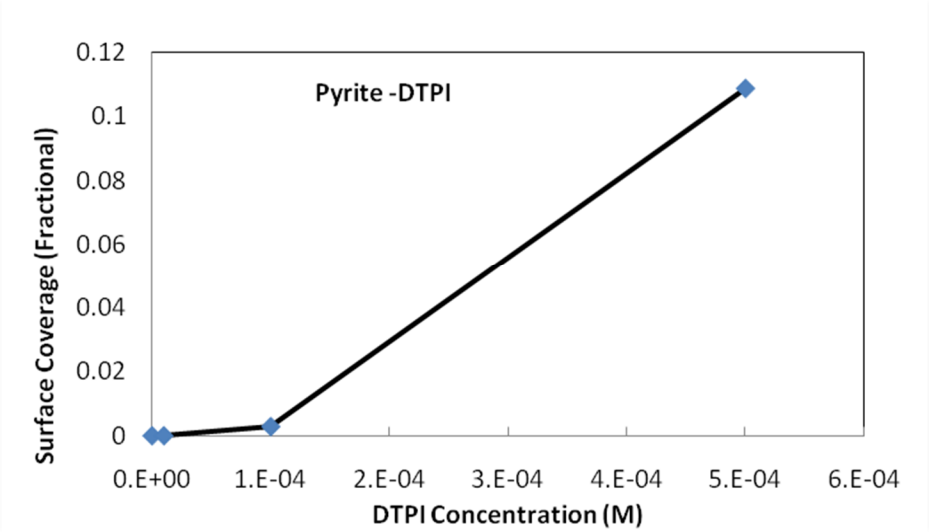

Figure 4.40. The relationship between the concentration of DTPI in solution and the surface coverage on the pyrite surface.

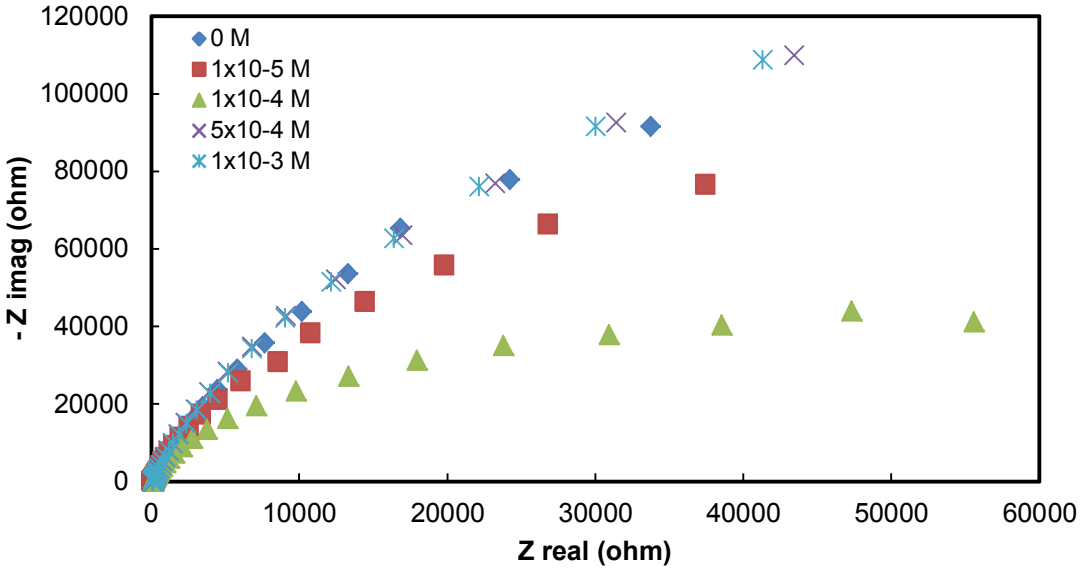

Figure 4.41. Nyquist plots as a function of applied frequency for pyrite in the presence of different concentrations of DTPI.

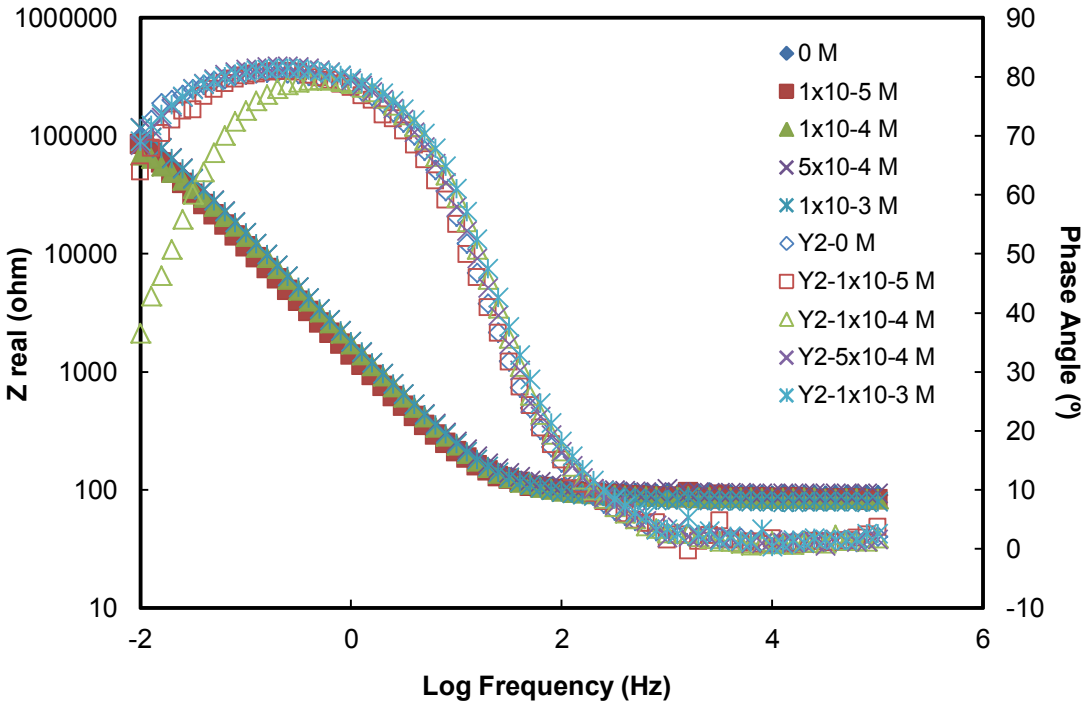

Figure 4.42. Impedance and phase angle plots as a function of applied frequency for pyrite in the presence of different concentrations of DTPI.

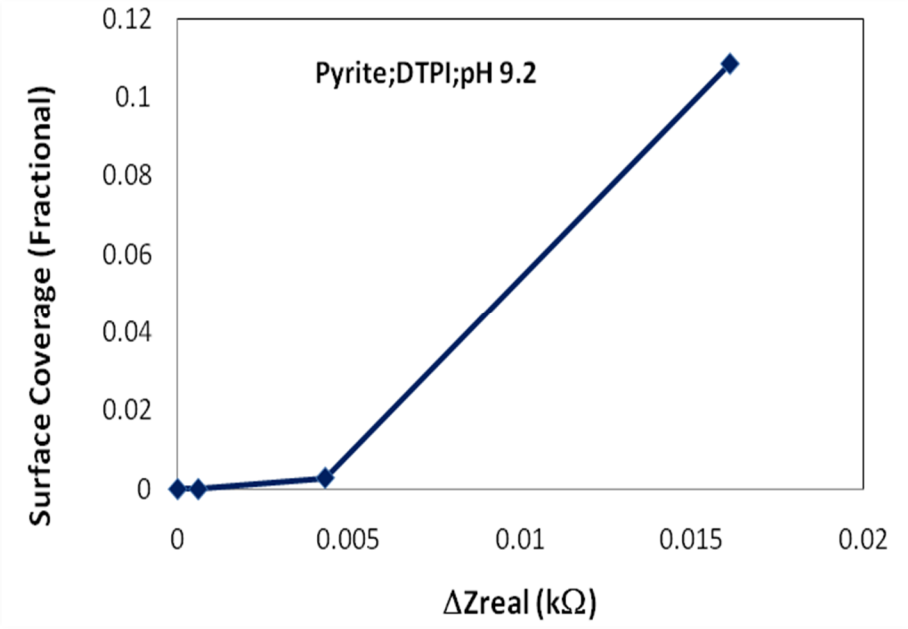

Figure 4.43. Surface coverage of DTPI on pyrite as a function of change in Z_{real} measured at a frequency of 1 Hz

4.4. Composite Mineral Electrodes

Up to this stage, EIS experiments were performed to determine the adsorption of collector on single mineral electrodes. However, the electrode system and the measurement methodology should also be capable of measuring the collector adsorption on composite particles. Thus, in this section combined chalcopyrite/pyrite mineral electrodes were fabricated to simulate the electrochemical behavior of composite particles.

Fabrication of composite electrodes was explained Chapter 3. These electrodes are considered to simulate the electrochemical behavior of liberated and composite particles. Cyclic voltammetry and EIS measurements of these electrodes were performed in the absence and presence of SIPX.

4.4.1. Cyclic Voltammetry

Results of the cyclic voltammetry experiments in the absence of the collector are given in Figure 4.44. The current densities of the mineral combination electrodes were higher than those of the single mineral chalcopyrite and pyrite electrodes. This was attributed to the influence of galvanic interaction between the two minerals with different rest potentials. Moreover, depending on the ratio of the minerals in the electrode, the electrochemical behavior of both chalcopyrite and pyrite could be observed within the same electrode.

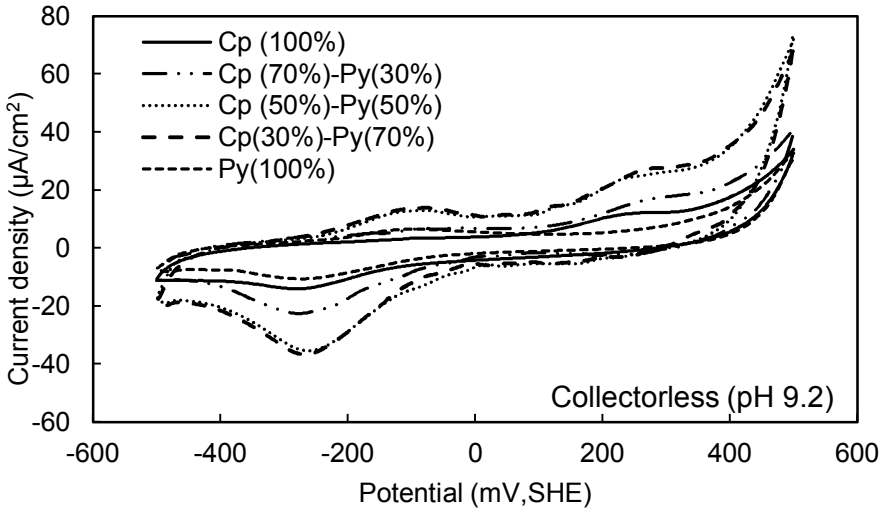

Figure 4.44. Voltammograms of chalcopyrite/pyrite mixture electrodes at pH 9.2.

According to the galvanic interaction model between chalcopyrite and pyrite, electron transfer between these two minerals occurs due to the difference in their rest potentials (Figure 4.45). The electrons flow from chalcopyrite to pyrite, resulting in a higher rate of anodic dissolution of chalcopyrite and more ferric hydroxide formation on the pyrite surface. This was observed in the form of an increase in current density of the anodic and cathodic peaks in the cyclic voltammogram (Figure 4.45).

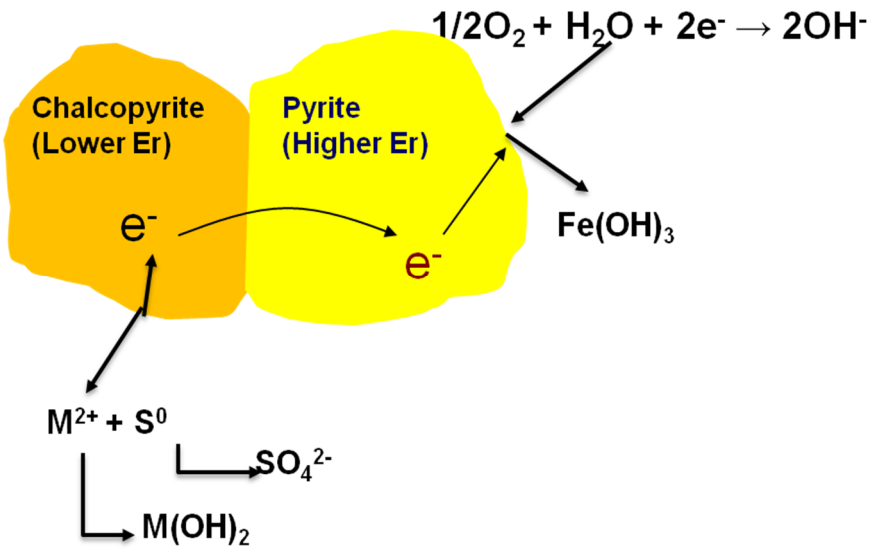

Figure 4.45. Galvanic interaction model between chalcopyrite and pyrite.

Similar cyclic voltammetry experiments were performed in the presence of 10^{-3} M SIPX (Figure 4.46). The adsorption of SIPX was detected clearly with the anodic peak starting at about 100 mV. This peak was not observed with the pyrite electrode. When Cp/Py combination electrodes were used, both the oxidation of pyrite (the peak at about -100 mV) and the adsorption of SIPX were observed in the form of two separate anodic peaks.

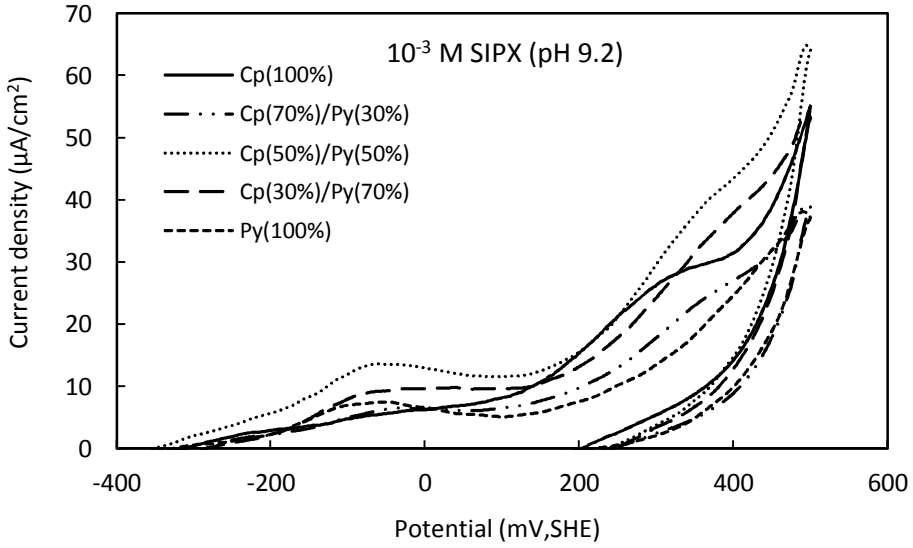

Figure 4.46. Voltammograms of chalcopyrite/pyrite mixture electrodes in the presence SIPX at pH 9.2.

4.4.2. Electrochemical Impedance Spectroscopy

The EIS was performed to observe adsorption of SIPX on surface of the composite particles. Bode and Nyquist plots of the EIS data are illustrated in Figure 4.47 and 4.48 respectively for the composite electrodes having different Cp/Py ratio.

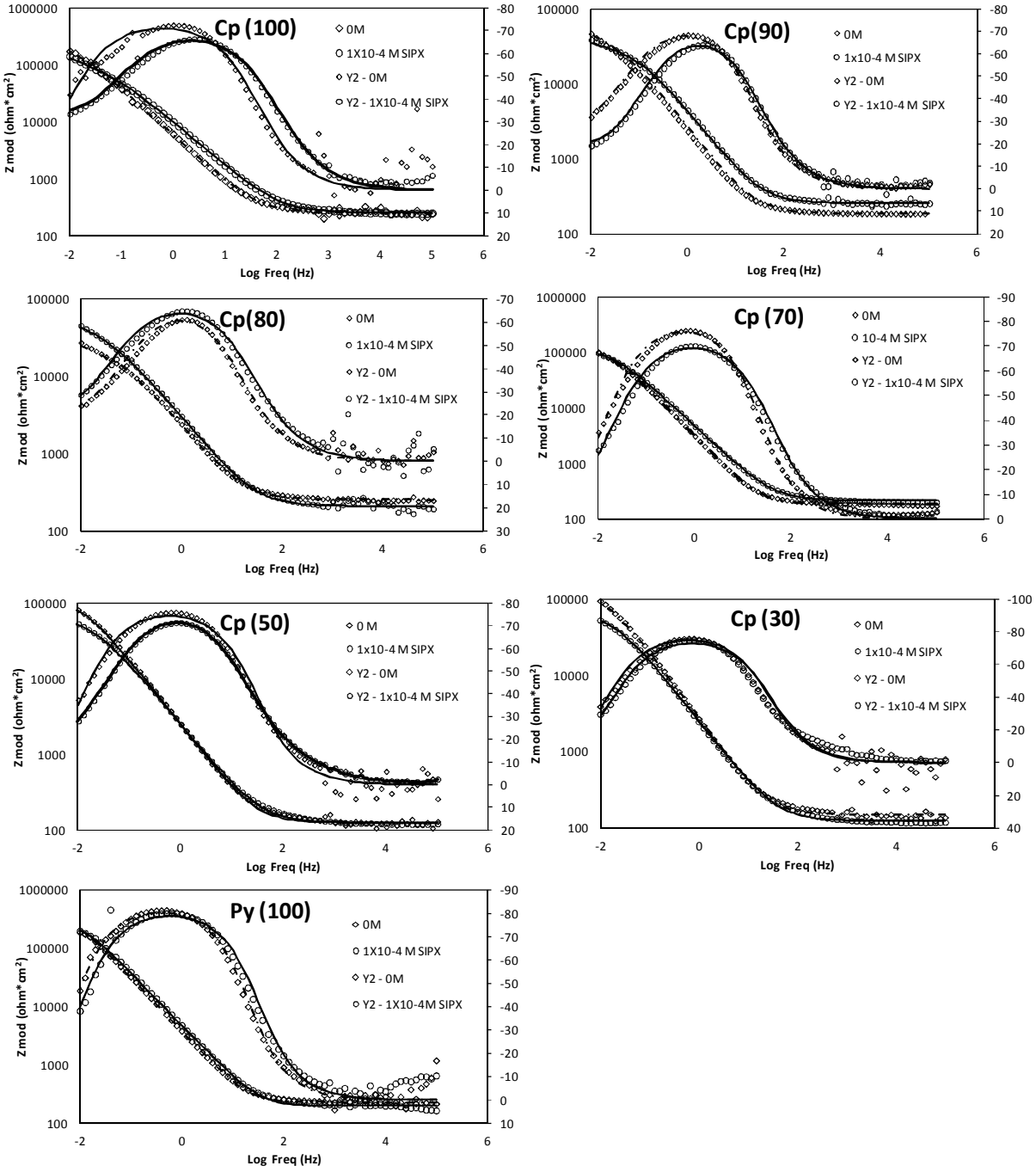

Figure 4.47. Bode graph of combined electrodes in the absence and presence of $1x10^{-4}$ M SIPX.

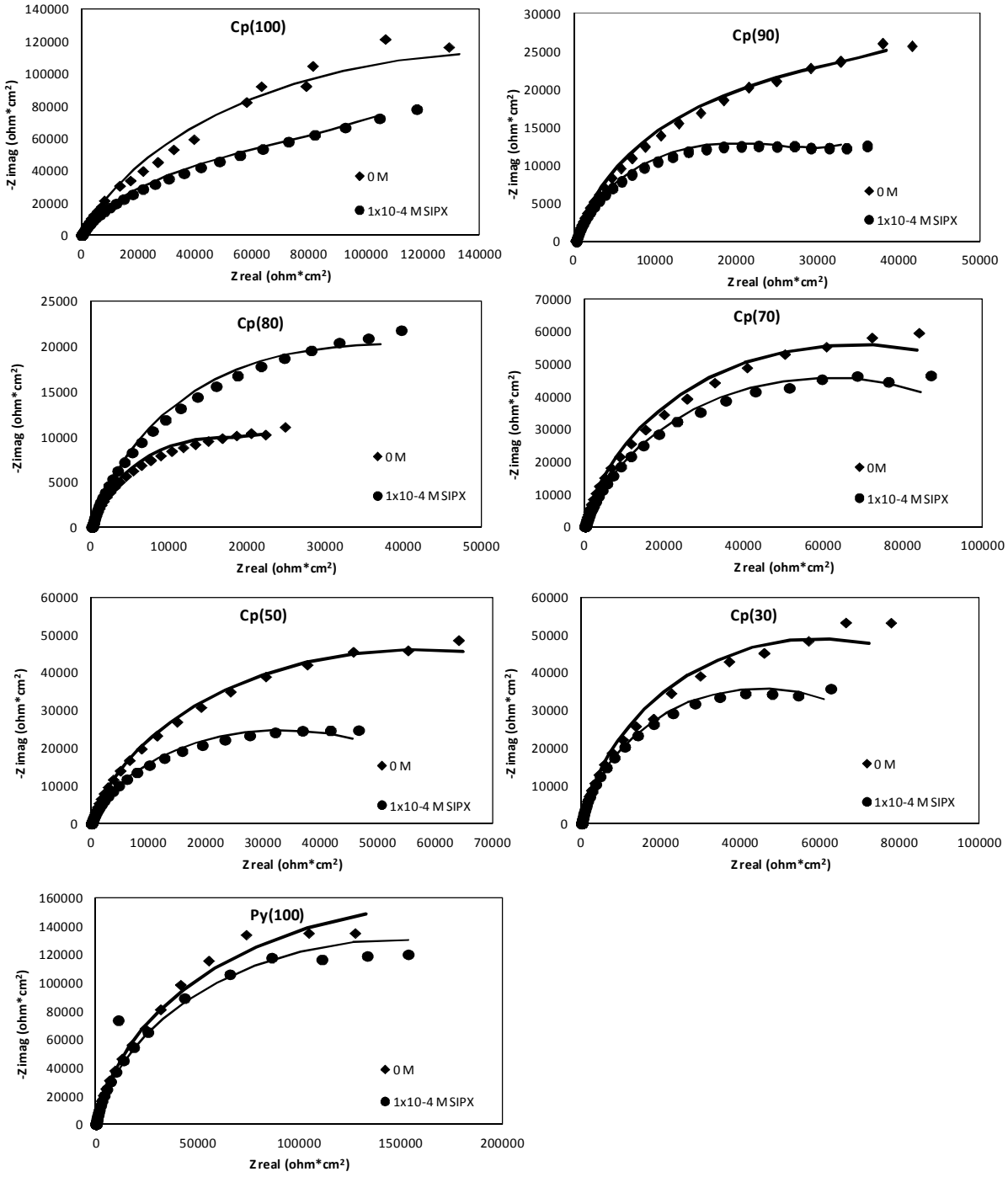

Figure 4.48. Nyquist graph of combined electrodes in the absence and presence of $1x10^{-4}$ M SIPX.

At higher frequency domain Zmod values are low and relatively constant as a typical response of a resistor to an AC with high frequency, corresponding to solution resistance. Medium frequency region represents capacitive behavior caused by the electrical double layer at the mineral/solution interface. In the

medium frequency region, the difference between impedance values of the measurements in the presence and absence of SIPX is higher for the electrodes with large Cp surface area and decreases for the electrodes containing less than 50% chalcopyrite. In order to present difference between resistance values before and after addition of SIPX clearly, Zreal versus ratio of Cp graph was drawn in Figure 4.49. In EIS measurement, changes in both capacitance and resistance can be used to determine surface coverage of collector on mineral surfaces. In Figures 4.49 and 4.50, the resistance component, Zreal impedance, is given as a measure of collector adsorption.

Figure 4.49 shows that chalcopyrite has higher resistance than pyrite. Z_{real} values of the combination electrodes lie between chalcopyrite and pyrite, but the decrease is not gradual. The presence of a small amount of pyrite decreases the Z_{real} of the combination electrodes to values very close to those of the pyrite electrode. This is attributed to the galvanic interaction between the chalcopyrite and pyrite minerals.

The addition of the collectors, SIPX and DTPI, results in an increase in Z_{real} values, due to the formation of an electrochemically passive layer at the surface attributable to collector adsorption. Hence, the collector addition at higher dosages results in higher Z_{real} values.

The greatest increase is observed with the chalcopyrite only electrode. The difference in the Z_{real} is larger with the chalcopyrite electrode than with the combination electrodes, indicating a higher density of adsorption on the liberated chalcopyrite particles. Both Figures 4.49 and 4.50 show clearly that the adsorption of collector is not proportional to the percentage of chalcopyrite in the composite electrode. The presence of a small amount of pyrite changes the surface characteristics of chalcopyrite and therefore the density of the collector adsorption.

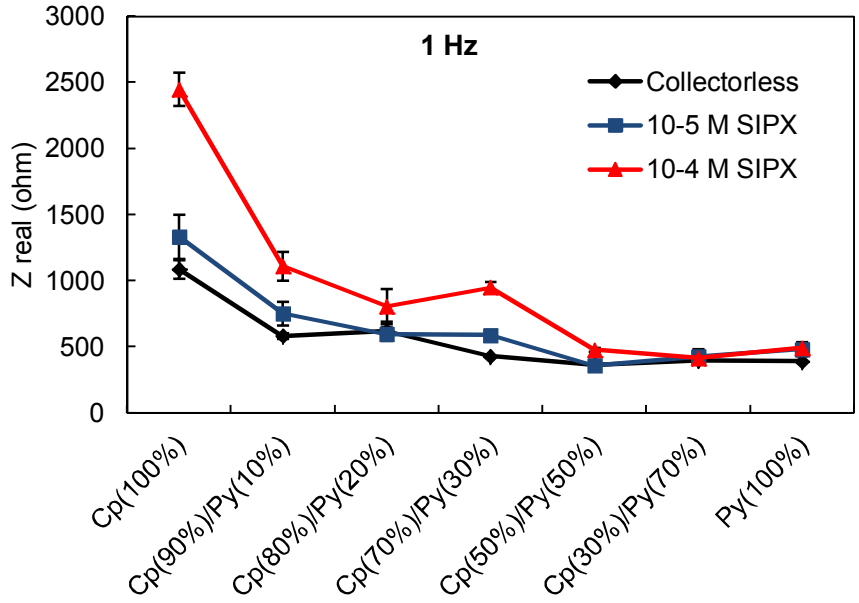

Figure 4.49. Changes in impedance characteristics of chalcopyrite/pyrite combination electrodes in the absence and presence of SIPX at pH 9.2.

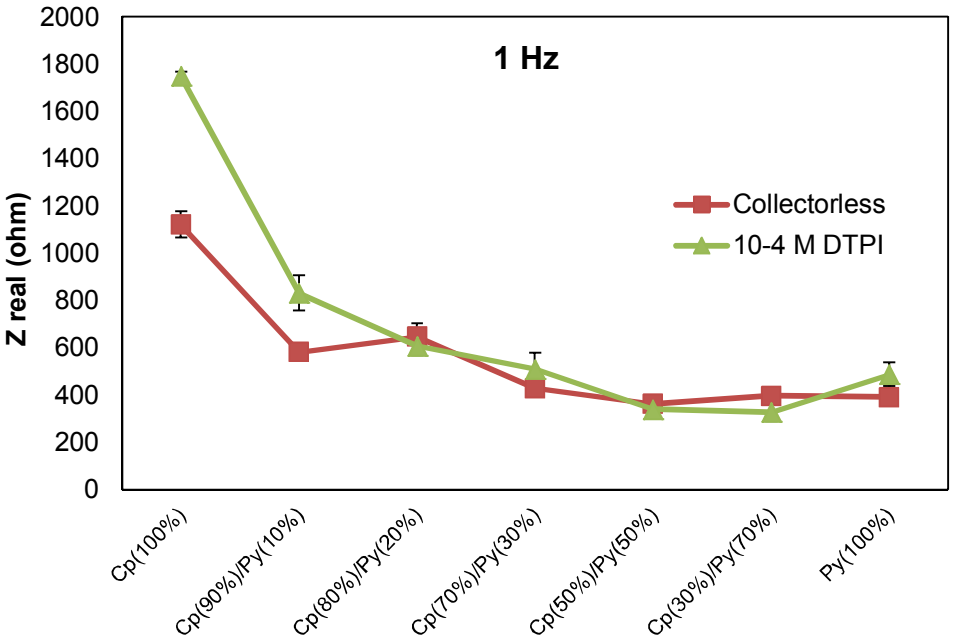

Figure 4.50. Changes in impedance characteristics of chalcopyrite/pyrite combination electrodes in the absence and presence of DTPI at pH 9.2.

The results given in Figures 4.49 and 4.50 correspond to the response of the entire combination electrode, i.e. chalcopyrite and pyrite. To differentiate the

changes on the surface characteristics of both chalcopyrite and pyrite, the measured impedance data were fitted to an equivalent electrical circuit model, shown in Figure 4.52. The two minerals are connected in parallel and the resulting simple circuit (with one capacitor and one resistor) is equivalent to the circuit shown in this section (Figure 4.51). The total capacitance was split between chalcopyrite and pyrite based on their relative surface area ratio in the electrode. Similar calculations can also be done for the measured resistance. Results of fitting to equivalent circuit model were illustrated in Table 4.1.

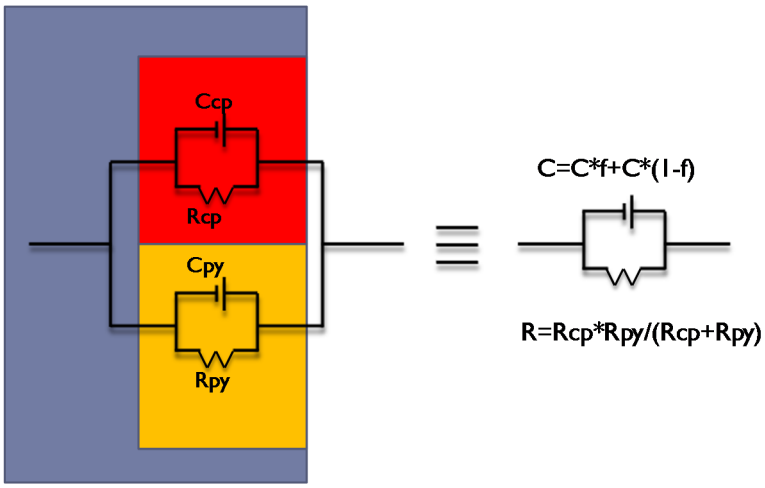

Figure 4.51. The schematic representation of the equivalent electrical circuit to model the behavior of composite particles

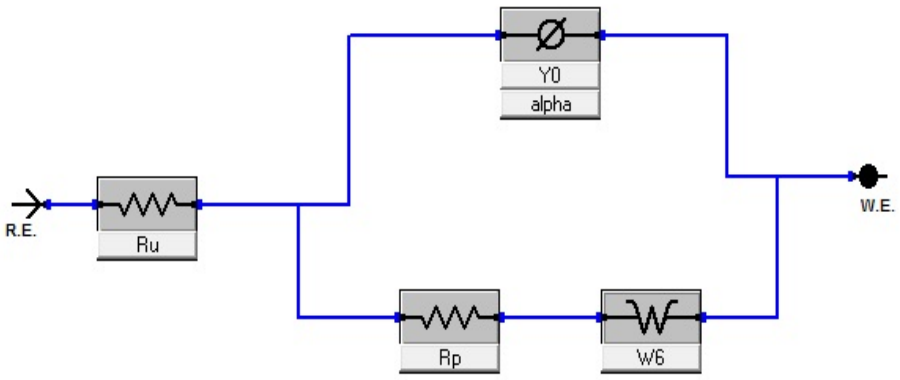

Figure 4.52: The schematic representation of the equivalent electrical circuit to model the behavior of composite particles

Table 4.1. Modelling data of composite particles

Collectorless							C_{total}*area	C_{total}*(1-area)
	Ru	Y_0	alpha	Wd	Rp	C_{total}(µF/cm^2)	**C-Cp (µF/cm^2)**	**C-Py (µF/cm^2)**
Cp(100)	254,6	3,77E-05	0,8236	3,31E-01	2,99E+05	63,213	63,213	
Cp(90)-Py(10)	186,2	8,07E-05	0,8301	1,87E-04	4,29E+04	104,131	93,718	10,413
Cp(80)-Py(20)	252,2	1,00E-04	0,7929	4,81E-04	2,25E+04	123,903	99,122	24,781
Cp(70)-Py(30)	188,2	6,32E-05	0,888	9,76E-04	1,31E+05	82,544	57,780	24,763
Cp(50)-Py(50)	126,3	8,20E-05	0,8667	9,80E-01	1,14E+05	115,561	57,781	57,781
Cp(30)-Py(70)	150,3	7,30E-05	0,8741	2,15E-02	1,20E+05	99,763	29,929	69,834
Py(100)	228,9	4,86E-05	0,9243	2,67E-01	3,45E+05	61,218		61,218
1x10^{-4} M SIPX							C_{total}*area	C_{total}*(1-area)
	Ru	Y_0	alpha	Wd	Rp	C_{total}(µF/cm^2)	**C-Cp (µF/cm^2)**	**C-Py (µF/cm^2)**
Cp(100)	256,8	2,31E-05	0,786	4,80E-05	1,03E+05	29,254	29,254	
Cp(90)-Py(10)	253,3	5,08E-05	0,813	3,57E-04	3,03E+04	56,096	50,486	5,610
Cp(80)-Py(20)	207,3	7,92E-05	0,787	3,09E-04	4,52E+04	111,953	89,563	22,391
Cp(70)-Py(30)	214,5	4,73E-05	0,819	7,60E-02	1,22E+05	69,623	48,736	20,887
Cp(50)-Py(50)	124,6	8,82E-05	0,823	5,52E-01	6,59E+04	128,964	64,482	64,482
Cp(30)-Py(70)	146,2	7,56E-05	0,856	2,93E-01	9,00E+04	104,234	31,270	72,964

The distribution of capacitance between chalcopyrite and pyrite is illustrated in Figures 4.53 and 4.54 respectively. High capacitance indicates a high Faradaic process. This is attributed to the galvanic interaction between the two minerals and it is entirely dependent on the surface area ratio of chalcopyrite and pyrite in the electrode. In the absence of the collector, the capacitance of chalcopyrite in the combination electrodes of Cp(90) and Cp(80) is substantially higher than in the single chalcopyrite mineral electrode and the remaining combination electrodes. This was attributed to the galvanic interaction between chalcopyrite and pyrite, as shown in Figure 4.45. The rate of the galvanic interaction, that is the rate of oxidation and reduction of the minerals, depends on the relative surface area ratio of chalcopyrite and pyrite in the same electrode. The presence of a very small amount of pyrite increases the Faradic process at the electrode surface. But when the ratio of pyrite was increased to 30% in the electrode, the rate of galvanic interaction was so high that excess oxidation took place, and the capacitance decreased due to the formation of a metal oxy-hydroxy species. For pyrite the situation is different (Figure 4.55). Pyrite is the cathodic mineral and the rate of

formation of ferric hydroxide in these particles is considerably higher, resulting in a low capacitance and a high charge transfer resistance.

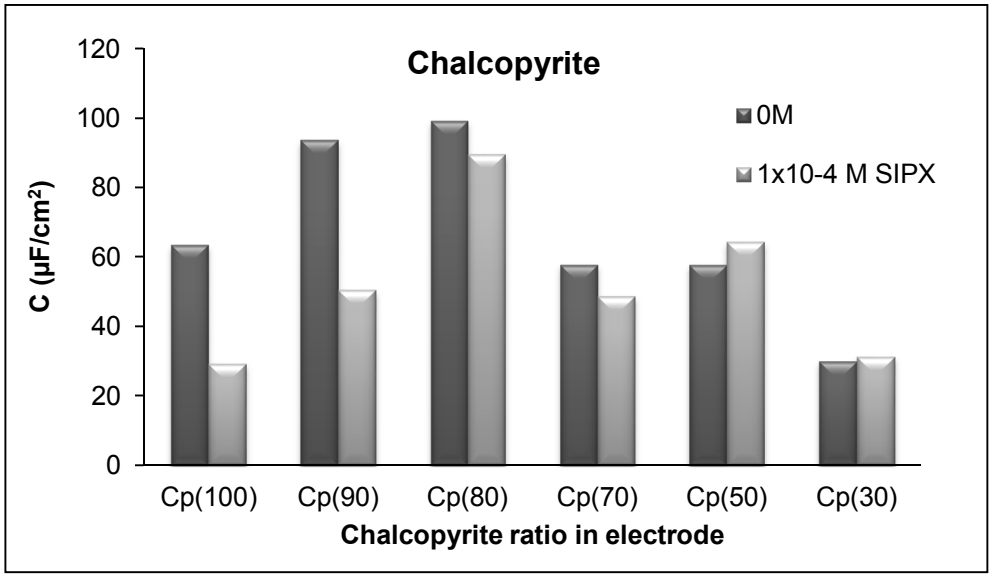

Figure 4.53. The distribution of capacitance with regard to the proportion of chalcopyrite in the composite electrode.

The difference between the capacitance values in the absence and presence of the collector can be correlated with the density of the collector adsorption. The greater the difference, the higher the density of the collector adsorption. Figure 4.53 shows that collector adsorption is high for the pure mineral [Cp(100)] and Cp(90), but decreases rapidly when the surface area ratio of pyrite increases to 20%. There is almost no collector adsorption on chalcopyrite in the electrodes containing 50% or less chalcopyrite.

The relationship between the difference in the capacitance of chalcopyrite before and after collector adsorption, and the surface area ratio of chalcopyrite in the electrode, is illustrated in Figure 4.54. A high ΔC indicates a higher collector adsorption. The results showed that there is an exponential relationship between the surface area of chalcopyrite and collector adsorption, and that the ΔC is below zero when the surface area of chalcopyrite is less than 50%.

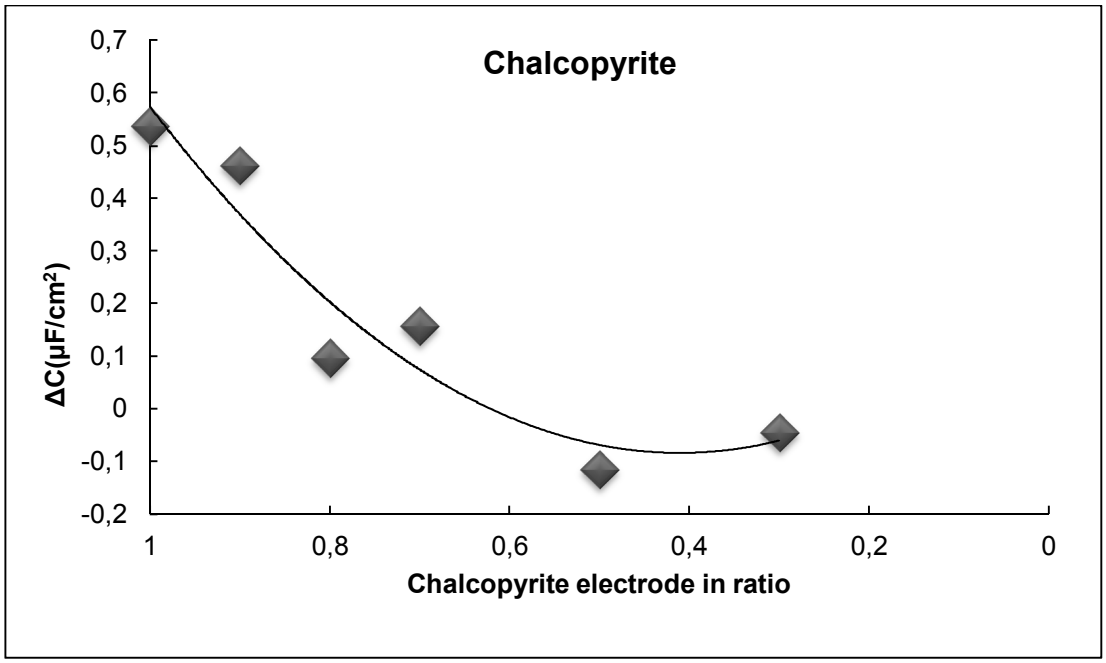

Figure 4.54. The relationship between the surface area ration of chalcopyrite in the chalcopyrite/pyrite combination electrode and the change in capacitance.

The calculated capacitance values of the pyrite in the combination electrodes are given in Figure 4.55. The capacitance of pyrite in the Cp(90), Cp(80) and Cp(70) electrodes was substantially lower than in the other electrodes. According to the galvanic interaction model given in Figure 4.45, pyrite is the cathodic mineral, so dissolved oxygen is reduced at the pyrite surface, producing a ferric hydroxide species. This reaction is dependent on the relative ratio of the two minerals in the electrode. When the surface area of chalcopyrite is larger than pyrite, the intensity of dissolved oxygen reduction on the smaller pyrite area will be higher. Consequently, a thick layer of hydrophilic ferric hydroxide forms on the surface and the capacitance decreases.

The differences in the capacitance values of pyrite in the absence and presence of the collector were very small (Figure 4.55). The adsorption of the collector on pyrite was found to be likely only for the Cp(90), Cp(80), Cp(70) and Py(100) electrodes. However, the only significant difference was observed with the pyrite only electrode, Py(100).

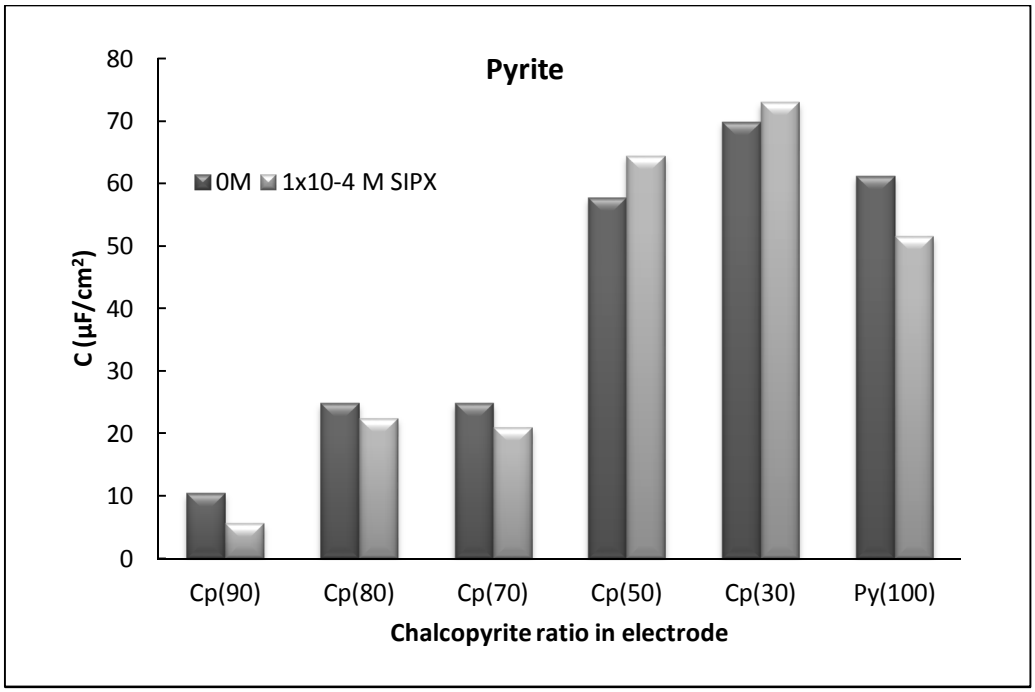

Figure 4.55. The distribution of capacitance with regard to the proportion of pyrite in the composite electrode.

4.5 Flotation Tests

4.5.1. Preliminary Laboratory Tests

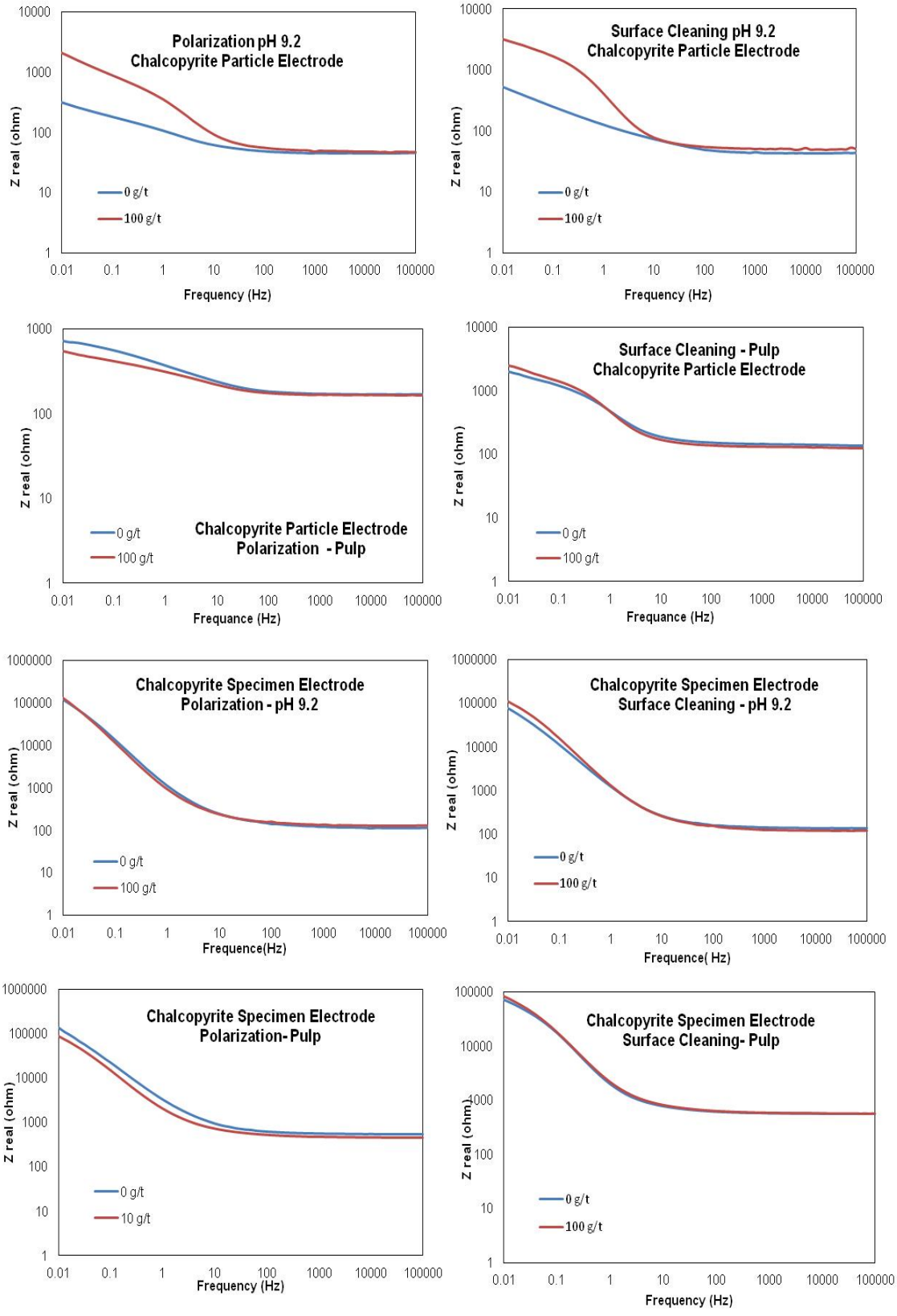

Figure 4.56. Bode Plots of preliminary laboratory tests

Both polarization and surface cleaning methodologies (impedance measurements taken in EC Cell) were found to be effective in determining the adsorption of the collector di-isobutyl dithiophosphinate (DTPI) at the surface of the chalcopyrite electrode. Bode plots of the results are illustrated in Figure 4.56 for polarization for all conditions. The adsorption of DTPI on the chalcopyrite mineral electrode was detected in the form of surface passivation due to adsorption of the collector, which resulted in higher Zreal values. But, the measurements performed in pulp cell were not as clear as in the EC cell.

The effect of collector addition was clearly observed with both the specimen electrode (Figure 4.56) and the particle electrode. However, this difference is not clear in Figure 4.56 due to the large logarithmic scale. Since chalcopyrite particle electrode is more conductive, Z real value is smaller and the logarithmic scale becomes more visible. But, the difference in particle electrode is considerably larger than the specimen electrode.

4.5.2. Batch Flotation Tests

4.5.2.2. Impedance Measurement

Bode plots of polarization; surface cleaning and pulp cell measurement were given at Figure 4.57, 4.58 and 4.59, respectively.

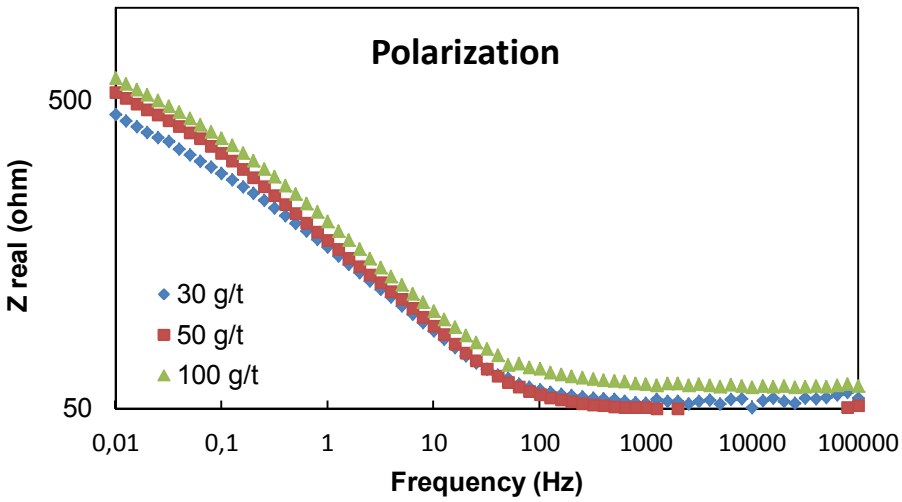

Figure 4.57. Bode Plot of impedance measurements of polarization experiments at different DTPI dosages.

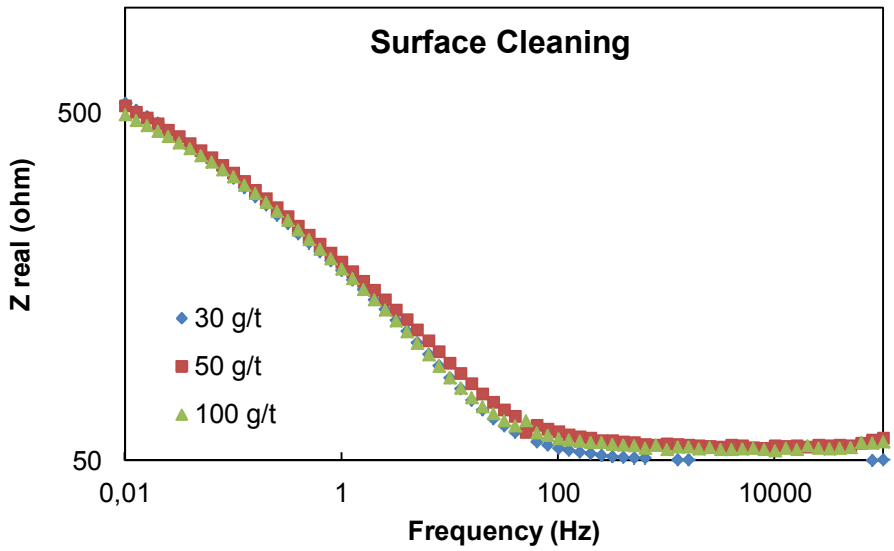

Figure 4.58. Bode Plot of impedance measurements of surface cleaning experiments at different DTPI dosages.

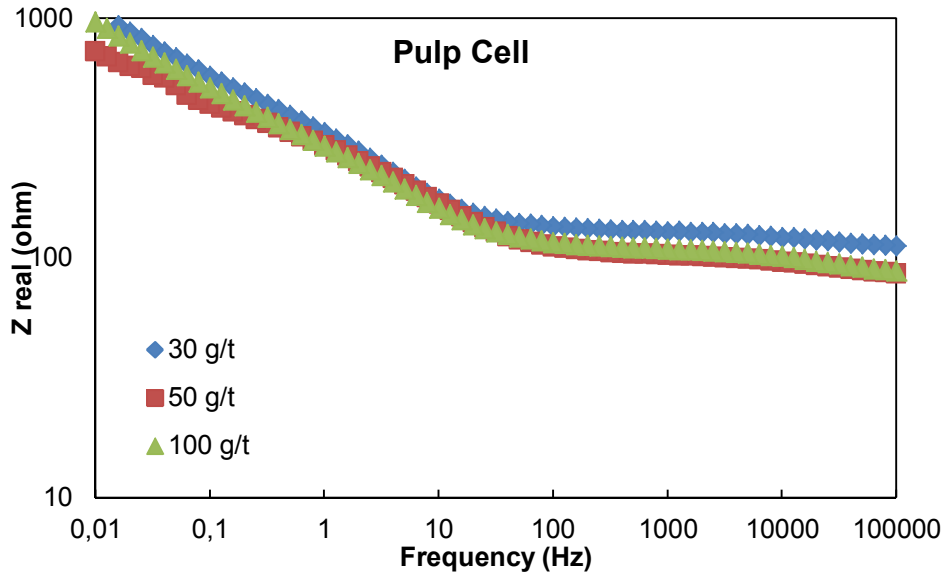

Figure 4.59. Bode Plot of impedance measurements of pulp cell experiments at different DTPI dosages.

Among these three methods, the most successful outcomes were obtained by polarization. Figure 4.57 clearly shows the difference among three different DTPI concentrations. Z real value was increased as the amount of collector increases. In surface cleaning (Figure 4.58) and pulp cell (Figure 4.59) measurements, a clear result could not be obtained even with the increased concentration.

Flotation experiments were fitted to the model by the equivalent electrical circuit in Figure 4.60. Data obtained from the model was given in Table 4.2.

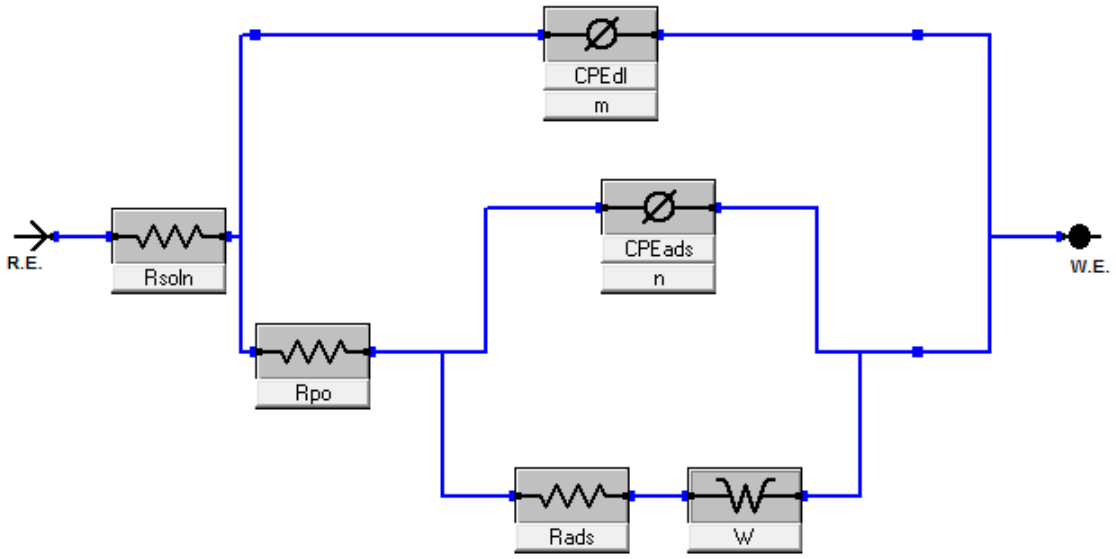

Figure 4.60. Equivalent circuit used to fit impedance data

The equivalent electrical circuit model given in Figure 4.60 was found suitable to simulate the adsorption phenomena on mineral surface. In this model, Ru represents the solution resistance between the mineral electrode surface and the reference electrode. The electrical double layer (Cdl) and coating capacitance (Cads) is modelled using Y_0, a Constant Phase Element (CPE) parameter. The CPE can be used to fit an electrochemical system better than an ideal capacitor, when the electrode surface is rough or the bulk conductivity of the oxide film changes with distance through the film. However, capacitance can be back calculated from the CPE value using the following equation.

$$C = (Y_0 * R)^{1/n}/R \qquad (4.6)$$

Where, R : polarization resistance at low frequency (ohm)

n : exponent derived during model fitting with CPE

R_{ads} is the polarisation resistance of the coated area. Wd is the Warburg diffusion element.

Table 4.2. Results of fitted data to impedance measurements

	Rsoln	Rads	Rpo	CPE_{ads}	n	CPE_{dl}	m	W	Goodness of Fit
30g/t	45,96	96,98	7,652	2,97E-04	0,857	2,66E-03	1,12E-01	1,75E-03	3,08E-03
50g/t	48,52	173,8	0,703	5,19E-04	0,745	2,19E-03	1,13E-01	1,40E-03	2,39E-03
100g/t	50	258,6	10,02	4,80E-04	0,741	2,01E-03	1,25E-01	1,10E-03	1,62E-03

4.5.2.3. Flotation Tests Results

The results of flotation experiments conducted together with impedance experiments were given in Table 4.3. In flotation experiments, copper concentrate with 25% grade was tried to be obtained by two cleaning stages. As expected, copper recovery was increased by the increase in the collector dosage. At different concentrations, the relation between the recovery and the resistance (R_{ads}) measured by EIS was shown in Figure 4.61. There is a logarithmic relationship between the resistance and copper recovery

Table 4.3. Flotation results of experiments at different DTPI concentrations

		Cu(%)	W (gr)	Rec % Cu
30 g/t	**Feed**	3,075	32,200	100
	Cu Conc.	25,950	55,650	**42,846**
	Cu Rgh. Tail	0,775	965,000	22,180
	Cu Cl 1 Tail	10,458	68,950	21,394
	Cu Cl 2 Tail	16,231	28,200	13,580
50 g/t	**Feed**	3,323	38,750	100
	Cu Conc.	24,237	79,250	**57,260**
	Cu Rgh. Tail	0,581	828,400	14,341
	Cu Cl 1 Tail	3,722	169,200	18,773
	Cu Cl 2 Tail	9,386	34,400	9,625
100 g/t	**Feed**	2,920	1105,465	100
	Cu Conc.	25,400	82,000	**64,565**
	Cu Rgh. Tail	0,276	558,764	4,783
	Cu Cl 1 Tail	1,150	419,046	14,930
	Cu Cl 2 Tail	11,131	45,596	15,722

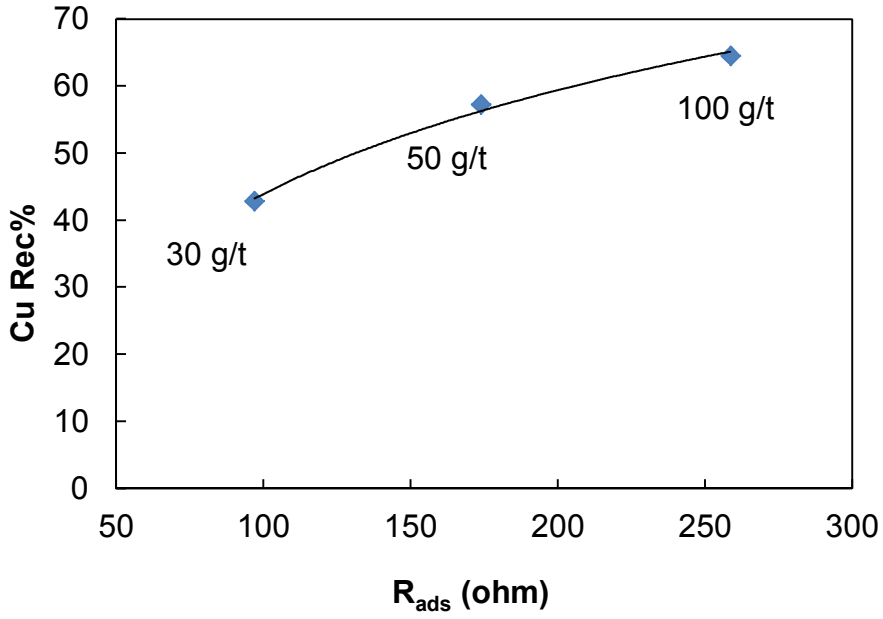

Figure 4.61. The relationship between resistance of chalcopyrite electrode and flotation recovery.

Modelling of EIS data using equivalent electrical circuits was performed for a single mineral electrode system, and surface coverage of the collector was successfully predicted using the capacitance values derived from the model.

The relationship between the measured resistance and flotation recovery is illustrated in Figure 4.61. The results given in Figure 4.61 showed clearly that it is possible to estimate the floatability of chalcopyrite by using EIS measurements.

In the next step, the density of collector adsorption on chalcopyrite was calculated by modelling of EIS data. Modelling studies were performed to fit EIS data to an equivalent electrical circuit. The first step in developing an equivalent electrical circuit for an electrochemical system is to analyse the nature of the overall current and potential. Large numbers of papers and books describing these procedures in detail are available in the literature. However, a brief outline of the main components of the electrical double layer forming at the mineral/water interface is provided here, to better understand the concept of modelling EIS data.

The model parameters for a chalcopyrite electrode were calculated using the model given in Figure 4.60 in the presence of different DTPI dosages. The relationship between the calculated capacitance and the DTPI dosage is given in

Figure 4.62. The capacitance decreased exponentially with the increase of the collector dosage, because the mineral surface is partially blocked with the adsorbed collector. The lower the capacitance, the higher the surface coverage of the collector.

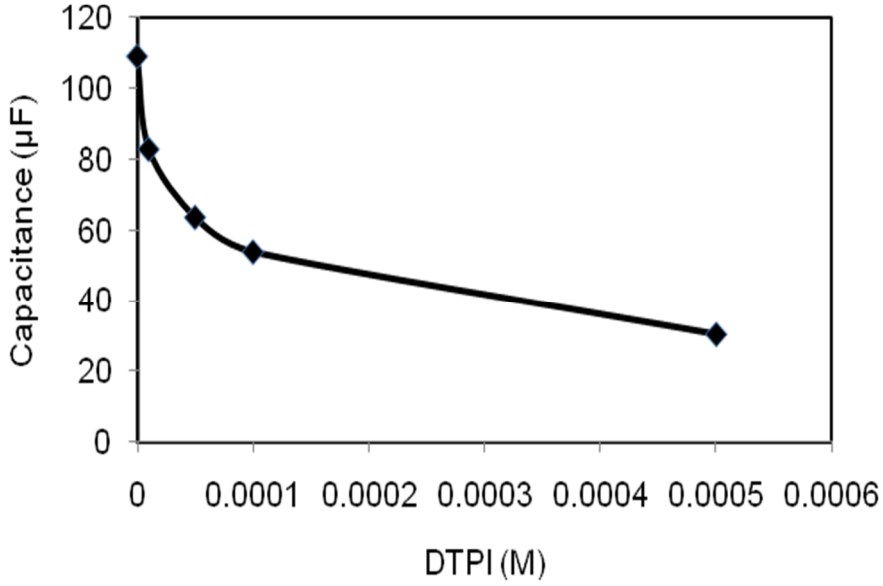

Figure 4.62. Variation of capacitance as a function of the DTPI dosage (chalcopyrite electrode, pH 11).

In the next step, surface coverage of the collector at a given concentration was calculated using the following equation;

$$\theta_i = \frac{C_0 - C_i}{C_0 - C_\infty} \qquad (4.7)$$

where, C_0: capacitance at zero concentration

C_∞: capacitance at infinite concentration

C_i: capacitance at a given concentration

The relationship between the collector coverage and the capacitance of the electrical double layer is illustrated in Figure 4.63. The capacitance value measured at $5x10^{-4}$ M DTPI was assumed as C_∞. However, the calculated surface coverage using EIS analysis should be confirmed by surface analytical methods, which can quantitatively measure adsorption of the collector directly. ToF-SIMS can potentially be used for this purpose. Mineral electrodes which can be used for both microscopic and ToF-SIMS analyses were designed for this purpose.

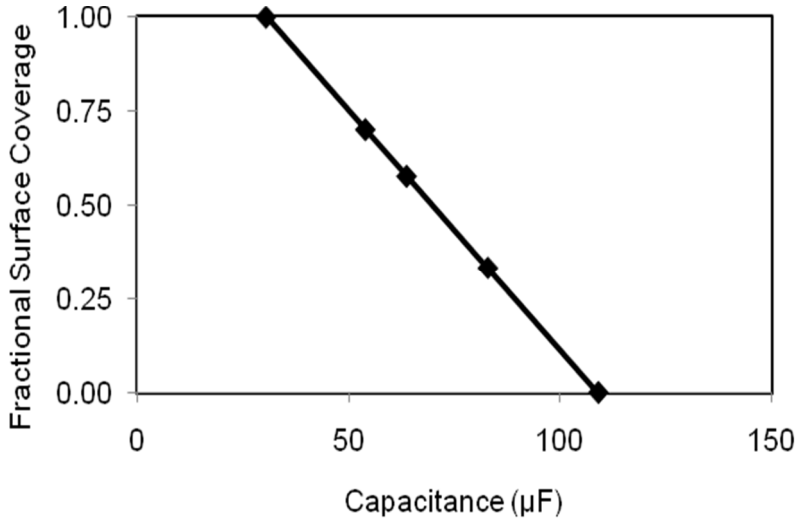

Figure 4.63. Prediction of surface coverage of SIPX on the chalcopyrite electrode by using capacitance values measured with the EIS technique.

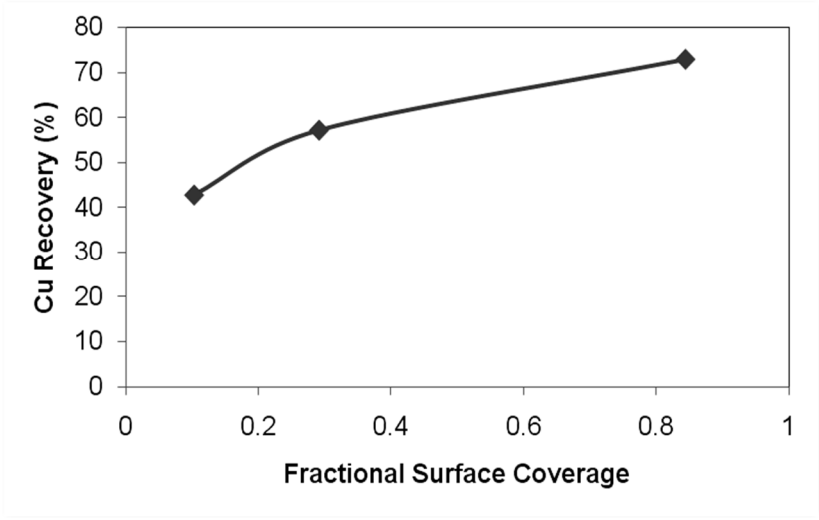

Figure 4.64. The relationship between the surface coverage of the collector and copper flotation recovery in the batch flotation of Çayeli Cu-Zn ore.

The relationship between the surface coverage of the collector and copper flotation recovery is given in Figure 4.64. There is almost a linear relationship between the collector coverage and floatability. The results showed clearly that the EIS methodology is capable of measuring floatability at collector dosages in the range of plant scale application.

5. CONCLUSIONS

In this thesis, various electrochemical methods were tested to measure surface coverage of collector on sulphide minerals and estimate the degree of hydrophobicity which can be used as a proxy to determine floatability of sulphide minerals.

Open circuit potential measurement is currently the only electrochemical method employed for plant scale measurements. However, the results showed that OCP was not sensitive enough at low collector dosages, particularly with collectors adsorbed through EC mechanism.

Cathodic stripping voltammetry was applicable at high collector dosages but not sensitive enough to detect the differences at low collector additions. Differential pulse voltammetry was found to be very effective at low collector dosages, but no response could be obtained with DTPI due to the difference in the adsorption mechanisms of SIPX and DTPI. The adsorption mechanism of SIPX is mainly through electrochemical reactions and it is relatively easy to detect the electron transfer to or from the mineral electrode surface. On the other hand, DTPI adsorption occurs through an electrochemical-chemical (EC) mechanism and it is difficult to observe the adsorption or desorption at the electrode surface, in the form of a pure Faradaic process. Consequently, chronoamperometry was found to be suitable for SIPX but not for DPTI.

Electrochemical impedance spectroscopy (EIS), based on the measurement of the resistance of the electrical double layer, was found to be capable of measuring the change in impedance arising from the adsorption of both SIPX and DTPI on different types of sulphide minerals. Two measures from EIS, resistivity (Zreal) and conductance (Cdl), were used to measure the adsorption density of collectors. The changes in the resistance of the electrical double layer were correlated with the surface coverage of the collector.

Combined mineral electrodes (chalcopyrite/pyrite) were prepared with various mineral ratios to simulate electrochemical behavior of the composite particles and measure collector adsorption. The results showed that the rate of galvanic interaction between chalcopyrite and pyrite depends on the relative surface area

ratio of the minerals in the electrode. The galvanic interaction determines the degree of surface oxidation and hence the adsorption of the collector.

EIS measurements in flotation pulps and the relationship between the resistance of the electrode surface and the copper recovery showed that it is possible to predict the floatability of chalcopyrite particles in the pulp by using an EIS measurement technique.

The studies planned to be done in the future in line with the results obtained in this thesis are as follows:

Fabricating combined electrodes also for other sulphide minerals in order to investigate galvanic interaction mechanism between different minerals.

Plant scale testing of the developed impedance method for measuring and controlling chemical parameters.

6. REFERENCES

Abramov, A.A., Avdohin, V.M., 1997, Oxidation of Sulphide Minerals in Benefication Processes, Gordon and Breach Science Publishers, p.1.

Allison, S: A. et al., 1972, A determination of products of reaction between various sulphide minerals and aqueous xanthate solution, and a correlation of the products with electrode rest potentials, Metallurgical Transactions, Vol. 3, 2613-2618.

Bard, A.J., 1980, Faulkner, L.R. Electrochemical Methods: Fundamentals and Applications, John Wiley&Sons, 833.Wang,2000).

Buckley, A.N.; Woods, R.; Chemisorption- the thermodynamically favoured process in the interaction of thiol collectors with sulphide minerals, 1997, International Journal of Min. Pocess., 51, pp.15-26.

Chander, S. and Briceno, A., 1987, Kinetics of pyrite oxidation, Miner. Metall. Process., 4, 171-176.

Chander, S., 1991, Electrochemistry of sulfide flotation: Growth characteristics of surface coatings and their properties, with special reference to chalcopyrite and pyrite, Int. J. Miner. Process., 33 (4),pp. 121-134.

Chander, S.; Briceno, A.; Pang, 1993, J. Mechanism of sulfur oxidation in pyrite. Minerals and Metallurgical Processing, 10(3), pp.113-118.

Dennen, W.H., 1959, Principles of Mineralogy, Roland Press, New York.

Derjaguin, B. V., Dukhin, S.S., 1961, Trans. IMM 70:221.

Ekmekçi, Z. and Demirel, H., 1997, Effects of Galvanic Interaction on Collectorless Flotation Behavior of Chalcopyrite and Pyrite, International Journal of Mineral Processing, 52, pp. 31-48.

Ekmekçi, Z., 2006, Electrochemistry of Sulphide Minerals – Comminution and Flotation, Lecture Notes, Chapter 1, p.4.

Finkelstein, N.P., Allsion, S.A., Lovell,V.M., Stewart, B.V., 1975, Advances in InterfPheno of Particulate/Solution/Gas Systems (Eds. P. Somasundaran and R. B. Grieves). AIChE:New York. 71(150), pp. 165- 175.

Fuerstenau D.W., Mischra, R.K.,1980, In: M.H.Jones (ed), Complex Sulfides 271-278. London: IMM. Harris, P.J.& N.P.Finkelstein, pp.271-278.

Fuerstenau M.C., et.al., Chemistry of Flotation, AIME/SME, New York., 1985.

Fuerstenau, D.W., 1980, in The Physical Chemistry of Mineral-Reagent Interactions in Sulphide Flotations,(P.E. Richardson, G.R. Hyde and M. S. Ojalvo, eds.), U.S. Bureau of Mines IC 8818.

Gardner, J.R. and Woods, R., 1979, A study of surface oxidation of galena using cyclic voltammetry, Journal of Electroanalytical Chemistry, 100, pp.447-459.

Gardner, J.R., and Woods, R., 1973, The Use of Particulate Bed Electrode for the Electrochemical Investigation of Metal and Sulphide Flotation, Australian Journal of Chemistry, No. 26, pp. 1635-1644.

Gaudin, A.M., 1932, Mc Graw-Hill Book Co., New York, 522p.

Glembotskii, V.A., Klassen, V.I., Plaksin, I.N., 1974, Flotation, Primary Sources, New York, 633p.

Goold, L.A., Finkelstein, N.P., 1972, The reaction of sulphide minerals with thiol compounds, NIMM, Johannesburg, South Africa, Report No. 1439.

Gorain, B.K., Franzidis, J.P. and Manlapig, E.V., 1996, The effect of gas dispersion properties on the kinetics of flotation, Proc. of 35th Annual Conferance of Metallurgist-Column 96, CIM, Montral, Canada, pp.299-313.

Gorain, B.K., Franzidis, J.P. and Manlapig, E.V., 1997, Studies on impeller type, impeller speed and air flow rate in an industrial scale flotation cell. Part 4: Effect of bubble surface area flux on flotation kinetics, Minerals Engineering, 10 (4), pp.367-379.

Guler, T., Hiçyılmaz, C., Gökağaç, G.,Ekmekçi, E., 2004, Voltammetric and drift spectroscopy investigation in dithiophosphinate-chalcopyrite system, Journal of Colloid and Interface Science, 279 (1), pp.46-54.

Guo H., Yen W.T., 2002, Pulp Potential and Flotability of Chalcopyrite, Minerals Engineering ,16, pp. 247-256.

Guy, P.J. and Trahar. W.J., 1985, In: Flotation of Sulphide Minerals, K.S.E. Forssberg(Ed.), Elsevier, Amsterdam, 91-109.

Güler, T.; Hiçyılmaz, C.; Gökağaç, G.; Ekmekçi, Z., 2005, Electrochemical behavior of chalcopyrite in the absence and presence of dithiophosphate, International Journal of Mineral Processing, 75, pp. 217-228.

Heyes, G.W. and Trahar, W.J., 1977, The Natural Flotability of Chalcopyrite, Int. J. Miner. Process., 4, 317-344.

Heyes, G.W. and Trahar, W.J., 1979, Oxidation-Reduction effects in the flotation of chalcocite and cuprite, Int.J.Miner.Process, 6 (3), 229-252.

Hope, G.A., Woods, R., Watling, K.,2003, A Spectroelectrochemical investigation of the interaction of diisobuthyldithiophosphinate wit copper, silver and gold surfaces. II. Electrochemistry and Raman Spectroscopy, Colloids and Surfaces A: Physicichem. Eng. Aspects, 214, pp.87-97.

Hu, W.; Sun, W; Wang, D. Electrochemistry of Flotation of Sulphide Minerals; Springer 2009.

Johnson R E., 1959, J. Phys. Chem. 63, pp, 1655.

Leja, J., 1982, Surface Chemistry of Float Flotation, Plenum Press, New York, Sec.Ed., 758 p.

Maulder et. al.,1995, Handbook of X Ray Photoelectron Spectroscopy, published by Physical Electronics.

Mellgren, O., 1966, Heat of adsorption and surface reactions of potassium ethylxanthate on galena, Trans. AIME , 235, 46-60.

Mendriatta, N. K., 2000, Kinetic studies of sulphide mineral oxidation and xanthate adsorption, PhD Thesis, Virginia Polytechnic Institute and State University,162.

Miller, J.D., Kappes, R., Simmons, G.L., LeVier, K.M., 2006, Pyrite activation in amyl xanthate flotation with nitrogen, Minerals Engineering, Volume 19, Issues 6-8, pp. 659-665.

Pecina E.T., Uribe, A., Finch, J.A., Nava, F., 2006, Mechanism of di-isobuthyl dithiophosphinate adsorption onto galena an pyrite, Minerals engineering, 19, pp. 904-911.

Pourbaix, M., 1966, Pergamon Press, London, 644 p.

Rand, D.A.J. and Woods, R., 1984, Eh measurements in sulphide mineral slurries, Int.J.Miner.Process., 13 (1), 29-42.

Salamy, S.G. and Nixon, J.C., 1953, In: Recent Developments in Mineral Dressing, IMM, London, 503-516.

Savassi, O.N., 1998, Direct estimation of the degree of entrainment and the froth recovery of attached particles in industrial flotation cells. PhD Thesis, University of Queensland,Australia, p.p 307.

Silverman, D.C. 1986, Primer on the AC impedance technique. In:Baboian, R. (Ed.), Electrochemical Techniques for Corrosion Engineering. NACE, Houston, pp. 73-79.

Skoog, D.A., Holler, F.H., Nieman, T.A., 2007, Enstrümental Analiz İlkeleri, (Çev. Esma Kılıç), Bilim Yayıncılık.

Smart, R, St.,C., 1991, Surface Layers in Base Metal Sulphide Flotation, Minerals Engineering, 4(7-11), pp. 891-909.

Sutherland K.L & Wark I.W., 1955, Principles of Flotation Australasian Institute of Mining and Metallurgy, Melbourne.

Taggart, A.F., Taylor, T.C. and Kroll, A.F., 1930, Amer. Inst. Min. Metall. Engrs., Tech. Publ., No 312, 3-33.

Tao, D.P.; Richardson, P.E.; Luttrell, G.H.; Yoon, R.H. Electrochemical studies of pyrite oxidation and reduction using freshly-fractured electrodes and rotating disc electrodes. Electrochimica Acta 2003, 48,pp. 3615-3623.

Tolley, W., Kotlyar, D., 1996, Fundemental electrochemical studies of sulphide mineral flotation, Minerals Engineering, Vol.9, No.6, pp.603-637.

Tolley, W., Kotlyar, D., Fundemental electrochemical studies of sulphide mineral flotation, Minerals Engineering, Vol.9, No.6, pp.603-637., 1996.

Tolley, W.; Kotlyar, D.; Van Wanoger, R., 1996, Fundamental Electrochemical Studies of Sulphide Mineral Flotation, Minerals Engineering, 9(6),pp. 603-637.

Valdivieso, A.L., Escamilla, C.O, Song, S., Lázaro Baez, I., Martinez, I.G., 2003, Adsorption of isopropyl xanthate ions onto arsenopyrite and its effect on flotation, International Journal of Mineral Processing,Volume 69, Issues 1–4, March 2003, Pages 175–184.

Velasquez, P.; Gomez, H.; Leinen, D; Ramos-Barrado, 1998, J.R. Electrochemical impedance spectroscopy analysis of chalcopyrite CuFeS2 electrodes. Colloids and Surfaces A:Physicochemical and Engineering Aspects, 140, pp.177-182.

Velasquez, P.; Leinen, D.; Pascual, J.; Ramos-Barrado, J.R.; Cordova, R.; Gomez, H.; Schrebler,R., 2001, XPS, SEM, EDX, and EIS study of an electrochemically modified electrode surface of natural chalcocite (CuS2), Journal of Electroanalytical Chemistry, 510, pp.20-28.

Venter, J.A., Vermaak, M.K.G., 2008, EIS measurements of dithiocarbonate and trithiocarbonate interactions with pyrite and copper, Minerals Engineering, 21,pp. 559-567.

Vermaak, M.K.G.,Pistorius, P.C., Venter, J.A., 2005,Electrochemical of Raman Spectroscopic Studies of the Interaction of ethyl xanthate with Pd-Bi-Te, Minerals Engineering,18,pp.575-584.

Vianna, S.M., 2004, The effect of particle size, collector coverage and liberation on the flotability of galena particles in an ore, PhD thesis, The University of Queensland, JKMRC Department of Mining, Minerals and Materials Engineering.

Walker, G.W., Electrochemical Flotation of Sulfides: Reactions of Chalcocite in Aqueous Solution, Int. J. of Min. Processing, 12, pp.55-72., 1984.

Walker, G.W., Stout III, J.V., Richardson, P.E., 1984, Electrochemical Flotation of Sulfides: Reactions of Chalcocite in Aqueous Solution, Int. J. of Min. Processing, 12, pp.55-72.

Wang, 2000, J. Analytical Electrochemistry, Second Edition, Wiley-VLC, 209p.

Wark, I.W. and Cox, A.B., 1934, Trans AIME, 112, 189-224.

Wills, B.A., Napier-Munn, T., 2006, Mineral Processing Technology, ISBN: 0750644508, Publisher: Elsevier Science & Technology Books, pp.216.

Woods, C.I, Kim, R., Basilio, D.S., Yoon, R.H., 1995, A spectroelectrochemical study of chemisorption of ethyl xanthate on gold, Colloids and Surfaces A: Physicochemicaland Engineering Aspects, Volume 94, Issue 1, pp. 67–74.

Woods, R. Electrochemistry of sulphide flotation. Proc. Aust. Inst. Min. Met.1972, 241, 53-61.

Woods, R., 1984, In: Principles of Mineral Flotation, M.H. Jones and J.T. Woodcocke (eds), pp. 91-115.

Woods, R., Basilio, C.I, Kim, D.S., Yoon, R.H., Chemisorption of ethyl xanthate on copper electrodes, Int.J.Miner.Process., 42, pp.215-223., 1994.

Yıldız, A., Genç, Ö., Bektaş, S., 1997, Enstrümental Analiz Yöntemleri, Hacettepe Üniversitesi Yayınları A-64, 2. Baskı.

Yordan, .J.L., Yoon, R.H., 1885, SME-AIME Annual Meeting, New Orleans, LA.